FESC
Florida Energy Systems Consortium

FESC Research, Education and Outreach Project Progress Reports

(Attachment to Main Report)

November, 2013

TABLE OF CONTENTS

Florida Atlantic University

Southeast National Marine Renewable Energy Center (SNMREC)
(Progress Report)

PI: Susan H. Skemp **Co-PIs:** Howard P. Hanson, James VanZwieten, Taghi Khoshgoftaar, Pierre-Phillippe Beaujean, Len Berry, Megan Davis, Jeanette Wyneken, Manhar Dhanak, Eric Chassignet, John Reed, Charles Messing, Karl vonEllenrieder, Julie Lambert, Hassan Mahfuz, Stewart Glegg, George Frisk, Bassem Alhalabi, Hari Kalva, Steve Kajura, Madasamy Arockiasamy, Francisco Presuel-Moreno, Isaac Elishakoff
Students: Student listing is appended

Description: The Southeast National Marine Renewable Energy Center (SNMREC) at Florida Atlantic University (FAU) was established by an award from the US Department of Energy in 2010 as an extension of FAU's Center for Ocean Energy Technology, which was originally founded in 2007 by the 2006 Florida State University System Center of Excellence Program. The SNMREC is investigating harnessing power from ocean currents, such as the Gulf Stream, as well as ocean thermal energy conversion to generate base-load electricity, thereby making a unique contribution to a broadly diversified portfolio of renewable energy for the nation's future. Key drivers for investigation are determined by the regulatory process at State and Federal levels and by market and technology gaps needed to commercialize MRE. The SNMREC's role is to bridge the gap between concept and commercial deployment of ocean energy technologies by providing at-sea testing facilities and technology development for both ocean current and thermal energy systems. Research areas span environmental, resource, economic, education, and technology topics.

Budget: $8,750,000

Universities: Florida Atlantic University, collaborating with the University of Central Florida, Florida State University, University of South Florida, Embry-Riddle Aeronautical University, University of Miami, Oregon State University, University of Washington, Pennsylvania State University, University of New Hampshire, University of Hawaii, University of Edinburgh, Heriot-Watt University, Nova Southeastern University, Virginia Polytechnic Institute and State University, and Florida Institute of Technology.

External Collaborators: Numerous industry partners, state and federal government agencies, FFRDCs such as the National Renewable Energy Laboratory, Oak Ridge National Laboratory, Woods Hole Oceanographic Institution, U.S. Department of Energy (Office of Energy Efficiency and Renewable Energy), U.S. Department of Interior (Bureau of Ocean Energy Management, Regulation, and Enforcement), U.S. Department of Commerce (National Oceanic and Atmospheric Administration), the Florida Fish and Wildlife Commission, and Florida Departments of Agriculture and Environmental Protection.

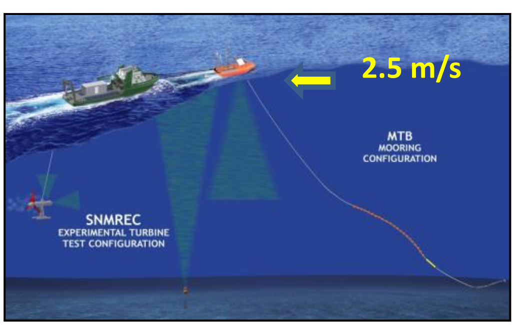

Project Description

The Southeast National Marine Renewable Energy Center is developing an open-ocean energy laboratory and test capability to advance research on *marine and hydrokinetic* (MHK) ocean current energy and thermal potential energy. The SNMREC is moving forward with strategically selected research, developing and testing key technology, infrastructure and systems as well as standards criteria to meet this need. The successful implementation of an in-water testing infrastructure for MHK off the coastline of Florida will be the first and only such capability globally. Already, companies from both the U.S. and internationally have expressed a desire to work with the SNMREC in defining not only their test requirements based on their design, but also are exploring both short term occupancy in Florida and potentially longer term manufacturing and grid connection in developing arrays for commercial enterprises. An MHK lease application on the outer continental shelf (OCS) was submitted to the U.S. Department of Interior, Bureau of Ocean Energy Management (BOEM). This is the first national application which will form the model for future lease applications. BOEM released the Final Environmental Assessment (EA) with a Finding of No Significant Impact (FONSI) on 12 August 2013. The EA and FONSI can be found on the Department of Interior's website at http://www.boem.gov/Florida-Revised-EA-FONSI-August2013/.

The DOE NEPA office is in the process of writing their FONSI required by law based on the EA. The Department of Environmental Protection, as the State of Florida's lead Coastal Zone Management Act agency, conducted a consistency determination review of the BOEM EA and FONSI. They notified the BOEM on 25 September 2013 that the issuance of a lease to SNMREC for hydrokinetic technology testing is consistent to the maximum extent practicable with the provisions of the Florida Coastal Management Program. It is anticipated that a lease will be granted to FAU and SNMREC in Q1 of CY2014.

The SNMREC is engaged in sensor and instrument acquisition, deployment, and analysis to more fully characterize offshore energy resources, and the benthic and pelagic environment. Second, fabrication of a small-scale hydrokinetic turbine system is in the final stages of completion. Testing is ongoing for components, sub-systems, and major systems of the turbine. Assembly and tow testing of the prototype prior to deployment of the test infrastructure will begin in November. Discussions are ongoing with over 40 companies to determine testing/validation requirements for open-ocean testing of their proposed experimental devices at the SNMREC's test facility. A centralized, standardized testing capability will be provided for testing current energy conversion prototypes; initially, scaled versions and eventually full-scale devices. In addition, critical environmental measurements will be obtained from the observational platform.

Sea trials were successfully conducted of a mooring and telemetry buoy to ready it for at-sea deployment. In-lab technology testing is underway with a scaled generator dynamometer which provides a platform to test offshore electrical systems before use and simulate offshore grids. Aerial surveys are being conducted to determine offshore turtle and marine mammal distribution and activity prior to install/test of MHK devices. Sub-sea surveys of installation sites are helping to identify deep water coral distribution and determine appropriate anchor areas.

Over fifty upper-division graduates and Principle Investigators have been engaged in research in marine renewable energy (MRE) to date. The Center developed a curriculum for upper-division high-school students to introduce the topic within secondary education.

To date, with the State of Florida funding, the SNMREC has successfully leveraged $5,717M of U.S. Department of Energy funds. Industry sponsored funding is at a level of $177,000.

3. Annual Progress Report 10/12 – 9/13

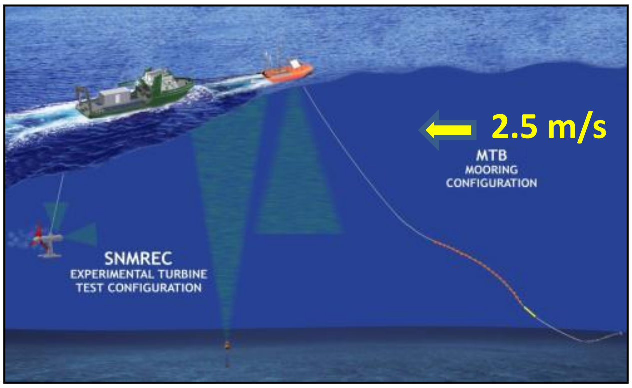

Figure 1. SNMREC Ocean Current Test Facility Setup

SNMREC is developing and installing the first open-ocean current energy conversion test facility in the U.S. consisting of at-sea equipment (Figure 1) for the purpose of investigating current energy conversion devices in the Florida Current, approximately 12 miles offshore Fort Lauderdale, Florida. Initially, the capability will be limited to scaled devices (⅛ – ¼ scale, or up to 7 meter diameter rotors or 100kW instantaneous maximum power production). The SNMREC facility will provide a centralized, standardized approach to testing for current energy conversion prototypes. In addition, the facility will serve as an observational platform from which critical environmental measurements can be obtained.

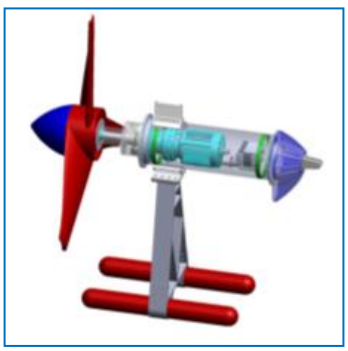

Figure 2. SNMREC 3-Meter Diameter Rotor, 20kw Instantaneous Max Power Prototype Turbine

A 3-meter rotor diameter, 20kW generically designed experimental research turbine (Figure 2) will provide a non-proprietary platform for component development at small scales. The test procedure/plan is laid out to incorporate monitoring and failure prediction systems, to gain experience in at-sea operations of this nature, and to support standards and protocol development. Industrial beneficiaries will be able to use the results of testing to enhance and accelerate prototype development. A major challenge, obtaining an outer continental shelf lease, is nearly met.

3.2 Areas of Significant Progress

3.2.1 Resource Assessment

The global analysis of ocean thermal energy conversion (OTEC) potential, a DOE-funded project undertaken jointly with the Lockheed-Martin Marine Systems and Sensors Division, has been completed, producing a publically available GIS database that is accessible at http://maps.nrel.gov/mhk_atlas. This GIS tool provides information pertinent to both OTEC and sea water air conditioning (SWAC). A screenshot of this tool is shown in Figure 1. Detailed assessments of both the OTEC and SWAC resources off Florida have also been conducted. Using the Hybrid Coordinate Ocean Model (HYCOM) results produced in data-assimilation mode by the Naval Research Laboratory (NRL) and *in situ* data, estimates of the net electric power that could be created utilizing a representative 100 MW OTEC plant have been made. It is estimated that such a plant could produce an average up to 112 MW of power if located off Key West, with power production decreasing with latitude up the east coast of Florida (Figure 3).

Florida Energy Systems Consortium

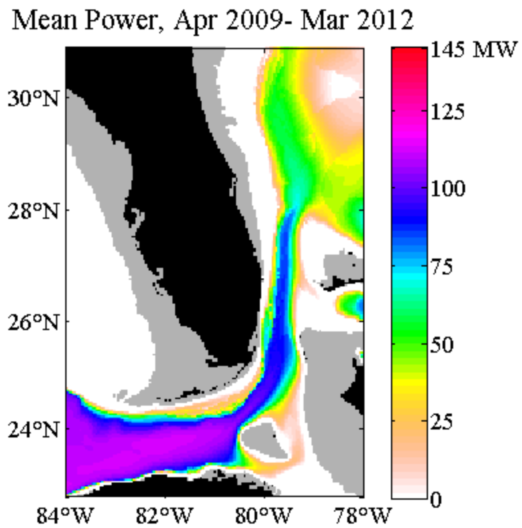

Figure 3. Average net electric power produced from a single representative 100 MW OTEC plant

OTEC plants create power by using the temperature difference between the warm surface water and cold deep water to produce electricity. For this reason they run large amounts of both cold and warm water through heat exchangers. Therefore, a first step in assessing the environmental impact of locating an OTEC plant in the Florida Straits is quantifying the percentage of the resource that will be used by a plant. It is calculated that an OTEC plant located along the transect line "A" in Figure 4 would use approximately 0.009% of the cold water (<9° C Figure 4, right) flowing past this line. To help put this into perspective Florida utilized approximately 26 GW of power in 2005. If this entire 26 GW of power were produced using OTEC (meaning 260 of the 100 MW OTEC plants discussed here) then these plants would utilize less than 2.5% of the cold water that flows between Florida and Cuba.

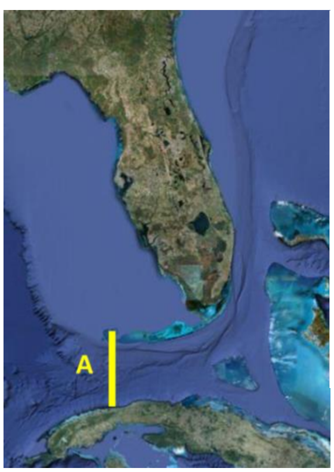

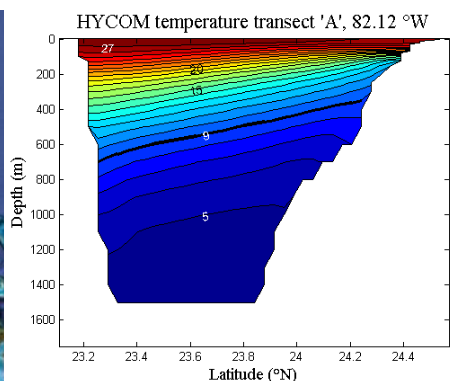

Figure 4. Thermal energy resource for (a) summer, (b) winter, (c) annual average

The DOE-sponsored global OTEC resource study relied on model results, from a data-assimilation version of the global HYCOM. Recently, the NRL has adopted a more recent version of HYCOM for its simulations of the Gulf of Mexico and the Straits of Florida, which version includes both very high resolution (~4 km horizontally and more vertical layers) and improved physics. Because of this, comparisons between SNMREC field datasets and HYCOM results such as those shown in Fig. 4 have improved markedly. These results will continue to be useful for ongoing OTEC assessments for Florida's future.

Finally, on May 22nd three Acoustic Doppler Current Profiler (ADCP) buoys were deployed. The ADCP measurements combined with a SeaSonde® ocean surface current measurements system will allow for estimations of the Florida Current's volumetric flow and power potential. The SeaSonde® system, manufactured by CODAR Ocean Sensors, consists of two pairs of antennas installed on land within close proximity to the shore at Hillsboro and Haulover Beach (Figure 5). At each site one antenna transmits a high frequency radar signal that is reflected on the ocean surface and received by the second antenna. At offshore locations where at least two radar signals intersect the total current speed and direction can be calculated.

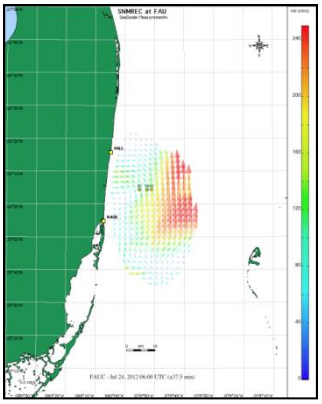

Fig 5. CODAR Installations

Concurrently as of mid-July 2012, SNMREC's 12 MHz SeaSonde® radar system has been collecting ocean surface current measurements (see figure 5 for location of ADCP buoys in relation to SeaSonde® coverage area).

Fortuitously, the ADCPs were operating during the passage of Hurricane Sandy and were recovered in December 2012. With the passage of Hurricane Sandy, however, wave action at the Hillsboro site caused serious beach erosion and, in the process, the northern of the two antennas was destroyed. However, data were obtained before the unit's loss to allow initial attempts to validate the SeaSonde® data by comparing to data collected from the ADCPs. Early results suggest that, at least during periods of variable winds, such as during the passage of the storm, there is no correlation between CODAR-measured surface currents and currents throughout the water column. It appears that it will be necessary to adopt other strategies for continuous monitoring of the current.

Eventually, wind data within the coverage area (which will be collected from the MTB anemometer when permission to deploy the MTB is granted) will be available to quantify the wind effects and improve the accuracy of the current profile prediction algorithms. In May 2013, four ADCPs were deployed in a modified diamond configuration to measure both latitude and longitudinal effects of variability in the current. Recovery of the ADCPs is planned for December 2013.

Finally, in July, notification came from a fisherman, that a buoy had been spotted floating in the current off Graciosa, the Azores and recovered. The buoy was equipped with two ADCPs, a 75 kHz and a 300 kHz. Serial numbers from the ADCPs were sent to the manufacturer and finally traced back to equipment purchased by SNMREC and deployed in February 2009. At the time of retrieval of the first four ADCPs in March 2010, it was discovered that the one located furthest east at an approximate depth of approximately 2,165 ft. in the core of the current was missing. Three years later, it turned up in the Azores. The instruments were recovered by SNMREC and the data is undergoing evaluation. Changes were made to the ADCP buoy design and a GPS monitoring device was installed to provide tracking data should ADCP buoys slip their mooring in the future.

3.2.2 Regulatory Environment

Continuing evolution of state and federal agency requirements is a challenge obtaining permits for open-ocean deployment of even experimental test systems. Pursuing any research and development in renewable energy on the Outer Continental Shelf (OCS) must comply with the federal Outer Continental Shelf Lands Act. With respect to the SNMREC deployments of prototype devices/systems, the major permits, approvals, and authorized actions necessary to construct, operate, maintain, and decommission project facilities while falling outside of State of Florida waters (i.e., greater than 3 miles offshore), will involve interaction with the Florida Fish and Wildlife Conservation Commission due to its agreements with the U.S. Fish and Wildlife Service. Shore-side activities in support of the offshore deployment will be conducted within State waters, at a commercial marina under the purview of the Florida Department of

Environmental Protection. These activities also engaged agencies such as the U.S. Army Corps of Engineers, the National Oceanic and Atmospheric Administration's Marine and Fisheries Service, the U.S. Coast Guard, the U.S. Navy, etc.

SNMREC submitted the first lease application in the nation to the U.S. Department of the Interior's Bureau of Ocean Energy Management (BOEM) to deploy equipment related to marine hydrokinetic energy conversion device on the outer continental shelf (OCS). The initial phase of a standalone testing and evaluation infrastructure without transmission of power to shore required an Environmental Assessment (EA) which was conducted by BOEM. BOEM released the Final Environmental Assessment (EA) with a Finding of No Significant Impact (FONSI) on 12 August 2013. The EA and FONSI are located on the Department of Interior's website at: http://www.boem.gov/Florida-Revised-EA-FONSI-August2013/. As required by law, the Department of Environmental Protection, as the State of Florida's lead Coastal Zone Management Act agency, conducted a consistency determination review of the BOEM EA and FONSI. They notified the BOEM on 25 September 2013 that the issuance of a lease to SNMREC for hydrokinetic technology testing is consistent to the maximum extent practicable with the provisions of the Florida Coastal Management Program. It is anticipated that a lease will be granted to FAU and SNMREC in Q1 of CY2014.

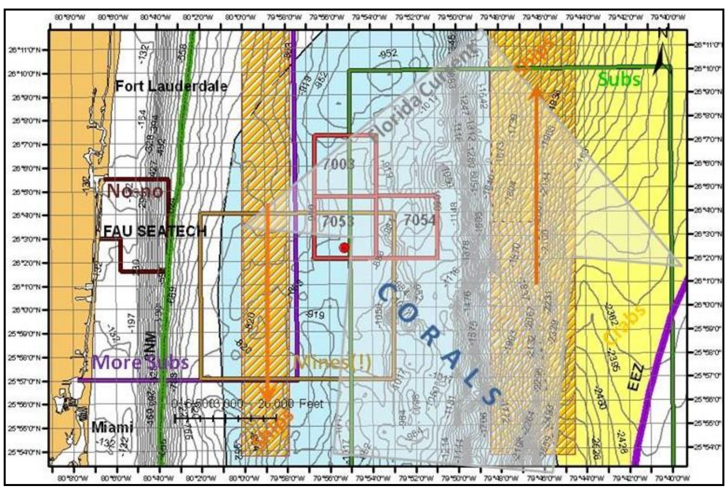

Figure 6. Map of SNMREC requested OCS Lease BOEM Blocks (7003, 7053 and 7054).

Efforts are underway to develop the Project Plan required by the EA. The Project Plan will include any specifics that were not detailed in the original lease application as well as any information necessary to comply with lease and EA stipulations. As this is the first such application for MHK on the OCS, there are still areas being worked out by the agencies.

The three-block area of interest requested in the application includes BOEM defined blocks 7003, 7053 and 7054, as shown with red outlines in Figure 6.

The map is a compilation of other identified areas of primary interests and potential user conflicts that were considered during selection of the final BOEMRE blocks.

Recent research results, some of which were supported by the SNMREC, have provided additional information about a newly discovered genus of corals that inhabit the outer parts of the Miami Terrace in the Florida Straits. The vulnerability of these corals to deep-trawl commercial fishing led the National Oceanic and Atmospheric Administration to designate a large part of the sea-bed offshore of Florida and Georgia as a Coral Habitat Area of Particular Concern. While this designation will result in relatively little disruption of the SNMREC's operations – the Center's two or three anchor systems can easily be deployed on the large, sandy patches that exist between coral beds – there will likely be significant challenges for commercial-scale deployments in the future.

3.2.3 Infrastructure

Figure 7. Mooring and Telemetry Buoy (MTB) during open-ocean sea trials.

SNMREC's proposed initial deployment, approximately 12 miles offshore Fort Lauderdale, Florida which regularly experiences 3-4 kts of current, will consist of an anchored mooring and telemetry buoy (Figure 7), to be used as an attachment point for work boats to deploy prototype systems for testing, and as an observational platform for a variety of environmental and met-ocean studies. The SNMREC's buoy, a design based on the familiar NOMAD weather buoys originally developed by the U.S. Navy in the 1940s, is undergoing final tune-up modifications following a series of successful sea trials earlier this summer. The initial deployment will provide testing capabilities for devices in the 100kW class and smaller.

Figure 8. Dynamometer for generator testing (left) and full-up data acquisition and control system (right)

One of the biggest unknowns in the operation of ocean current turbine (OCT) systems concerns the behavior of the generator sub-system as it experiences both variable loads and the torque differentials associated with changing currents acting on the rotor. In order to provide a capability to test generators under conditions as realistic as possible without actually having to go to sea, SNMREC has developed a computer-controlled dynamometer system, located at the FAU SeaTech facility in Dania Beach. This capability is further being developed in conjunction with oceanographic measurements and modeling to simulate rotor behavior as it would behave in the current. The 20 kW dynamometer (Figure 8) has been fitted with the SNMREC's experimental research turbine power and health management systems, and is generating data for Prognostics and Health Monitoring (PHM) research. In addition, preliminary work has been completed to emulate rotor behavior in wave conditions and from collected offshore measurements. Testing will continue to include optimization of *in situ* data integration and 20kW research turbine electrical and sensor system testing.

3.2.4 Environmental Monitoring / Demonstration

Monthly aerial diversity and distribution surveys are being conducted to assess sea turtle and marine mammal populations. The surveys employ the currently accepted protocol – human observers viewing transect areas from a plane flying approximately 500 ft. from the ocean surface. Twenty-four cross-channel and 20+ coastal surveys were completed. Additional along-shore surveys with available historical data are underway.

Figure 9. Aerial survey areas offshore Ft. Lauderdale, to determine sea turtle and marine mammal population

Because preliminary data suggests significant population activity near shore, these transects will provide higher resolution data to support analysis efforts. The research team is working with the National Oceanic and Atmospheric Administration's, National Marine Fisheries Service to evaluate the SNMREC's enhanced approach as an expansion of currently accepted methods. The survey areas currently being assessed are depicted in Figure 9.

3.2.5 Education and Outreach

3.2.4.1 Professional Community

The Southeast National Marine Renewable Energy Center (SNMREC) will provide a centralized, standardized testing capability for ocean current energy conversion prototypes; initially, scaled versions and eventually full-scale devices will be tested. Initial testing in the lease area will be with SNMREC's experimental prototype turbine components and subsystems. SNMREC is working with over forty individual companies as well as industry organizations on a research agenda that is compatible with strategic industry, government, and academic requirements. Balancing the portfolio to meet the diverse priorities is a challenge. Technology R&D, specifically in areas related to intelligent monitoring and environmental assessment will continue as Marine Hydrokinetic (MHK) commercial devices are developed to ensure safety and reduce risk. The Center supports participation on two International Electrotechnical Commission (IEC) U.S. Technical Advisory Groups (TAG) in developing global standards and conformity assessment practices for marine renewable energy. The two areas of focus of the Technical Committees are wave, tidal and ocean current design, performance and operation (TC114) and mechanical vibrations, shock and condition monitoring (TC108).

Discussions are ongoing to determine testing/validation requirements for open-ocean testing of company's proposed experimental devices at the SNMREC's test facility. Further, critical environmental measurements will be obtained from the observational platform. Additional test berths will need to be installed as commercial devices progress through development gates (including grid-connection and moored stand-alone systems in the 1:4 and 1:1 scale). A future permanent ocean observing system co-located with offshore test facilities will provide real-time environmental measurements, resource characterization, and device performance data. The environmental measurements and assessments, in conjunction with device deployments, will allow for the investigation of interaction with installed MHK systems after baseline ecological activity information is gathered. Education and outreach programs will continue to be fostered in all levels of curricula to populate the growing economic sector, and a publicly available and useful data clearinghouse will provide related and integrated data specifically for MHK and Ocean Thermal Energy Conversion development.

3.2.4.2 Education

SNMREC created and implemented a summer internship program with HBOI, and the United States Coast Guard Academy for the summer of 2013. This ongoing initiative will ran from July 2012 - the summer of 2013, and will continue annually. The cadet selected to participate in the program this year used her research to submit a poster to the National Oceans Conference. This program will enhance cooperation between the U.S. Coast Guard and the SNMREC while educating future officers about projects which will be installed in coastal areas.

The SNMREC continues to partner with the South Broward High School's Marine Magnet Program and presents programs to the students using the SNMREC's curriculum as a basis. The focus of this program is technological while also highlighting interactions with the environment.

SNMREC staff worked with professors and students at FAU's School of Communications and Multimedia Studies' to create an interactive educational display game. In partnership with HBOI, the SNMREC is designing and installing a kiosk in their Ocean Discovery Center. The kiosk is anticipated to be installed by January 2014 and will create a hands-on experience which educates the public about future ocean energy projects. This effort will be leveraged to provide similar kiosks to science and discovery museums. The intent is to provide an opportunity to engage all ages in a hands-on, fun and educational experience about ocean renewable energy production. The kiosks will increase knowledge of real, cutting- edge research in renewable energy from the ocean as well as, incorporating valuable Science Technology Engineering & Math (STEM) content to foster a well- informed *constituency that* understands the importance of renewable energy production in the U.S.

In collaboration with Florida Atlantic University's Lifelong Learning Society (LLS), the SNMREC presented two lectures to members of the LLS. The LLS at FAU is a 20,000 member strong organization providing an opportunity to introduce MHK energy to a wider age spectrum of the population.

A seventh lesson is in development for the SNMREC curriculum for high school based on civics/social studies. This lesson instructs the students on the important role that the government has in renewable energy production and advancement. The lesson is based on the same educational model as the original curriculum, the "5E's"; Engaging, Exploring, Explaining, Elaborating and Evaluation. Appropriate activities and Sunshine State Standards are included.

Funding Leveraged

To date, with the State of Florida funding, the SNMREC has successfully leveraged $5,455,675 of U.S. Department of Energy funds. DOE has identified an additional $250,000 pending development of a Statement of Work and associated detailed budget against the current grant. Three proposals are in process and will be submitted in May and June.

University of Florida

Database Infrastructure for Integrative Carbon Science Research (Updated)
(Final Report)

PI: Sabine Grunwald **Co-PI:** Timothy A. Martin
Students: C.W. Ross (M.S. completed); X. Xiong (Ph.D., completed)
Technical staff: Brandon Hoover and Risa Patarasuk

Description: Rising CO_2 concentrations in the atmosphere and effects on global climate change have been well documented, and future impacts are uncertain but potentially devastating. Florida's natural and agro-forest ecosystems have much potential to sequester carbon in biomass and soils due to unique climatic and landscape conditions. However, research gaps exist to accurately assess carbon pools and fluxes at coarse scales, ranging from county to the region and larger. The overarching objective of this project is to address these obstacles by developing a terrestrial carbon information system (called "TerraC") for the carbon science community, focused on ecosystems in Florida. The information system will be administered through the UF Carbon Resources Science Center (http://carboncenter.ifas.ufl.edu), a multi-disciplinary Center dedicated to research in support of enhanced agricultural and natural resource carbon management.

Budget: $199,440
Universities: UF
External Collaborators: Natural Resources Conservation Service-U.S. Department of Agriculture

Progress Summary
We developed the TerraC system (Terrestrial Carbon Information System) [http://terraC.ifas.ufl.edu] that synthesizes terrestrial carbon and environmental data into an online database structure and facilitates data sharing and synthesis analysis. This project helped to leverage a $20 million NIFA-USDA funded project (PINEMAP: "Integrating Research, Education and Extension for Enhancing Southern Pine Climate Change") that has adopted TerraC as the centralized data infrastructure for the project.

The overall goal of this project was to develop a carbon data information system for the carbon science community focused on Florida and the southeastern U.S. The specific objectives were to develop a web-based database infrastructure and toolsets that integrate carbon and environmental data and facilitate collaboration and interactions among scientists and others interested in carbon and global climate change sciences. Terrestrial carbon is a key indicator in the global carbon cycle that interrelates with the global climate and other biogeochemical cycles. Energy consumption and fossil fuel emissions have impacted severely the carbon cycle and lead to warming effects in the atmosphere. It is critical to integrate data, information, and knowledge related to carbon and other environmental properties to enhance our knowledge and develop adaptation and mitigation strategies to counteract negative impacts in the future.

The TerraC system provides support to synthesize and integrate carbon and environmental data to assess impacts of global climate and land use change, investigate adaptability to natural and anthropogenic induced forcings and disturbances, vulnerability and risk assessment related to the terrestrial carbon balance, ecosystem services (e.g. carbon sequestration), and more.

Goals and Objectives

The overall goal of this project was to develop a carbon data information system for the carbon science community focused on Florida and the southeastern U.S. The specific objectives were to develop a web-based database infrastructure and toolsets that integrates carbon and environmental data and facilitates collaboration and interactions among scientists and others interested in carbon and global climate change sciences.

1. Motivation for Project

Rising CO_2 emissions in the atmosphere and effects on global climate change have been well documented, and future impacts are uncertain but potentially devastating. In the southeastern U.S., specifically Florida, natural and agro-forest ecosystems have much potential to sequester carbon in biomass and soils due to unique climatic and landscape conditions. However, research gaps exist to accurately assess terrestrial carbon content/density, carbon pools, and carbon fluxes at coarse scales, ranging from county to the region and larger. This project was motivated to address these obstacles by creating a database infrastructure for the carbon science community, focused on ecosystems in Florida and the southeastern United States. The TerraC system provides support to synthesize and integrate carbon and environmental data to assess impacts of global climate and land use change, investigate adaptability to natural and anthropogenic induced forcings and disturbances, vulnerability and risk assessment related to the terrestrial carbon balance.

2. TerraC Architecture

We developed a SQL-based (SQL = structured query language) web-accessible data infrastructure to compile carbon and environmental data into a centralized tool. TerraC manages user accounts at a variety of permission levels, provides tools to store, view, query, access, and download carbon data. A new .NET application was built to handle the interaction between the client and the database to accommodate fast streaming of large data files. With the growth and demand of modern datasets, this technology is a requisite for tools such as TerraC.

Description of the TerraC Information System

TerraC provides a data engine which allows managing, archiving, sharing, editing, modifying, and querying carbon and associated environmental data. These data are derived from various projects and sources; thus, provide a wide array of different carbon measurements, in various ecosystems and geographic regions, and spatial and temporal scales. The TerraC data engine facilitates synthesis and modeling to gain better insight into carbon cycling from micro, plot, field, watershed, basin, large region, and global scales.

Data Sharing and Usage Policy

Data users submitting data to or use data from the TerraC Information System agree to abide by the terms and conditions explained in this document. Data users may be held responsible for any misuse that is caused or encouraged by failure to abide by this agreement.

Definitions

Project: Set of one or more datasets that contain carbon (and related) environmental data.

Dataset: Set of data comprised of one or more data fields that contain carbon (and related) data that is part of a single project.

Roles of users

Project owner (leader): Principal Investigator or person with similar credentials responsible for collecting and managing the original, quality controlled data generated by a specific project. The project leader needs to initiate a project before a dataset can be submitted to TerraC and is responsible for the quality of all datasets under his/her projects. The project leader controls the levels of data sharing and can assign one or more data managers to each of his/her projects.

Data contributor (or manager): User that has read/write access to a dataset in TerraC. The data manager has privileges to submit a new dataset to a project and access and modify existing ones in part or as a whole. The project leader needs to assign a user manager status before he/she can submit a new dataset or modify an existing one in a project.

Data user: User that can view a dataset in TerraC. The data user can read public datasets and also private datasets as long as he/she has been granted access to them by the project leader. The data user cannot submit a new dataset or modify existing ones unless he/she receives manager status from the project leader to a project.

Data sharing: Data stored in TerraC can be shared at three access levels. The access levels are chosen by the project leader to control access to their projects by different users. Different access levels can be assigned to different users, the level being project- and user-specific. Levels 1 and 2 mirror the roles of data user and data manager, respectively. Level 3 in the most restricted access level.

Levels of data sharing:

Level 1 – Public with read-only access: Access to the data is open to all TerraC users. Any person that has a TerraC user account (i.e. data users) can view the data, but not modify it directly from the TerraC database. Only the project leader can modify/edit data.

Level 2 – Private read/write access: Access to the data is open to data managers who were assigned (approved) by the project leader to have permissions to view and modify/edit data directly from TerraC. *Private read/write access* is password-protected.

Level 3 – Private read-only access: Access to the data is restricted to the project leader and users selected by the project leader. Users can only view the data, but not modify it directly from TerraC.

The project leader controls the sharing of data in TerraC. He/she provides leadership for collaboration with new partners on behalf of the project teams. The project leader can switch sharing levels from Level 3 to 2 and 1, but not vice versa, meaning if the data are released to other users or the general public this right cannot be reversed. Data users who are interested in to gain access to a specific protected dataset can contact the project leader and negotiate agreement of data use of a specific project. The project leader may agree to share data with the data user to collaborate on a joint project, work on a co-authored research publication, or use them for other purposes.

Data usage: Data users are expected to use data obtained from TerraC to the highest level of professional integrity and ethics. Data users must abide by the following guidelines when distributing or publishing data obtained from TerraC:

Data sharing and usage in TerraC is governed by the **Attribution Non-Commercial Share Alike** license provided by Creative Commons (summary: http://creativecommons.org/licenses/by-nc-sa/3.0; legal code: http://creativecommons.org/licenses/by-nc-sa/3.0/legalcode), which observes the following rules:

Attribution: The data user must give credit to the project leader (or project) in the manner specified by him/her (but not in any way that suggests that the project leader endorses the data user or his/her use of the data);

Noncommercial: The data user may not use TerraC data for commercial purposes; data should be used for reserach and non-profit applications;

Share Alike: If the data is modified in any manner or used to derive other products, the data user may distribute the resulting work only under the same or similar license to this one;

Credits and publications derived from TerraC usage:

- The data user must inform or consult the project leader about his/her intentions to use the data for publication well in advance of submission of the publication; the project leader should be given the opportunity to read the manuscript and, if appropriate, be offered co-authorship;
- The data user must give credit to the project leader (or project), which can be in the form of co-authorship, citation, or acknowledgement, according to the requirements imposed by the project leader; any deviation from this rule must be formally agreed between the data user and project leader;
- The data user must cite or acknowledge TerraC as the data host used to obtain the data;
- Any modification to the data originally obtained from TerraC by the data user must be fully documented.

Carbon Data and Associated Environmental Data

(1) Core Data Fields:

- Identification number for each observation (ID)
- Replication number (REPN)
- X coordinate (X) {Geographic Coordinate - longitude in decimal degrees, World Geographic System 1984, WGS 1984}
- Y coordinate (Y) {Geographic Coordinate - latitude in decimal degrees, World Geographic System 1984, WGS 1984}
- Sample date (DATE) {MM/DD/YYYY}
- Time (TIME) {HH:MM:SS}

- Height or depth of measurement (Z) {in cm; below the soil surface negative numbers; above the soil surface positive numbers}
- Carbon measurements (variable names, data values, and meta data: analytical methods & units of measurement in Standard International Units)
- Biogeochemical or other environmental data (variable names, data values, and meta data: analytical methods & units of measurement in Standard International Units)

(2) Project Elements (meta data):

- Project title
- Project description (description of sampling design, sampling protocol, quality assessment, data constraints such as below detection limit treatment, missing values, etc.)
- Project owner (typically Principal Investigator of a research project; or Project Leader for agency lead project)
- Project contributor (optional)
- Project user (optional)
- Contact information (Project Owner)
- Funding source
- Project location (description of geographic location of project; size of project area)
- Project period (YYYY to YYYY)
- Link to project homepage
- Publications from project
- Acknowledgements

Data Quality and Standards

Data format: TerraC focuses on terrestrial carbon and related environmental data. Data submitted to TerraC must contain carbon data and have the following format:

- Data organized n rows and columns, with cases (observations) listed in the rows and properties (attributes) listed in the columns;
- Carbon and other measured properties must be presented as variables in specific columns:
    - Each column must only contain properties measured using the same method; if the same property was measured using more than one method (e.g. total carbon vs. carbon fractions), each method must be presented as a separate column;
- Spatial coordinates (horizontal and vertical) and time stamps must be presented, whenever available, as variables in specific columns;
- Repeated measures (e.g., the same property collected at different times or replicated) must be treated as separate cases (i.e. listed in separate rows):
    - A column indicating that the cases are repeated measures of the same property must be included (e.g. using the same sample identifier for the repetitions);
    - A column indicating the number of the repetition (i.e. 1, 2, 3…) must be included;
- Quality assurance/quality control (QA/QC) data should not be included in the dataset, but instead in the metadata of the property it pertains to.

Data preparation: You can use any relational data base software of spreadsheet program to prepare your data for upload into Terra C. For example, Excel, MS Access, SQL or similar to organize your data listing cases (observations) in rows and properties in columns. A data template provided by TerraC helps to setup datasets ready for upload into the system.

Notes:

- Data values can be represented in form of strings, boolean (yes or no; 1 or 0), continuous (float), or discrete (integer) data
- Null values should be represented in the data as "0" or "0.0"
- To represent missing data leave fields empty (blank); do not use "N/A"
- To mark any special data values you may use codes "-999", "-9999" or similar (outside the data range for a specific measurement). The meaning of such special values should be included in the meta data
- Below detection limits (BDL) should be marked in data fields with a value (numeric data value) instead of listing "BDL" (string). The numeric data value can either represent the "true" BDL for a specific analytical method (e.g. 0.0005) or a designated arbitrary value (e.g. -99999). Mixing of different data types in one variable should be avoided (e.g. mixing of numeric and string values; or decimal values and text)

3. Datasets incorporated in TerraC Information System

Several large carbon and environmental datasets were integrated into TerraC covering Florida and the southeastern U.S. Environmental data are focused on climate and other relevant information, such as land use and vegetation, pertaining to the carbon cycle.

Soil Carbon Data – Florida
Soil carbon data from various projects, covering the Santa Fe River Watershed and the State of Florida, from different time periods (1965 to current) are included in TerraC.

PRISM (Parameter-elevation Regressions on Independent Slopes Model)
These data sets were created using the PRISM climate mapping system, developed by Dr. Christopher Daly, PRISM Climate Group director. PRISM is a unique knowledge-based system that uses point measurements of precipitation, temperature, and other climatic factors to produce continuous, digital grid estimates of monthly, yearly, and event-based climatic parameters. Continuously updated, this unique analytical tool incorporates point data, a digital elevation model, and expert knowledge of complex climatic extremes, including rain shadows, coastal effects, and temperature inversions. PRISM data sets are recognized world-wide as the highest- quality spatial climate data sets current l y available. PRISM is the USDA's official climatological data. http://prism.oregonstate.edu

Variables representing 1970-2010 included in the PRISM dataset are: Precipitation (average monthly), Minimum Temperature (average monthly), Maximum Temperature (average monthly), Dew Point Temperature (average monthly), Mean Temperature (average of Minimum and Maximum Temperature)(average monthly) , Vapor Pressure (average monthly) .

Idaho Geospatial
This gridded data set was developed by Dr. John Abatzoglou from the University of Idaho. These climate data combines spatial attributes of gridded climate data from PRISM with temporal attributes of a region-al-scale and daily gauge -based precipitation. The gridded was based on observations from various weather stations including RAWS, AgriMet, AgWeatherNet and USHCN-2. The dataset is intended for users who require daily climate data to drive ecological or hydrological models as well as other applications. The original files came in a netCDF format. Then these netCDF were reformat ted and imported in ArcGIS. http://inside.uidaho.edu/webapps/search/epscor_browse.aspx

Variables representing 1979-2011 included in the Idaho Geospatial dataset are: Precipitation (average monthly) , Precipitation(total monthly accumulations), Maximum Relative Humidity (average monthly) , Minimum Relative Humidity (average monthly), Specific Humidity (average monthly), Downwelling Short wave Radiation at Sur face (average monthly) , Wind Direction (average monthly), Minimum Temperature (average monthly), Maximum Temperature (average monthly) , Wind Speed (average monthly) .

NARCCAP (The North American Regional Climate Change Assessment Program)

NARCCAP is a joint international program that aims to produce climate change simulations in order to investigate uncertainties in regional scale projections of future climate and generate climate change scenarios. NARCCAP is a database that hosts climate change projections for North America. NACCAP dataset are generated by various GCMs (Global Climate Models) , from which, various climate change projections (scenarios) are derived. GCMs use grids of spatial resolution e.g., 300 km * 150 km grids. These GCMs are downscaled by various RCMs (Regional Climate Models) to spatial resolution of 50 * 50 km grids.

NARCCAP projections have been made for two 30-year time period using each GCM-RCM combination. These are: 1) Current time period of 1971-2000, usually known as the "baseline" projection, and is received by forcing the GCMs with historic CO2 emissions, till the year 2000. A perfect GCM-RCM combination should simulate a climate almost identical to the climate that was actually observed during the period of 1970-2000. 2) The future time period of 2041-2070 representing projections into the future under various assumptions for scenarios.

The NARCCAP climate variables are projected in a very high temporal resolution. For example, temperature, precipitation and surface pressure are all represented on a 3-hourly time scale. However, other variables such as minimum/maximum surface air temperature are represented on a daily scale (http://www. narccap.ucar.edu/data/data-tables.html).

The original data set comes in netCDF format. Ferret (from NOAA) and Cdat (from NCAR) were used to aggregate the data into the monthly scale. Some variables such as the monthly minimum temperature were derived from the NARCCAP daily data. Then these aggregate monthly scales were imported to ArcGIS.

Variables available in the NARCCAP dataset are: Sur face Air Temperature, Precipitation, Downwelling Shortwave Radiation at Surface, Surface Pressure, Specific Humidity, Minimum Surface Air Temperature, Maximum Surface Air Temperature. PINEMAP has derived the following: Number of Frost Days, Average Minimum Surface Air Temperature, Average Maximum Daily Sur face Air Temperature.

Tier 1 and 2 site-specific data from PINEMAP project have been included in TerraC. Those will be complemented by tier 3 site-specific data as soon as measurements become available.

4. Building of a TerraC User Community and Visualization of Carbon Data

TerraC has an intricate user structure (data/project owners, data contributors, and data users) [levels 1 to 3] that have different permissions to control/access data in the system. Users can come together in TerraC not only to share carbon and environmental data but also to collaborate. The system provides citation lists, where project owners can add citations to articles that have been published using the data in their project. The system also provides the ability to upload meta data and additional descriptions in form of PDF documents attached to each data table so that other users can fully understand project data. Graphing functions allow viewing and exploring data, which not only work in PC-based web browsers, but also on tablets and handheld portable devices.

Terra C is enhanced with a Google Earth apps that allows creating maps using global positioning system (GPS) points from client data to give a brief view of where the data is being collected. The idea is that users can use this tool to visualize their data and superimpose them onto other readily available aerial photographs and spatial maps.

1. Funds leveraged/new partnerships created

TerraC is now providing the data infrastructure for a $20 million integrated research, education, and extension project. This large-scale project funded by the United State Department of Agriculture (USDA) – National Institute of Food and Agriculture (NIFA) – Agriculture and Food Research Initiative (AFRI) Regional Project "PINEMAP: Integrating Research, Education and Extension for Enhancing Southern Pine Climate Change" (2011-2016) allows to populate TerraC and cross-fertilizes several research idea centered around carbon budgets and assessments, carbon change in dependence of global climate change and other stressors, and carbon sequestration and regulation as an ecosystem service. Many other similar synthesis projects are facilitated through TerraC-PINEMAP. Dr. Martin (co-PI of this FESC project) is the PI of the PINEMAP project and Dr. Grunwald (PI of this FESC project) is one of the 50+ co-PIs of the PINEMAP project. More information about PINEMAP can be found at: http://www.pinemap.org.

The PINEMAP project goals are to create, synthesize, and disseminate the necessary knowledge to enable southern forest landowners to:

- harness pine forest productivity to mitigate atmospheric carbon dioxide
- more efficiently utilize nitrogen and other fertilizer inputs
- adapt their forest management approaches to increase resilience in the face of changing climate.

PINEMAP has a multi-tier data structure representing different scales including:

- Tier 1 (historic measurements of tree response in dependence of treatments at about 700 locations across the southeastern U.S.)
- Tier 2 (new base measurements at hundreds of sites across the southeastern U.S.)
- Tier 3 (high-intensity measurements to capture water and carbon cycle at 4 sites)

The PINEMAP project has added almost 4GB of data which accounts for millions of rows for vegetation, climate, and atmospheric data. All of this data is being consumed by faculty, research staff, post-docs and students spread throughout the southeastern United States.

Concluding Remarks

All project goals and objectives of this project were met. We like to remark that this FESC-funded project was able to spawn a $20 million research, extension and education project, which is itself a big success. Carbon and climate related research is profoundly important and TerraC plays a major role in the southeastern U.S. to facilitate to make progress towards better understanding of the terrestrial carbon balance threatened by numerous human-made disturbances, including global climate and land use changes.

Publications

Peer-reviewed Publications:

Ross C.W., S. Grunwald, and D.B. Myers. 2013. Spatiotemporal modeling of soil carbon stocks across a subtropical region. Science of Total Environ. J. 461-462: 149-157.

Cao B., S. Grunwald and X. Xiong. 2012. Cross-regional digital soil carbon modeling in two contrasting soil-ecological regions in the U.S. *In* Minasny B.**,** B.P. Malone, and A.B. McBratney (eds.). CRC Press, Taylor and Francis, 2012. ISBN: 978-0-415-62155-7.

Xiong X., S. Grunwald, D.B. Myers, J. Kim, W.G. Harris and N.B. Comerford. 2012. Which soil, environmental and anthropogenic covariates for soil carbon models in Florida are needed? *In* Minasny B.**,** B.P. Malone, and A.B. McBratney (eds.). CRC Press, Taylor and Francis, 2012. ISBN: 978-0-415-62155-7.

Xiong X., S. Grunwald, D.B. Myers, J. Kim*, W.G. Harris and N.B. Comerford. 2012. Which soil, environmental and anthropogenic covariates for soil carbon models in Florida are needed? The 5th Global Workshop on Digital Soil Mapping 2012, Sydney, Australia, April 10-13, 2012.

Xiong X., S. Grunwald, D.B. Myers, J. Kim, W.G. Harris and N.B. Comerford. 20__. Optimal selection of predicting variables for soil carbon modeling in Florida, USA. Environ. Modeling and Software J. (in review).

Xiong X., S. Grunwald, D.B. Myers, J. Kim, W.G. Harris, N.B. Comerford, and N. Bliznyuk. 20__. Bayesian geostatistical modeling of soil organic carbon with uncertainty analysis across a highly heterogeneous landscape. Biogeoscience J. (in review)

Xiong X., S. Grunwald, D.B. Myers, W.G. Harris, and N.B. Comerford. 20__. Soil organic carbon stock change and its link to land use and land cover conversion and climate gradient. Science of Total Environ. J. (in review)

Patarasuk R., S. Grunwald, T.A. Martin and B. Hoover. 20__. Integrative modeling of tree response along geographic and ecological trajectories in the southeastern U.S. Ecological Modeling J. (in preparation).

Theses and Dissertations

Ross C.W. 2011. Spatiotemporal modeling of soil organic carbon across a subtropical region. M.S. thesis. University of Florida, Gainesville, FL.

Xiong X. 2013. Geospatial modeling of soil organic carbon and its uncertainty. Ph.D. dissertation. University of Florida, Gainesville, FL.

Presentations

Grunwald S. 2012. Soil carbon variability across large landscapes. Soil and Water Science Research Forum, Gainesville, FL, Sept. 7, 2012.

Grunwald S., B. Hoover, and R. Patarasuk. 2012. Terra C and Pinemap data resources. Webinar series Pinemap project. Gainesville, FL, July 13, 2012.

Grunwald S. 2011. Geospatial and spectral soil carbon modeling across large regions. NRCS, National Soil Survey Center (NSSC), Lincoln, NE, May 13, 2011.

Grunwald S., T. A. Martin, B. Hoover, G.M. Vasques, B. Zhong, and D.L. DePatie Jr. 2010. Terrestrial carbon (TerraC) information system. 2010 Florida Energy Systems Consortium (FESC) Summit, Orlando, FL, Sep. 27-29, 2010.

Grunwald S., T.A. Martin, G.M. Vasques and B. Hoover. 2009. Database infrastructure for integrative carbon science research. Florida Energy Systems Consortium Summit, Tampa, FL, Sept. 29-30, 2009.

Hoover B., S. Grunwald, T.A. Martin, G.M. Vasques, N.M. Knox, J. Kim, X. Xiong, P. Chaikaew, J. Adewopo, B. Cao and C.W. Ross. 2011. The Terrestrial Carbon (Terra C) Information System to facilitate carbon synthesis across heterogeneous landscapes No. 264-10. Symposia Spatial Predictions in Soils, Crops and Agro/Forest/Urban/Wetland Ecosystems, ASA-CSSA-SSSA Int. Meeting, San Antonio, TX, Oct. 16-19, 2011.

Hoover B., N.M. Knox, S. Grunwald, T.A. Martin, X. Xiong, P. Chaikaew, J. Kim, and B. Cao. 2011. Synthesis tools for carbon assessment in ecosystems. FESC Summit, University of Florida, Gainesville, FL, Sept 28-29, 2011.

Hoover B., G.M. Vasques, B. Zhong, S. Grunwald, T. A. Martin, and D.L. DePatieJr. 2010. The terrestrial carbon (TerraC) information system Vers. 1.0. 11th Annual Soil and Water Science Research Forum, Gainesville, FL, Sep. 10, 2010.

Xiong X., S. Grunwald, D.B. Myers, W.G. Harris, A. Stoppe and N.B. Comerford. 2011. Are soil carbon models transferable across distinct regions or scales in Florida? No. 262-8. Symposia Spatial Predictions in Soils, Crops and Agro/Forest/Urban/Wetland Ecosystems, ASA-CSSA-SSSA Int. Meeting, San Antonio, TX, Oct. 16-19, 2011.

Snapshot of the Terrestrial Carbon (TerraC) Information System website.

Project setup in TerraC.

Data setup in TerraC.

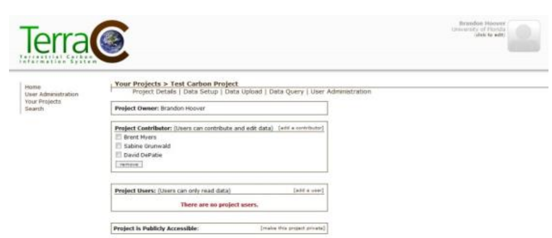

User administration tools.

Data query.

TerraC tutorials.

University of Florida

Development of Low-Cost CIGS Thin Film Hot Carrier Solar Cells (Final Report)

PI: Gijs Bosman **Co-PI:** Tim Anderson
Students: Yige Hu, PhD**.**

Description: PV has entered into a period of record growth. Most of the current production is based on crystalline Si technology. However, there are fundamental limits to the ultimate Si costs that may inhibit it from achieving the desired level of contribution to worldwide energy production. In contrast, thin-film PV technology can reach the desired outcome due to fast deposition rates and lower cost. Our study is focused on hot carrier solar cells for cell conversion efficiency improvement in a low cost, high throughput CIGS system. The rapid thermalizaton loss of hot photoexited carriers interacting with the lattice can potentially be reduced through phonon engineering in the absorber layer; the subsequent extraction of the hot carriers may be realized through device engineering of energy selective contacts.

Goals and Objectives

Efficiency improvement in a low cost, high throughput $CuIn_xGa_{1-x}Se_2$ (CIGS) system

Budget: $ 126,112.00 ($76.6K for this 12 month period)
Universities: UF

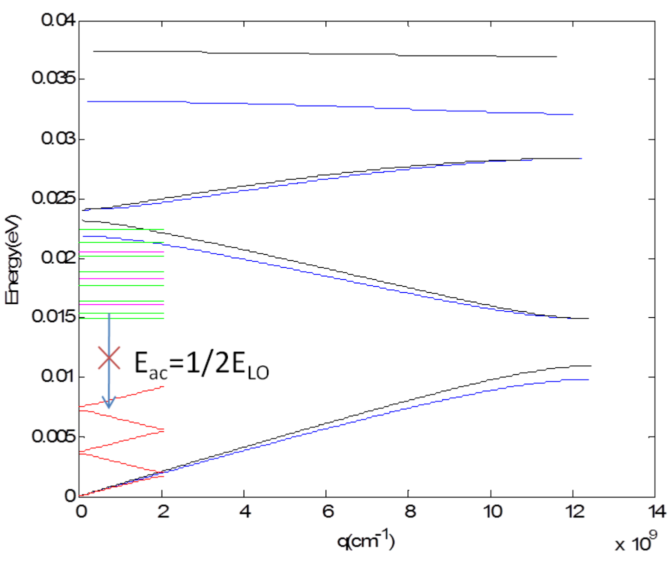

Figure 1. Phonon dispersion curve of CIGS bulk and SL structure. Black lines represent the CGS bulk phonon dispersion curve; blue lines represent the CIS bulk phonon dispersion curve; green, purple and red lines are the phonon dispersion curves for the SL structure of 1nm CIS with 2 nm CGS

Executive Summary

The research has been focused on hot carrier solar cells for cell conversion efficiency improvement in a low cost, high throughput $CuIn_xGa_{1-x}Se_2$ (CIGS) system.

The rapid thermalizaton loss of hot photo-exited charge carriers interacting with the lattice can potentially be reduced through phonon engineering in the absorber layer; the subsequent extraction of the hot carriers may be realized through device engineering of energy selective contacts. Simulations and modeling are presented for a novel hot carrier solar cell design with a superlattice structured absorber consisting of copper indium diselenide / copper gallium diselenide(CIS/CGS) and a quantum-well-structured energy selective contact of aluminum

nitride/gallium nitride(AlN/GaN). The phonon dispersion curve of a CIS/CGS absorber is shown in Figure 1. Mini phononic gaps appear in acoustic and optic phonon branches of a CIS/CGS superlattice structure. The mini gaps reduce the possibilities of optic phonons decaying to acoustic phonons, which propagate energy away as heat loss. The localized optic phonons transfer energy back to reheat the photo generated carriers. Therefore, the CIS/CGS superlattice structure provides a way to slow down the carrier cooling rate. The AlN/GaN contact provides confinement for hot carrier extraction. The electron transmission probability of an AlN/GaN/AlN DBQW contact is shown in the Figure 2. Carriers having energies outside the transmission band will be rejected to prevent scattering loss. Varying barrier and well thickness results in different resonant band locations for optimized collection.

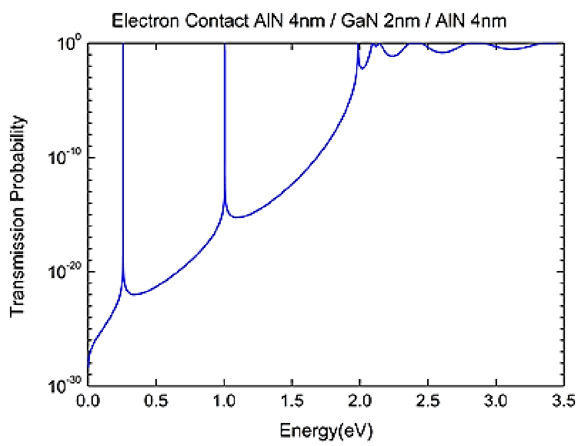

Figure 2. Transmission probability of an AlN double barrier quantum well electron contact with 4nm barrier and 2nm well.

Experiments were performed on a national renewable energy laboratory (NREL) conventional solar cell. The cell absorption spectrum has an upper limit of 375 nm, limited by the ZnO and CdS layers, and a lower limit of 1000 nm due to the CIGS absorber band gap cutoff. Four wavelengths, 395nm, 455nm, 633nm and 740nm are selected to represent the CIGS absorption range. The sample device is illuminated by LEDs at each wavelength under reverse external bias. The measured photocurrent is normalized to its value at zero bias to eliminate differences due to LED intensity variations as shown in Figure 3.

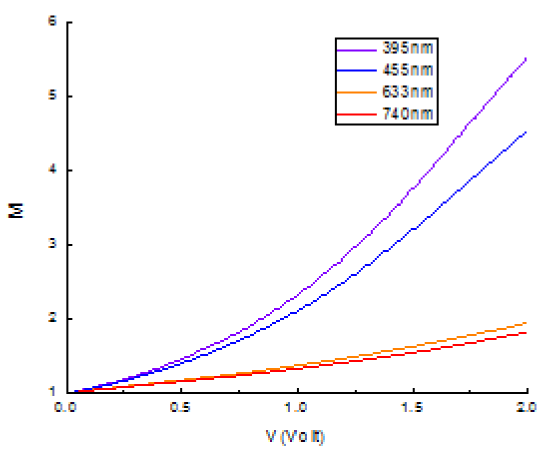

Figure 3. Normalized photocurrent M of the CIGS cell under 395nm, 455nm, 633nm and 740nm illumination, respectively, as a function of applied reverse bias.

In a thin film solar cell the photo current is expected to be a constant. However, the experimental curves increase with bias and are wavelength dependent. It is believed that the carrier temperatures play a role. Hot photo generated carriers with enough excess energy may impact ionize causing the current to increase under reverse bias.

The wavelength-dependent impact ionization rates are extracted from the current voltage measurements to reveal the existence of hot carriers in a conventional solar cell. The experimentally obtained ionization rates from current voltage measurements on the NREL solar cell are shown in Figure 4. Ionization rates increase with increasing maximum electric field E_m from the right to the left except for the extremely high and low field regions. For the short wavelengths of 395nm and 455nm, the ionization rates drop down when $1/E_m$ is below 6×10^{-6}cm/V. The reason is that the assumption of no hole multiplication may not be valid at extremely high fields [1]. For the long wavelengths of 633nm and 740nm, the impact ionization increase as $1/E_m$ is above from 8×10^{-6}cm/V. This artifact may be caused by an inaccurate multiplication factor determination at lower reverse bias.

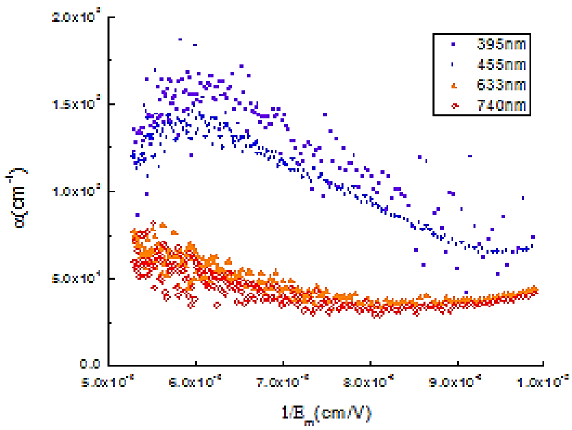

Figure 4 Impact ionization rates versus maximum electric field inverse for the CIGS cell.

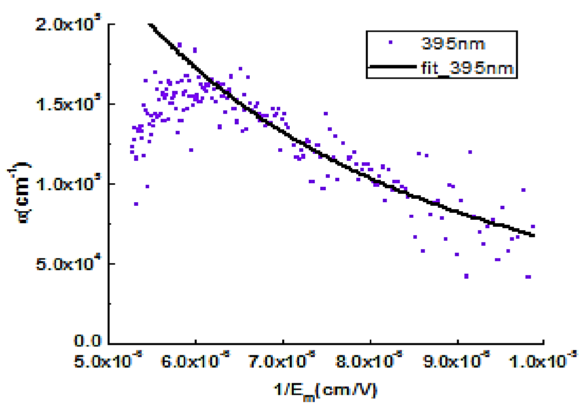

Figure 5 The ionization rates of 395nm illumination on the CIGS cell with the fitting function of λ and E_{av}.

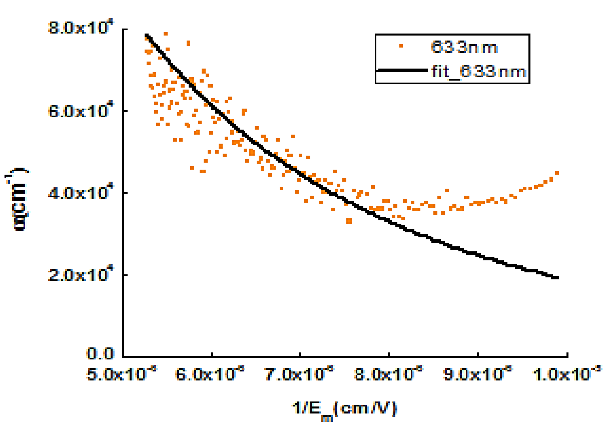

Figure 6. The ionization rates of 633nm illumination on the CIGS cell with the fitting function of λ and E_{av}.

The ionization rates for short wavelengths are in the order of 10^5/cm, which indicates an acceleration distance in the order of 100 nm for impact ionization to occur. Considering that the SCR is 100 to 200 nm long for the CIGS cell in the measured bias range, most short wavelength photogenerated carriers are expected to initiate impact ionization within the SCR even under low reverse bias. The ionization rates for long wavelengths are in the range of [3~8] $\times10^4$/cm, resulting in an acceleration distance of 125 to 300 nm. Impact ionization is not expected to take place at low bias, but at high reverse bias the electric field increases and the SCR expands, thus impact ionization is expected to occur. The observed ionization rate difference for short and long wavelengths is due to the respective differences in carrier temperatures. The higher the initial carrier energy, the lower the acceleration distance that is needed, corresponding to a higher α. A modified Shockley lucky electron model is developed to extract the initial carrier energies and the phonon mean free paths by applying the hot carrier concept to the traditional thin film CIGS cell design. In the conventional Shockley model, the kinetic energy gained from the field by accelerating over distance *l* to reach the threshold energy is given by $q\varepsilon l=E_{th}$, which allows the impact ionization rate α to be written in terms of the field: $\alpha=\frac{P_l}{l}=\frac{q\varepsilon}{E_{th}}e^{\frac{-E_{th}}{q\varepsilon\lambda}}$. The new model introduces a term for the initial energy of electrons as a result of a higher energy photon. The impact ionization threshold energy comes from the field acceleration and the initial kinetic hot carrier energy: $E_{th}=q\varepsilon l+E_{av}$, where E_{av} is the electron kinetic energy from high energy photons after a rapid initial loss:

$E_{av}=E_{photon}-E_g-E_{raploss}$. For the modification to include E_{av}, it is convenient to have a new term for the energy derived from the field, E'_{th}, that distinguishes from the real threshold energy, E_{th}: $E'_{th}=q\varepsilon l=E_{th}-E_{av}$. The ionization rate is modified as $\alpha=\frac{P_l}{l}=\frac{q\varepsilon}{E_{th}'}e^{\frac{-E_{th}'}{q\varepsilon\lambda}}$. The terms λ and E_{th}' are used as fitting parameters for the ionization rates at different wavelengths of the NREL cell. The fittings for 395nm and 633nm are shown in Figure 5 and 6 respectively. For short wavelength when $1/E_m$ is less than 6×10^{-6}cm/V, the fitting curve and the data diverge. It is currently unknown why the ionization rate data is independent of the field in this region. For long wavelength, the fitting curve is below the data when $1/E_m$ is above 8×10^{-6}cm/V. It might be again that the ionization rate data is inaccurate due to a distorted multiplication factor when the bias is close to zero. The initial electron energy, E_{av}, is extracted from the data by the difference of E_{th} in CIGS layer and E_{th}'.

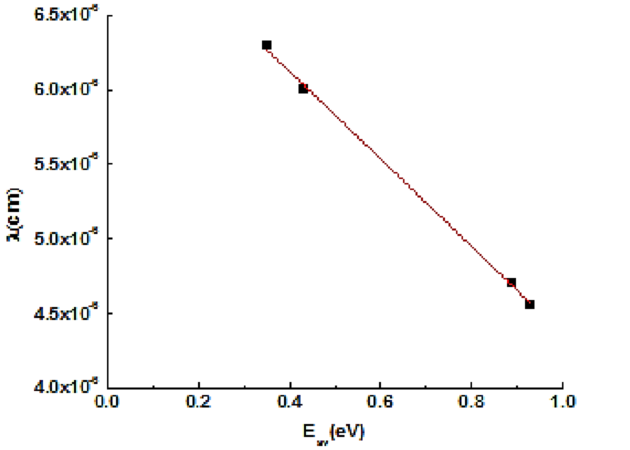

Figure 7. Phonon mean free path plotted versus the kinetic energy E_{av} after an initial rapid loss before phonon scatterings.

In Figure 7, λ is plotted against E_{av}, which reveals a linear relationship. As a general trend, the hotter an electron is, the more frequently it scatters (smaller λ). Based on the data analysis, the mean free path seems to decrease inversely proportional with increasing E_{av}. To confirm that the fitting result is reasonable, the obtained λ is compared with published data. The relaxation time of hot carriers is on the order of 0.1ps [2]. The mean free path of phonon scattering is then $0.1\text{ps}\times10^{7}\text{cm/s}=10^{-6}$cm. This number agrees well with the CIGS cell experiment results. Once the phonon mean free path is obtained, it can be used to calculate the energy of hot carriers reaching the cell contacts.

The wavelength dependent ionization rates suggest that the photo generated carriers do not lose all their energy above the band gap. Hot carriers may reach the top contact under operating forward bias. A conduction band barrier is proposed to utilize the hot carrier effect. A conduction band barrier is inserted between the CIGS layer and the n-ZnO layer to prevent thermal carriers in the ZnO layer from diffusing to cancel photo current while allowing the photo-generated hot carriers to pass through from the opposite direction. The barrier thickness, location and height need to be optimized to allow most photo-generated hot electrons to cross for collection while the detrimental diffusion is suppressed.

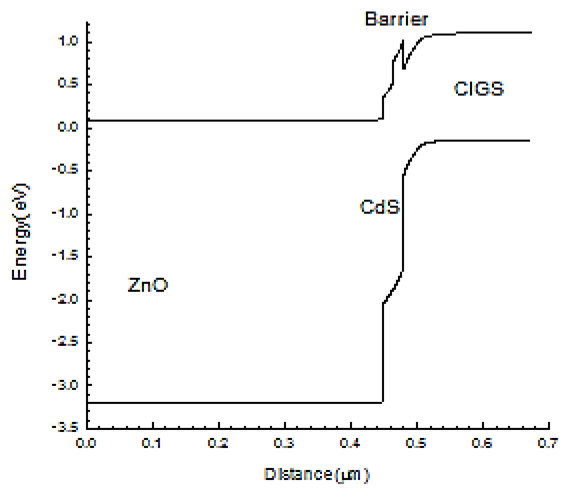

Figure 8. Band diagram of the proposed barrier structure.

A Medici model is constructed to simulate the way current under forward bias is affected by a barrier between the CdS and the CIGS layers. For simplicity, the barrier is assumed to have the same thickness and material properties as CdS, except for the higher conduction band offset and a change in band gap that keeps the valence band of the barrier and the CdS lined up. The conduction band offset is selected for the barrier relative to CdS in terms of kT, in our example as 10kT. The band diagram for the insert barrier structure is shown in Figure 8. The simulated current density voltage characteristics with illumination at wavelengths of 395nm for a 10kT barrier height and the curve without a barrier are shown in Figure 9. The open circuit voltage at 395nm increases for the barrier structure while the short circuit current density at 395nm stays constant. The added barrier between the CIGS and CdS layers improves the efficiency under short wavelength illumination.

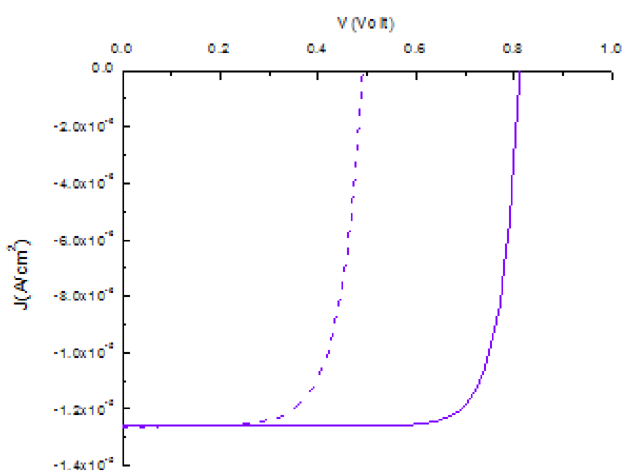

Figure 9. Medici simulated JV characteristic of the CIGS cell without barrier (dashed line) and with barrier (solid line) between the CdS and CIGS layers for a barrier height of 10kT at 395nm illumination.

The current density analysis of the entire solar spectrum is more complicated than the single wavelength analysis: hot electrons from different photons may or may not cross the barrier, depending on its energy height. Therefore, the barrier height should be optimized to limit most cold carrier diffusion while allowing maximum numbers of electrons generated from different wavelengths to pass through. A complete study of the optimized barrier height for the whole solar spectrum and barrier material should be done in the future.

References:

[1] R. D. Baertsch, “Noise and Multiplication Measurements in InSb Avalanche Photodiodes,” J. Appl. Phys., vol. 38, no. 11, pp. 4267–4274, 1967.

[2] C. Jacoboni and L. Reggiani, “The Monte Carlo method for the solution of charge transport in semiconductors with applications to covalent materials,” Rev. Mod. Phys., vol. 55, no. 3, pp. 645–705, Jul. 1983.

Results: The dynamics of hot carriers in a traditional device was studied. Current voltage characteristics of the conventional CIGS solar cell under different wavelength illuminations were measured at reverse bias, where a rapid increase of current with increasing reverse bias was observed which can be attributed to the impact ionization of hot carriers. The wavelength-dependent impact ionization rates were extracted from the current voltage measurements to reveal the existence of hot carriers in a conventional solar cell. A modified Shockley lucky electron model was developed to extract the ionization data. This process was then used to obtain the initial energies and the phonon mean free paths of the photo generated carriers under different wavelength illuminations.

The hot carrier effect was used to improve the solar cell efficiency by embedding a barrier in a traditional solar cell. The potential improvement was analyzed by simulating the corresponding open circuit voltage and short circuit current under a short wavelength illumination in Medici. The barrier embedded between the CdS and the CIGS layers showed an improved open circuit voltage.

University of Florida

Development of Novel Water Splitting Catalysts for the Production of Renewable Hydrogen

(Final Report)

PI: Helena Hagelin-Weaver
Students: Justin Dodson (Ph.D.)

Description: This project focuses on the development of iron-based catalysts for the thermochemical splitting of water into hydrogen and oxygen. The thermochemical process of splitting water is particularly well-suited for the utilization of solar energy to provide the heat for the reaction and is a way to produce a renewable hydrogen fuel. As hydrogen is difficult to transport and store, producing hydrogen on site for power plants using proton exchange membrane (PEM) fuel cells or internal combustion engines to generate electricity or for the production of chemicals, such as liquid hydrocarbon fuels, is a very attractive approach. The project uses a two-step process in which water is passed over a reduced iron oxide to generate hydrogen while the oxygen is taken up by the oxygen-deficient iron oxide (Step 1: $FeO_{x-1} + H_2O \rightarrow FeO_x + H_2$). In the second step the resulting iron oxide is heated to desorb oxygen and regenerate the oxygen-deficient iron oxide to close the catalytic cycle (Step 2: $FeO_x \rightarrow FeO_{x-1} + \frac{1}{2}O_2$). The main objectives of the project are to develop mixed metal oxide catalysts that 1) will release oxygen at temperatures lower than 1500°C (Step 2), while still maintaining water-splitting activity (Step 1) and 2) are stable up to the temperature necessary for the oxygen desorption step.

Budget: $ 100,000
Universities: UF

Summary
A reactor system for the thermochemical splitting of water was designed and built as part of this project. Two types of catalysts were evaluated in this reactor system, iron oxide supported on nanoparticle zirconia (FeO_x/n-ZrO_x) and iron oxide supported on yttria-stabilized (8 mol%) zirconia (FeO_x/8-YSZ). In addition to the two supports, the effect of iron loading was also investigated between 10 % and 20 % of iron by weight. The two zirconia supports yield very different results. The iron supported on the 8-YSZ gives a higher initial hydrogen yield per cycle, but the decrease in yield with increasing cycle number is higher for this catalyst compared with the FeO_x/n-ZrO_x catalyst. The FeO_x/n-ZrO_x with a 10 wt% iron loading exhibited the most stable hydrogen yield during the ten cycles. At iron loadings of 20 wt% a significant deactivation is observed with increasing number of cycles. Apparently, this loading is too high for sufficient stabilization from the zirconia support. Initial results on a 15 wt% FeO_x/n-ZrO_x catalyst are very promising, and this catalyst is currently under investigation.

Goals and Objectives

The goals of this project were two-fold; 1) develop catalytic materials that are stable up to temperatures of 1500°C and have reasonable catalytic activity for more than one cycle and 2) develop mixed metal oxide combinations that will release oxygen at temperatures lower than 1500°C (Step 2), while still maintaining water-splitting activity (Step 1). Iron oxide was chosen as the metal oxide since iron has several stable oxidation states and has been shown to have water-splitting activity, i.e. can remove oxygen from water and release hydrogen.

Our approach also involved using nanoparticle oxides of ZrO_2 as supports for the iron oxide. This is a novel approach since nanoparticles are normally not considered as supports for this reaction due to the high reaction temperatures. However, using nanoparticle oxide supports has significant potential as they could form mixed metal oxides with the iron and positively influence the catalytic activities.

Project Results

This project focused on the development of novel iron-based catalysts for the two-step thermochemical splitting of water into hydrogen and oxygen. The thermochemical process of splitting water is particularly well-suited for the utilization of solar energy to provide the heat for the reaction and is a way to produce a renewable hydrogen fuel. As hydrogen is difficult to transport and store, producing hydrogen on site for power plants using either proton exchange membrane (PEM) fuel cells or internal combustion engines to generate electricity or for the production of chemicals, such as liquid hydrocarbon fuels, is a very attractive approach. In this project, a two-step thermochemical process was used in which water is passed over a reduced iron oxide to generate hydrogen while the oxygen is taken up by the oxygen-deficient iron oxide (Equation 1). In the second step the resulting iron oxide is heated to desorb oxygen and regenerate the oxygen-deficient iron oxide to close the catalytic cycle (Equation 2). The main objectives of the project were to develop metal oxide catalysts that I) will release oxygen at temperatures lower than 1500°C (Equation 2), while still maintaining water-splitting activity (Equation 1) and II) are stable up to the temperature necessary for the oxygen desorption step.

$$FeO_{x-1} + H_2O \rightarrow FeO_x + H_2 \qquad \text{Equation 1}$$

$$FeO_x \xrightarrow{\Delta} FeO_{x-1} + \tfrac{1}{2}O_2 \qquad \text{Equation 2}$$

Reactor System. As part of the proposed research, a bench scale reactor system was designed, constructed and calibrated to evaluate the various catalysts for activity in the water-splitting reaction. The system design is shown in Figure 1 below, and a picture of the completed system is presented in Figure 2.

The reactor system is configured to run both thermal reduction (Equation 2) and water splitting (Equation 1) sequentially. In the first step, the catalyst is heated in a flow of argon until the oxygen desorbs and the oxygen-deficient iron oxide is generated. This step is done at a maximum temperature of 1500 °C. When no more oxygen is generated, the reactor is switched to water-splitting mode and the temperature decreased to 1000 °C. Water is pumped into the evaporator to generate steam, which is brought to the

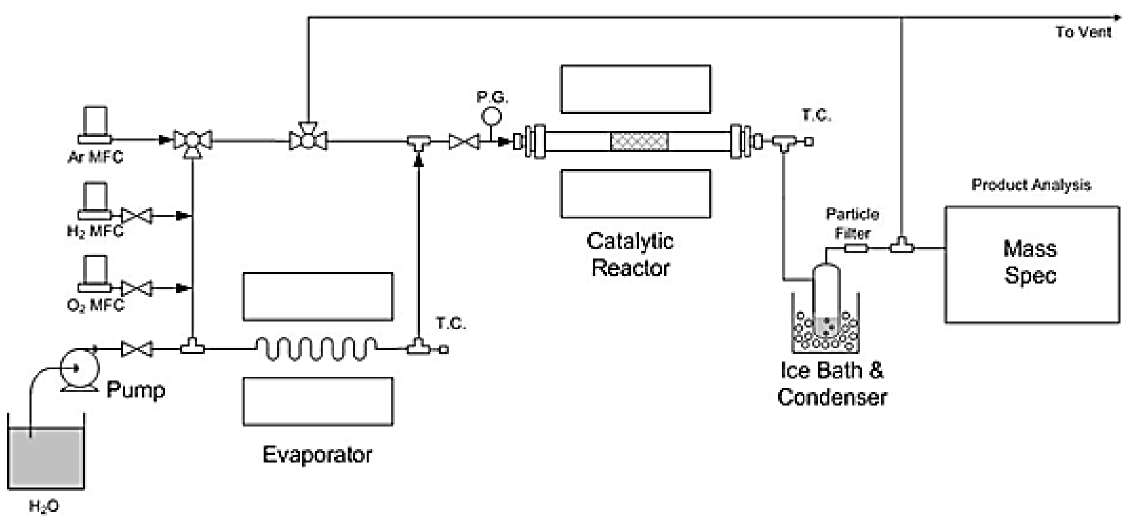

Figure 1. Flow diagram of the bench scale water-splitting reactor system.

reactor using argon as the carrier gas. The steam is then decomposed over the oxygen-deficient iron oxide at 1000 °C to produce hydrogen and iron oxide. When no more hydrogen is generated, the reactor is switched back to thermal reduction mode and heated in a flow of argon to 1500 °C again to regenerate the active iron oxide species. In both steps the product gas composition is measured continuously using a mass spectrometer which is attached to the outlet of the reactor system (after the condenser to remove unreacted water). These cycles are repeated six to ten times to determine the stability of the catalysts.

The oxygen and hydrogen mass flow controllers (MFCs) in Figure 1 were used to calibrate the mass spectrometer and allow quantification of the hydrogen and oxygen in the product stream during the reaction runs.

Figure 2. Completed bench scale water-splitting reactor system.

Catalyst Preparation and Evaluation. Two different iron oxide catalysts, with varying iron loading, were synthesized and tested for activity and stability in the thermochemical splitting of water. More specifically, the iron oxide was precipitated onto two commercial zirconia supports, a nanoparticle ZrO_2 (n-ZrO_2) and an yttria-stabilized zirconia with 8 mol% of yttria (8-YSZ), since zirconia is known as a high temperature ceramic. The precipitation was done by slowly adding a sodium hydroxide solution to a dispersion containing the support (either n-ZrO_2 or YSZ) and an aqueous solution of iron nitrate. The catalyst was then recovered by filtration and dried over night at 105 °C, before being heat-treated at 800 °C to decompose the iron hydroxide and form iron oxide (Fe_2O_3) on the surface of the catalysts. Before reaction, these catalysts were first thermally activated by heating to 1500 °C to generate the oxygen-deficient iron oxide, the active component in the water decomposition step. During the activation the Fe_2O_3 on the ZrO_2 is reduced to FeO (or a mixture of Fe_3O_4 and FeO), and some particle growth occurs due to the high temperatures. The oxygen evolution was monitored during this step to make sure that the reduction was complete (i.e. no more oxygen desorbed from the catalyst) before the water-splitting step. Once the catalyst had been activated, the temperature was decreased to 1000 °C and water (steam) was introduced and the hydrogen evolution monitored (Figure 3). In this step the FeO is reoxidized to Fe_3O_4 (Equation 1). Fe_2O_3, which was present on the fresh catalyst before activation, will not form under these conditions. When no more hydrogen evolved from the catalyst, the temperature was once again increased to 1500 °C to reduce the Fe_3O_4 back to FeO (Figure 4). These steps, water splitting and thermal reduction, were repeated at least six times, as it takes a few cycles to reach a stable productivity (Figures 3 and 4).

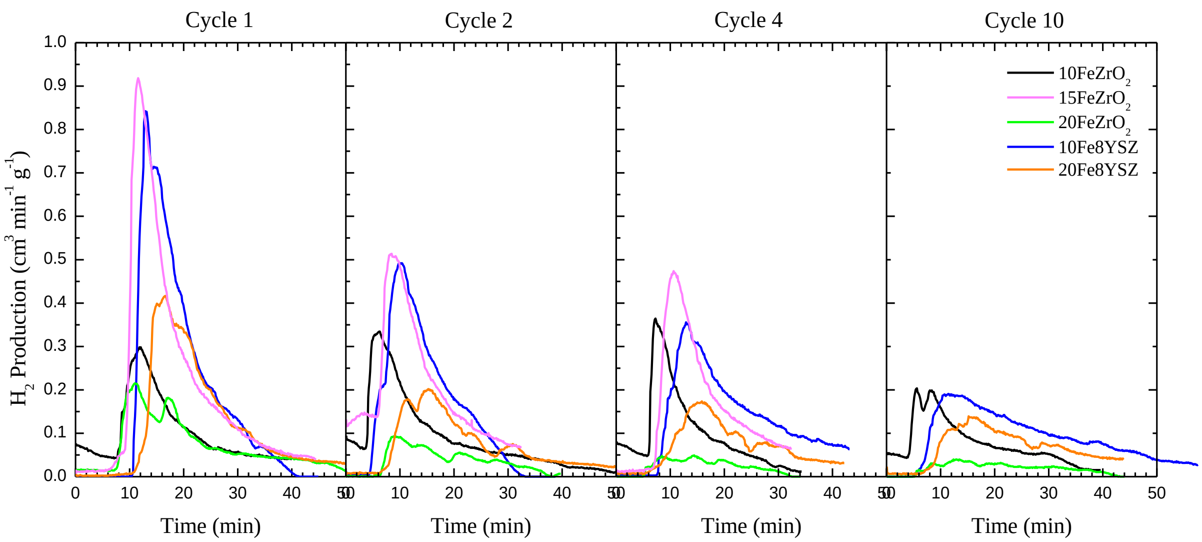

Figure 3. Hydrogen production step for cycles 1, 2, 3 and 10. ——— 10wt% FeOx/n-ZrO2, ——— 15wt% FeOx/n-ZrO2, ——— 20wt% FeOx/n-ZrO2, ——— 10wt% FeOx/8-YSZ, ——— 20wt% FeOx/8-YSZ.

As is evident in Figure 3, the first step generates the most hydrogen. This reveals that the catalyst is not stable after the activation step, and that further particle growth likely occurs during the second thermal reduction. The result of iron oxide particle growth is that a smaller fraction of the iron is available for reaction, i.e. a smaller fraction of the Fe_3O_4 is reduced during the thermal reduction and less FeO is then available for reaction with water. However, after the first cycle the subsequent cycles give more consistent hydrogen evolutions. This is true for all catalysts, except those with an iron content of 20 wt%. The hydrogen evolution obtained from the 20-FeO_x/ZrO_2 catalyst continues to decline with increasing number of cycles (Figure 3). This is clearly due to the fact that a smaller fraction of iron is being reduced in each cycle (Figure 4).

The same is true for the 20-FeO_x/YSZ catalyst, although the trend is not as severe as for the 20-FeO_x/ZrO_2 catalyst. The highest hydrogen production is obtained over the 15 wt% FeO_x/ZrO_2 and the 10 wt% FeO_x/YSZ catalysts. The results indicate that there is an optimal iron loading on these catalysts. At low iron loadings the reaction is limited by the amount of iron present at the surface, while at higher loadings the iron is not sufficiently stabilized by the support and severe sintering occurs (see characterization section below), which reduces the available iron oxide. Comparing the iron catalysts supported on n-ZrO_2 to those supported on yttria-stabilized ZrO_2 indicates that the FeO_x/ZrO_2 catalyst is more stable than the FeO_x/YSZ catalyst, as the hydrogen evolution is more consistent over the FeO_x/ZrO_2 catalyst through ten cycles. Thus, while more hydrogen is generated during the first cycles over the FeO_x/YSZ catalyst, after ten cycles the hydrogen production is very similar over the FeO_x/YSZ and FeO_x/ZrO_2 catalysts. Since the 10-FeO_x/ZrO_2 catalyst exhibited a very stable hydrogen evolution, while the 20-FeO_x/ZrO_2 catalyst showed significant deactivation even after a few cycles, a catalyst with a 15 wt% iron loading was added to the study. As is evident in both Figures 3 and 4, this catalyst shows significant promise as it has a high and stable hydrogen production, together with a stable thermal regeneration step (oxygen evolution) through four cycles.

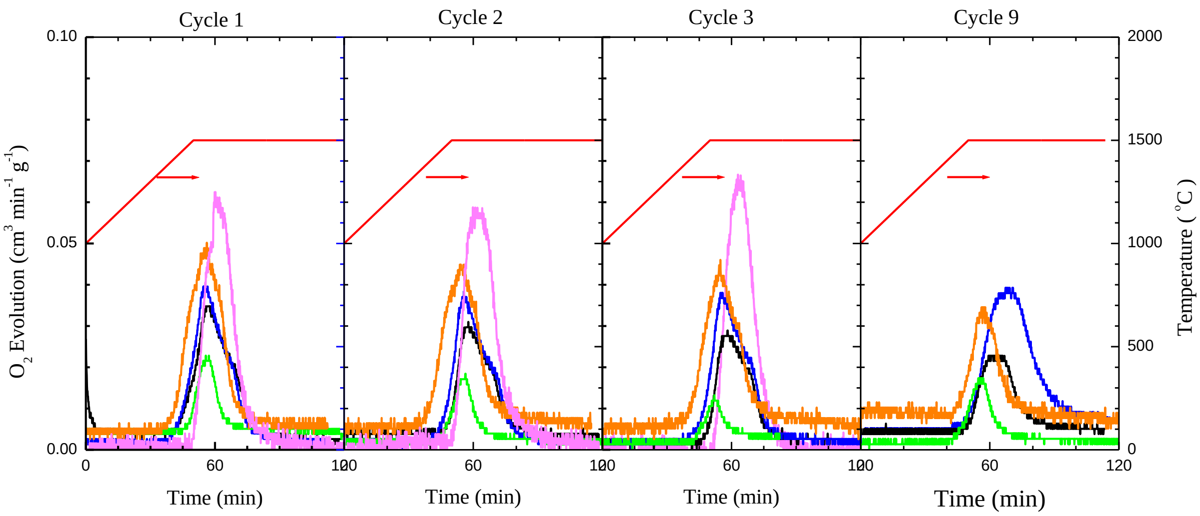

Figure 4. Thermal reduction step for cycles 1, 2, 3 and 9. 10wt% FeOx/n-ZrO2, 15wt% FeOx/n-ZrO2, 20wt% FeOx/n-ZrO2, 10wt% FeOx/8-YSZ, 20wt% FeOx/8-YSZ.

Catalyst Characterization. The fresh and spent catalysts were subjected to a number of catalyst characterization techniques, such as Brunauer-Emmett-Teller (BET) surface area analysis, x-ray diffraction (XRD) measurements, and scanning electron microscopy (SEM) studies, to determine how the properties of the catalysts are altered during reaction. These measurements will help in determining the reasons for decreases in activity, and can identify important catalytic properties. Some sintering (particle growth) is observed on all of these catalysts. However, sintering at temperatures of 1500 °C can be very severe and lead to complete activity loss due to particle growth which results in a single sintered block of material. Most of the catalysts in this study were still in powder form after the ten consecutive cycles of water decomposition and thermal regeneration (Figure 5).

Figure 5. Spent FeOx/n-ZrO2 catalyst after 10 cycles.

The BET surface areas for fresh and spent catalysts are presented in Table 1. The fresh catalysts all have surface areas of approximately 10 m^2/g. Evidently, the catalysts with an iron loading of 20% have lower surface areas (6-8 m^2/g) compared with the 10 wt% Fe catalysts (10-12 m^2/g), which indicates that the added iron block some of the pores in the support. The surface areas of the catalysts after reaction are an order of magnitude lower than before reaction. A lower surface area is expected due to sintering at the high temperatures of reaction. However, the data reveal that the catalysts are not completely destroyed during reaction.

Table 1. BET specific surface area measurements for select catalysts before (fresh) and after (spent) ten reaction cycles.

Catalyst	Fresh (m^2/g)	Spent (m^2/g)
10-Fe/n-ZrO_2	10.0	1.6
20-Fe/n-ZrO_2	7.8	0.7
10-Fe/8-YSZ	12.2	1.5
20-Fe/8-YSZ	6.3	0.79

The surface area is an important catalyst property, as it gives an indication of the surface area available for reaction. The smaller surface area of the 20 wt% Fe catalysts is consistent with the lower activity of these catalysts compared with the 10 wt% Fe catalysts. However, the differences in fresh (or spent) surface areas between the 10-Fe/n-ZrO_2 and 10-Fe/8-YSZ cannot explain the differences in behavior of these catalysts. Thus properties other than the BET surface area are also important.

The catalysts were subjected to XRD measurements, and the XRD patterns are shown in Figure 6. The XRD spectra clearly reveal that the crystal phase of ZrO_2 is different in the n-ZrO_2 and the YSZ. The nanoparticle ZrO_2 is monoclinic, while the yttria-stabilized zirconia is cubic (Figure 6). As expected the iron is present as Fe_2O_3 on the fresh catalysts, and the particle size is smaller on the catalysts with a 10 wt% iron loading compared to those with a 20 wt% iron loading. The larger size of the particles is evident in the XRD patterns as peaks with higher peak intensities. The XRD data reveal that the catalysts supported on YSZ behave differently from those supported on the nanoparticles ZrO_2. The peaks due to the monoclinic ZrO_2 are not significantly affected by exposure to the reaction conditions during the ten cycles. In contrast, significant particle growth is observed for the YSZ support (as is evident in cubic zirconia peaks with a higher intensity after reaction). The iron on the FeO_x-ZrO_2 catalysts is reduced to Fe_3O_4 after the water-splitting step, while no features due to iron oxide is detected in the XRD pattern obtained from the FeO_x/8-YSZ after the reaction cycles. This indicates that the iron oxide is incorporated into the lattice of the YSZ, which has been observed previously.[1] The increase in particle size of the YSZ

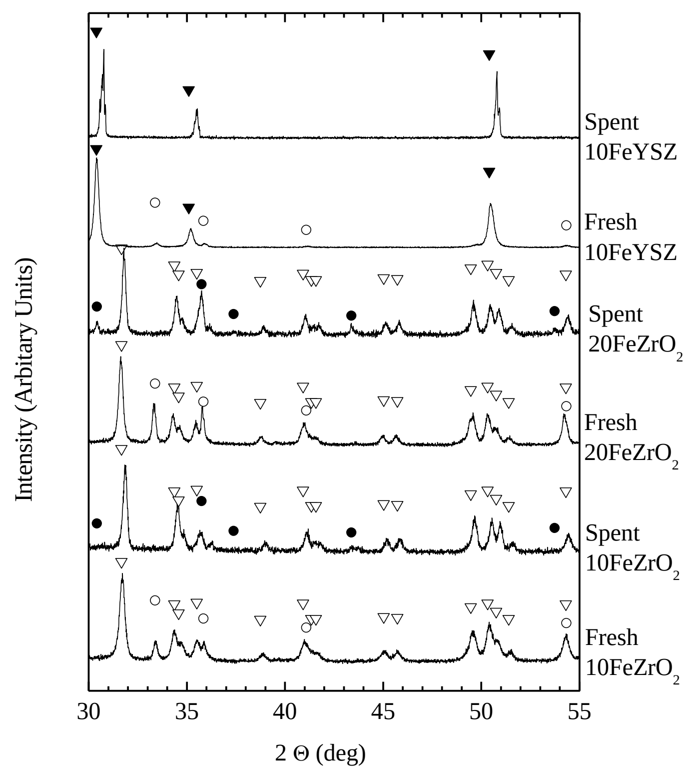

Figure 6. XRD spectra obtained from iron oxide precipitated on n-ZrO_2 and 8-YSZ. ▽ ZrO_2 (monoclinic), ▼ YSZ (cubic), ○ Fe_2O_3, ● Fe_3O_4.

[1] N. Gokon, T. Hasegawa, S. Takahashi, T. Kodama, "Thermochemical two-step water-splitting for hydrogen production using Fe-YSZ particles and a ceramic foam device," Energy 33 (2008) 1407-1416.

support may explain why this catalyst is not stable and exhibit a continuous decline in the hydrogen production with increasing reaction cycles.

SEM images were also obtained from fresh and spent FeO_x/ZrO_2 and FeO_x/8-YSZ catalysts with a 10 wt% iron loading (Figures 7). The particle growth due to sintering is evident for both catalysts when comparing the fresh and spent catalysts. The fresh catalysts contain significantly smaller particles on the surface compared with the spent catalysts. The difference between the nanoparticle ZrO_2 and the YSZ support is also evident in the SEM images. Consistent with the BET and XRD data, the FeO_x/8-YSZ catalyst exhibit a more significant particle size increase compared with the FeO_x/ZrO_2 catalyst. The energy dispersive spectroscopy (EDS) line scans and mapping confirm the presence of iron, oxygen, zirconium, and yttrium (for the YSZ support) on the surface with iron present across large portions of the surfaces for both catalysts. EDS confirms that after the reaction cycles YSZ and zirconia are now predominantly found on the catalysts surfaces but iron can be identified by differences in geometries between the catalyst support and the iron (Figure 8).

a) b) c) d)

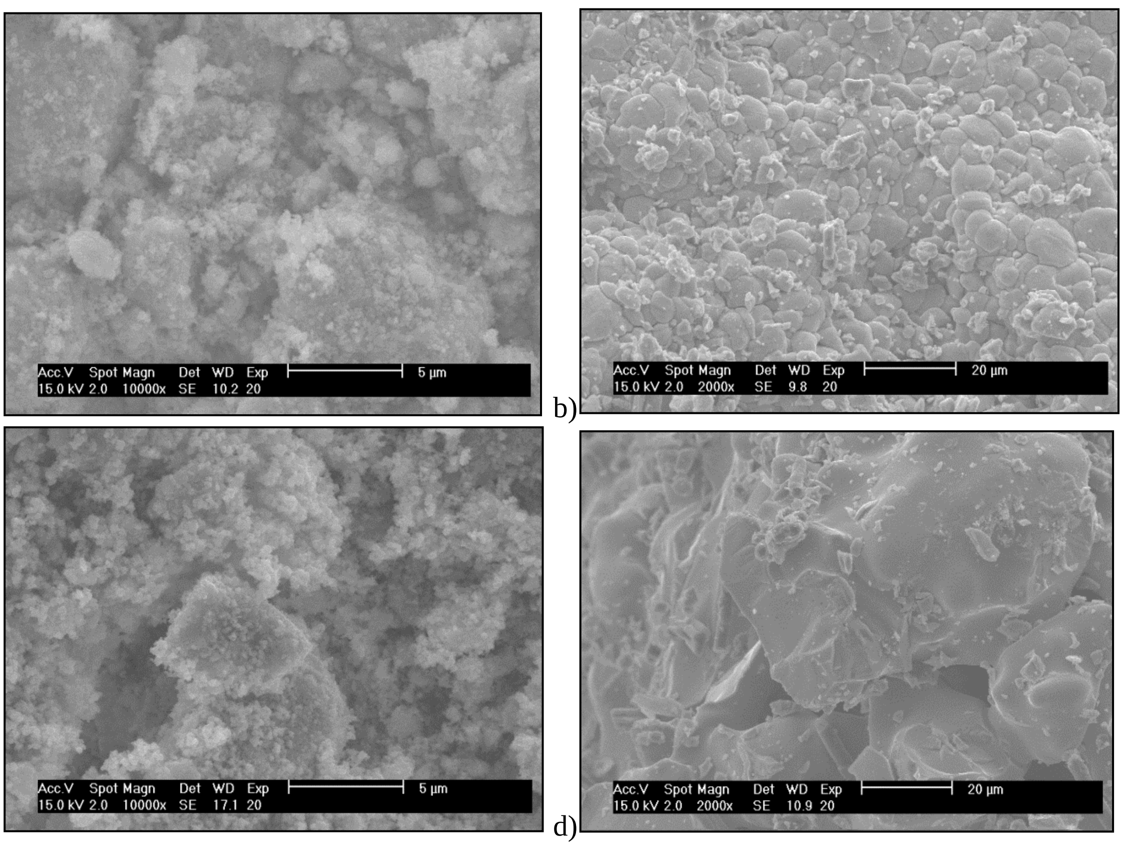

Figure 7. SEM images of fresh (a) and spent (b) 10wt% FeOx/n-ZrO2 and fresh (c) and spent (d) 10wt% FeO_x/8-YSZ.

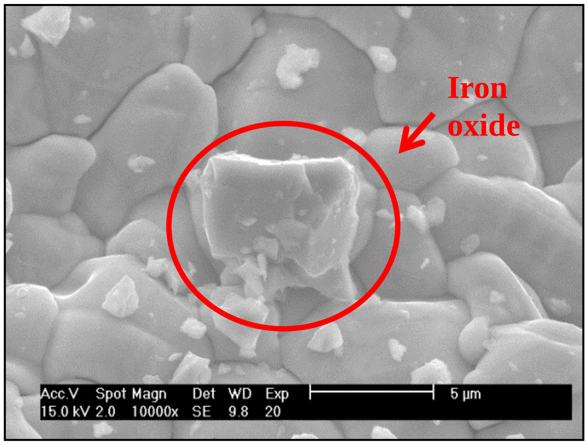

Figure 8. SEM image obtained from spent 10wt% FeO_x/ n-ZrO_2. An EDS line scan was done over this section of catalyst to identify the iron oxide particle shown in the figure.

Concluding Remarks

The iron oxide supported on zirconia is a promising catalyst combination for the thermochemical splitting of water. Future research will look into the addition of other components and other catalyst preparation methods to determine the factors of importance for stable and active catalysts under the thermochemical water splitting conditions.

University of Florida

UFTR Digital Control System Upgrade for Education and Training of Engineers and Operators

(Progress Report)

(Project was initiated by Dr. Aliriza Haghighat. Dr. Haghighat left the University of Florida. The project was transferred to Dr. Kelly Jordan. FESC provided an additional $45K as equipment support towards the completion of the project. The new project title is **"Equipment Support for the University of Florida Training Reactor Digital**")

PI: Kelly Jordan
Students: Geoffrey Bickford, MS; Robert Beard, MS; Raymond Fortin, MS.; Ryan Kelley, Ph.D.

Original Project Description: The goal of this project is to contribute to a major initiative on design, licensing and construction of a fully digital control system for the University of Florida Training Reactor (UFTR). This makes the UFTR the first operating nuclear power plant in the United States that uses a fully digital control system. This facility will provide for the training and education of the necessary workforce in the area of digital control and instrumentation for nuclear reactors. With this effort, a new focus/certificate on digital control and instrumentation will be developed at the Nuclear and Radiological Engineering (NRE) Department. Further, the UFTR facility will offer training courses for community colleges (Central Florida, Indian River, and Jacksonville) in the State of Florida, personnel from nuclear utilities and government agencies including the Nuclear Regulatory Commission (NRC). The project has already received significant funding from industry and government in form of grants, contracts, equipment/systems, and engineers' time.

Budget: $308,000 + additional new funding of $45,000
Universities: UF
External Collaborators: Indian River State College, Florida International University, Florida Power and Light, Duke Energy

Summary of Annual Progress

As nuclear power plants age, analog safety instrumentation obsolesces and becomes difficult to maintain. Adoption of advanced digital instrumentation and control (I&C) technologies in the nuclear sector has significantly lagged that of other industries. Utilities have been slow to implement these systems due to regulatory licensing uncertainty and a lack of internal expertise with new systems. As the previous generation of the nuclear workforce retires, the pool of available expertise in analog technology declines. The experience at Japan's Fukushima Power Station shows the need to continually modernize and augment reactor safety and operational systems.

The UFTR has undertaken an ambitious project to replace its 50-year old analog I&C systems with new, modern digital systems. Once modified, the facility will provide training and education for the future workforce as well as a demonstration platform in the area of advanced digital I&C for nuclear reactors. This effort ushers in a new focus on advanced digital I&C research, development, and testing, and greatly augments the existing Nuclear Engineering Program at UF. Further, the UFTR facility will offer training courses for other educational institutions in the state, such as Indian River State College, who provide the majority of nuclear technician education in Florida, as well as training for personnel from nuclear utilities and government agencies, including the Nuclear Regulatory Commission.

As part of the digital controls upgrade project, the UFTR has completed several major upgrades this year, including an NNSA-funded security system ($460k), a renovated HVAC system ($250k), a new stack exhaust monitor and high plume exhaust system funded by DOE ($212k).

FESC funding is being used to design, purchase, and install new control blade drive systems for the UFTR. We are working on a design with ITG in Jacksonville, using Siemens servo actuators and gear reduction boxes. The large gear reduction ration of 28000:1 (3600 rpm down to 0.125 rpm) presents a design challenge. We will have a design complete by December 2013 and ready for manufacture.

Two new partnerships have been formed in this reporting period: an industrial training partnership and international research collaboration. A new partnership has been formed for nuclear training with FIU and IRSN as primary educational partners. The UFTR has linked up with the $3M-funded Regional Center for Nuclear Education and Training hosted at IRSN and Florida Power and Light / NextEra to develop an enhanced program for training of non-nuclear engineers in the nuclear industry.
The UFTR is also partnering with the Swiss Federal Institute of Technology, Lausanne (EPFL) and the CROCUS reactor to develop new methods for characterizing safety performance of research reactors. This collaboration has a financial commitment of $300k from EPFL to aquire new graduate students and postdoctoral scientists to work with UF in this area.

Funds leveraged/new partnerships created

UFTR – IRSN – FPL Workforce Development Partnership

Formed a partnership with Indian River State College and Florida Power and Light on NUCLEAR WORKFORCE DEVELOPMENT To ensure growth and sustainability of Florida's nuclear energy industry, there is a need to enhance Florida's nuclear careers. Training next generation nuclear workforce will provide the skillset needed to expand industry in the state of Florida, engagement at all levels of education (including the graduation of new engineers, technicians and outreach to K-12). Collaboration of Florida academic institutions and industrial partners is paramount to success. Both organizations have appointed representatives to the UFTR advisory board and committed funds for acquiring a nuclear plant simulator, should federal funding also become available.

UFTR – EPFL Research Reactor Safety Collaboration

The principal aim of the project is, in collaboration with the University of Florida and the University of Florida Training Reactor (UFTR) facility, to develop and validate a detailed coupled multiphysics models of the zero-power CROCUS reactor at EPFL and the UFTR, for the comprehensive analysis of the reactor behavior under transient (neutronic or thermal-hydraulic induced) conditions.

These two reactors differ significantly in the core design and thermal power output, but share unique heat transfer and flow characteristics (single-phase laminar flow in complex geometries with the possibility of mechancially entrained air bubbles). Validation experiments will be design to expand the validation domain of these existing models and computational codes and techniques. In this process, emphasis will be put to validate the coupled models developed and get confidence in their applicability for safety analysis.

EPFL will be principally responsible for the design and implementation of transient experiments to generate a database of reactor parameters, i.e. flow distribution, power profile and power evolution to be used to validate against code predictions. UF will focus on the generation of the coupled neutron kinetics and thermal-hydraulic models, including implementation of a TRACE/PARCS reactor simulator model, a

PARET model, and development of full-field computational fluid dynamics models (using OpenFOAM) for refined thermalhydraulics physics treatments. In this subtask of the project, the aim is to verify by means of CFD the validity of TRACE predictions for atmospheric pressure water flow.

The work in this project will serve as a basis to develop two Ph.D.s, one at each University. The scientific understanding of these multiphysics domains will be expanded and the validation base of commonly-used calculation methods will be expanded to cover a new range of research reactor types. From a practical perspective, CROCUS and the UFTR will have fully validated reactor dynamic and transient models for accident analysis. With these validated models, both facilities will have improved capabilities and flexibility for extended operations. CROCUS and the UFTR will be able to make future reactor modifications with reduced regulatory resistance. A feasibility analysis of future power uprates at these facilities will also result.

University of Florida

Unifying Home Asset & Operational Ratings: Adaptive Management via Open Data & Participation

(Progress Report)

PI: Mark Hostetler **Co-PI:** Hal S. Knowles, III
Student: Hal S. Knowles, III (Ph.D. Student, UF School of Natural Resources & Environment)

Description: Recent environmental, social, and economic challenges are fostering a wave of interest in maximizing energy efficiency and conservation (EE+C) in existing U.S. homes. Long standing programs, ratings, and metrics are being reapplied into new stimulus initiatives such as the *Recovery through Retrofit*[2] program. Simultaneously, electric and gas utilities are expanding their demand side management (DSM) programs from weatherization and conventional technology replacement incentives to include conservation behavior campaigns with "recommendation algorithms" designed to assist in homeowner energy retrofit decision making. Furthermore, loan programs are emerging to address the financial barriers that commonly limit initiation of the necessary retrofits.

Collectively, these approaches most often project future home energy performance based on engineering models of the physical characteristics of homes (i.e., "asset ratings"). Yet to date, the marketplace is inadequately integrating historical household energy consumption patterns (i.e., "operational ratings") into the decision tree to optimize retrofit program efficacy and consumer benefits. Moving toward the unification of asset and operational ratings is crucial for successful program management, proper monitoring/measurement/verification (MMV), loan risk assessment, and for the persistence of reduced home energy use over time. However, unification will not be easy. This research project combines qualitative and quantitative research methods in social science and building science using Florida case studies to evaluate the opportunities and constraints of asset and operational rating unification and the steps necessary to get there. Relationships between our project and the collaborative, transparent, and participatory nature of "open government" initiatives are also being explored.

Budget: $24,000 over two years ($12,000 from 01/01/2011 to 12/31/2011 and $12,000 from 01/01/2012 to 12/31/2012)
Universities: UF
External Collaborators: Nick Taylor (Ph.D. Student, UF School of Natural Resources & Environment), Jennison Kipp (Assistant In, UF Program for Resource Efficient Communities)

Progress Summary
Summary of Progress since April 15, 2013

Collaboration with both Talgov Utility Billing Services Division and JEA in Jacksonville is underway. Some preliminary data has been exchanged (e.g., energy conservation and demand side management participation records) and Hal Knowles has begun to clean and consolidate the data in order to generate a treatment group from these conservation programs and to generate a control group from stratified random samples across both utility service territories. As previously reported, we anticipate a few hundred homes with the highest resolution 15-minute or hourly interval smart meter billing data. However, we also anticipate a much larger sample of approximately 2,500 to 5,000 homes with daily interval smart meter billing data from both utilities. After evaluating the R statistical software, Hal Knowles has determined

[2] See, http://www.whitehouse.gov/assets/documents/Recovery_Through_Retrofit_Final_Report.pdf

that MATLAB is a better fit for the project research and analysis needs. Project methodology is being adjusted as appropriate to work within the MATLAB statistical software. Plans are to analyze these large data sets of home energy consumption to detect how homes follow weather patterns and respond to weatherization efforts.

Funds Leveraged/New Partnerships Created

New collaborations		
Partner name	Title or short description of the collaboration	Funding, if applicable
Djundi Tjindra	UF/PREC is providing intellectual, data sharing, and logistical support for a related master's thesis and Djundi is providing new insights and visualizations into residential energy consumption in relation to residential density and urban development pattern	Not applicable
FAIRWINDS Credit Union	As seeded by the Osceola Energy Initiative (OEI), an ARRA funded program, UF/PREC has entered a 10-year partnership with FAIRWINDS Credit Union to administer a 7-county, $5 million residential energy efficiency finance program.	Tied to revenue from the delivery of the loan program
Several Building Contractors	UF/PREC is currently building partnerships with building professionals to serve as "Participating Independent Contractors" in the loan program.	Tied to revenue from the delivery of the loan program

Proposal #1						
Title	**Agency**	**Reference Number**	**PI, Co-investigators and collaborators**	**Funding requested**	**Project time frame (1 year, 2 years, etc.)**	**Date submitted**
NOT APPLICABLE DURING THIS REPORTING PERIOD						

Grants / Contracts Awarded #1					
Title	**Agency**	**Reference Number**	**PI, Co-investigators and collaborators**	**Period of Performance**	**Funding awarded**
The BEERE Menu: Pre-Packaged Technology Retrofit Options for PACE Financing	US DOE Better Buildings	DE-FOA-0000829 CFDA #: 81.086	PI: EcoCity Partners Co-PI: Hal Knowles, Craig Miller, Nick Taylor Collaborators: Pierce Jones and Jennison Kipp	3 year	$128,420.89 (UF Subcontract portion on a $669,102 overall proposal)

Hal Knowles, Co-PI and the primary supported person on this FESC project was a University of Florida Program for Resource Efficient Communities (UF/PREC) point person and contributor to the development of this new successfully awarded federal grant. UF/PREC will provide the following major services as a subcontractor for this energy efficiency financing and retrofit program: (1) energy pre-screening; (2) retrofit package specification development and standardization; (3) quality control; and (4) measurement and verification. As summarized on the proposal abstract:

"This project seeks to accelerate commercial property assessed clean energy (PACE) financing by small commercial building owners. We will simplify pathways to project completion and finance by designing and offering standardized, pre-packaged technology retrofit options arranged by building type and size, business type, climate zone and other factors. We will prove the reliability of pre-project estimates of energy and cost savings through post-project audits, monitoring & verification. This will enable us to develop critical informational resources for building owners to select from a menu of options for buying energy-efficiency and renewable energy solutions (the "BEERE Menu").

Successful projects included in the BEERE Menu will generate a minimum of 20% energy savings and be capable of accurate estimation. This will facilitate scalability of small commercial energy-efficiency solutions using PACE financing by streamlining pre- and post-energy audit requirements, and will simplify underwriting, approval and financing. Finally, the project will facilitate easier aggregation of PACE projects for pooled financing arrangements. The results will be made available to other PACE program administrators through a white paper and an industry-targeted webinar.

UNIVERSITY OF SOUTH FLORIDA

Design, Construction and Operation of CSP Solar Thermal Power Plants in Florida

(Progress Report)

PI: D. Yogi Goswami **Co-PIs**: Elias Stefanakos, Muhammad M. Rahman, Sunol Aydin, Robert Reedy
Students: Gokmen Demirkaya (Ph.D.); Ricardo Vasquez Padilla (Ph.D.);
Huijuan Chen (Ph.D.); Rachana Vidhi (Ph.D. Chemical Engineering);

Description:
This project targets the development of solar thermal power technology for bulk power and distributed generation, which will diversify energy resources in Florida and reduce greenhouse emissions by utilizing renewable sources. The project has three main tasks; the first one is to develop design methodologies and standards for the proven solar thermal power technologies in combination with bio or fossil fuels based on Florida conditions and resources. Secondly, the project aims to set up demonstration and test facilities for these technologies for optimization for Florida conditions, and the final task is to develop and commercialize innovative technologies based on new thermodynamic cycles.

Budget: $882,000
Universities: USF, UF, UCF
External Colaborators: Sopogy Corporation

Progress Summary
Research Objectives for Current Reporting Period: The main research objective is the development of a test facility and a pilot demonstration system based on parabolic trough technology.

Progress Made Toward Objectives During Reporting Period

Figure 1. Solar Field and power block for the 50 kWe power generation system

Construction of the solar field and the power block for the demonstration solar power plant is almost complete. The picture in Fig. 1 shows the status of construction of the 50kW$_e$ solar power system. Soponova 4.0 (Sopogy Inc.) parabolic trough collectors have been used in the solar field for providing 430 W/m^2 of thermal energy after losses. The solar field was designed to work in conjunction with a thermal energy storage system using a phase change material (PCM) as the storage material. Because of cost overruns, the designed thermal energy storage system could not be built in the system, although provision has been made to add a thermal energy storage system later.

Daily integration (DI) approach was used to obtain the average direct normal solar radiation for the location of the pilot demonstration solar plant (USF, Tampa, Fl). The direct normal solar radiation obtained for Tampa is shown in Fig. 2. The annual average for this location is 4.6 kWh/m^2-day. These solar radiation values and the solar shading analysis for solar collector rows were used for the solar field calculation.

The power block that will convert the thermal energy to electricity is based on Organic Rankine Cycle. This power block will have a nominal capacity of 50 kW_e. A preliminary study on passive cooling methods for dry cooled condensers for solar thermal plants was conducted and additional research is being conducted to develop a cost effective dry cooling technology.

The following describes a summary of the background research that was needed to move forward with the design and construction of the power plant.

Parabolic Trough Concentrators

The performance of parabolic trough based solar power plants over the last 25 years has proven that this technology is an excellent alternative for the commercial power industry. Compared to conventional power plants, parabolic trough solar power plants produce significantly lower levels of carbon dioxide, although additional research is required to bring the cost of concentrator solar plants to a competitive level. The cost reduction is focused on three areas: thermodynamic efficiency improvements by research and development, scaling up of the unit size, and mass production of the equipment. The optimum design, performance simulation and cost analysis of the parabolic trough solar plants are essential for the successful implementation of this technology. A detailed solar power plant simulation and analysis of its components is needed for the design of parabolic trough solar systems which is the subject of this research.

Preliminary analysis was carried out by complex models of the solar field components. These components were then integrated into the system whose performance is simulated to emulate real operating conditions. Sensitivity analysis was conducted to get the optimum conditions and minimum levelized cost of electricity (LCOE). A simplified methodology was then developed based on correlations obtained from the detailed component simulations.

A comprehensive numerical simulation of a parabolic trough solar power plant was developed, focusing primarily on obtaining a preliminary optimum design through the simplified methodology developed in this research. The proposed methodology is used to obtain optimum parameters and conditions such as: solar field size, operating conditions, parasitic losses, initial investment and LCOE. The methodology is also used to evaluate different scenarios and conditions of operation.

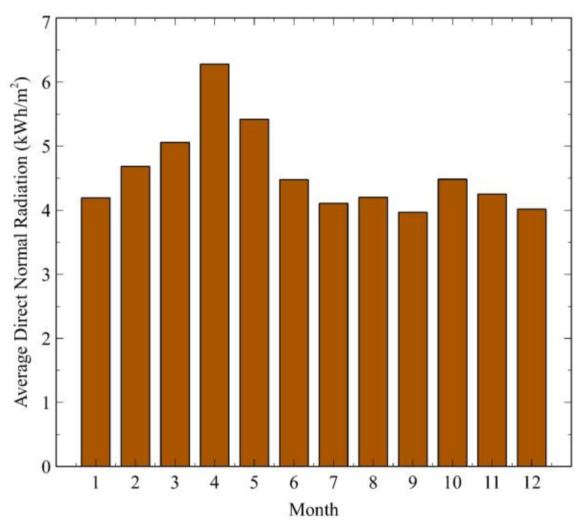

Figure 2. Direct Normal Radiation for Tampa, FL

The new methodology was implemented for a parabolic trough solar power plant for two cities: Tampa and Daggett. The results obtained for the proposed methodology were compared to another physical model (System Advisor Model, SAM) and a good agreement was achieved, thus showing that this methodology is suitable for any location.

Power Cycles for Solar Thermal Power

Low-grade heat sources below 300ºC, are abundantly available as industrial waste heat, solar thermal using low cost solar concentrators, and geothermal, to name a few. However, they are under-exploited for conversion to power because of the low efficiency of conversion. The utilization of low-grade heat is advantageous for many reasons. Technologies that allow the efficient conversion of low-grade heat into mechanical or electrical power are very important to develop.

Supercritical Rankine cycles were investigated for the conversion of low-grade heat into power. The performance of these cycles was studied using ChemCAD linked with customized excel macros written in Visual Basic and programs written in C++.

The selection of working fluids for a supercritical Rankine cycle is of key importance. A rigorous investigation into the potential working fluids was carried out, and more than 30 substances were screened out from all the available fluid candidates. Zeotropic mixtures were proposed to be used in supercritical Rankine cycles to improve the system efficiency. Supercritical Rankine cycles and organic Rankine cycles with pure working fluids as well as zeotropic mixtures were optimized for efficient conversion of low-grade heat into power. The results show that it is theoretically possible to extract and convert more energy from such heat sources using the cycle developed in this research than the conventional organic Rankine cycles. A theory on the selection of appropriate working fluids for different heat source and heat sink profiles was developed to customize and maximize the thermodynamic cycle performance.

The outcomes of this research will eventually contribute to the utilization of low-grade waste heat more efficiently.

Combined Power/Cooling Cycle

Binary mixtures exhibit variable boiling temperatures during the boiling process, which leads to a good thermal match between the heating fluid and working fluid for efficient heat source utilization. This study presents a theoretical and an experimental analysis of a combined power/cooling cycle, which combines the Rankine power cycle and the absorption refrigeration cycle to produce power and refrigeration in the same cycle, while power is the primary goal. This cycle, also known as the *Goswami Cycle*, can be used as a bottoming cycle to utilize the waste heat from a conventional power cycle or as an independent cycle using low to mid-temperature sources such as geothermal and solar energy. A thermodynamic analysis of power and cooling cogeneration was conducted. The performance of the cycle for a range of boiler pressures, ammonia concentrations, and isentropic turbine efficiencies were studied to find out the sensitivities of network, amount of cooling and effective efficiencies. The thermodynamic analysis covered a broad range of boiler temperatures, from 85 °C to 350 °C. The first law efficiencies of 25-31% are achievable with the boiler temperatures of 250-350 °C. The cycle can operate at an effective exergy efficiency of 60-68% with the boiler temperature range of 200-350 °C. An experimental study was conducted to verify the predicted trends and to test the performance of a scroll type expander. The experimental results of vapor production were verified by the expected trends to some degree, due to heat transfer losses in the separator vessel. The scroll expander isentropic efficiency was between 30-50%, the expander performed better when the vapor was superheated. The small scale of the experimental cycle affected the testing conditions and cycle outputs. This cycle can be designed and scaled from a kilowatt to megawatt systems. Utilization of low temperature sources and heat recovery is definitely an active step in improving the overall energy conversion efficiency and decreasing the capital cost of energy per unit.

Task 1: Development of simulation and design methodology for parabolic trough and parabolic dish

The objective of the task one is to develop a simulation and design methodology for the parabolic trough and parabolic dish based technologies for Florida conditions. Solar radiation, solar collector and thermal storage topics are the subtasks, and following progresses have been made during the period.

Parabolic trough solar systems are currently one of the most mature and prominent applications of solar energy for production of electricity. Compared to conventional power plants, parabolic trough solar power plants produce significantly lower levels of emissions and carbon dioxide. Thermal simulations and cost analysis of the system are used to evaluate the economic feasibility. Complex models and components are integrated to emulate real operating conditions, such as: Solar Radiation Model, Solar Thermal Collector, Thermal Energy Storage, Solar Field Piping, Power Block, Cost Analysis, and Integration of all Systems. This progress report presents a preliminary design method to calculate solar radiation data and thermal collector efficiency which are used to determine the size and the cost of solar field.

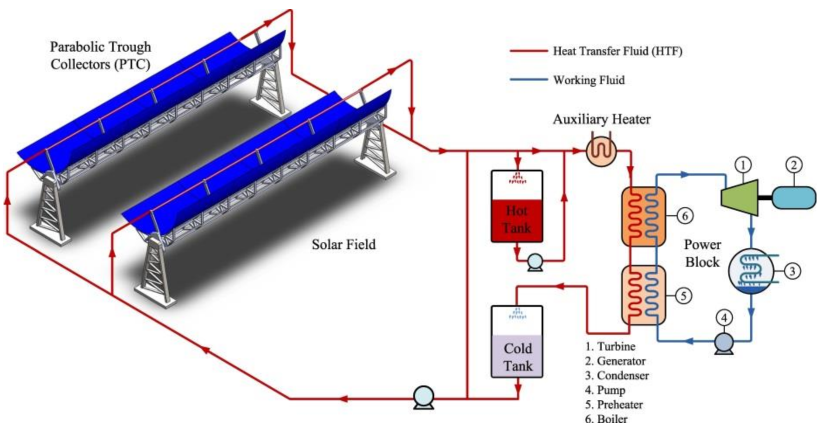

Figure 3. Parabolic trough Power Plant

An hourly solar radiation model is necessary to calculate the energy input that come from the sun, since the solar collector performance changes during the whole day. The inputs for the hourly solar radiation model are the long term average values of total horizontal and diffuse radiation, which can be obtained by ground or satellite measurements. Satellite data provide information about solar radiation and meteorological conditions in locations where ground measurement data are not available. Gueymard developed a Daily integration approach model to predict the monthly-average hourly global irradiation by using a large dataset of 135 stations with diverse geographic locations (82.58N to 67.68S) and climates. The results showed that the daily integration model is most accurate than previous hourly models.

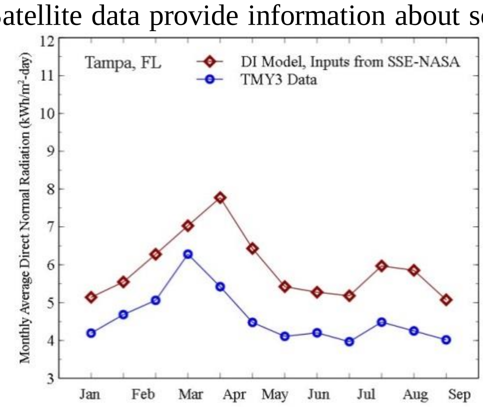

Figure 4. Comparison of two models

The second part of this report is about the numerical heat transfer model. The receiver consists of an absorber surrounded by a glass envelope. The absorber is typically stainless steel tube with a selective absorber surface. The glass envelope is an antireflective evacuated glass tube which protects the absorber from degradation and reduces heat losses. The Solar receiver uses conventional glass to metal seals and bellows to achieve the necessary vacuum enclosure and for thermal expansion.

The heat transfer model is based on an energy balance between the heat transfer fluid and the surroundings (atmosphere and sky). A comprehensive radiation model between the absorber and the envelope is included in this study. The results showed that the new model has lower RMSE than the NREL Model (0.985% and 1.382% respectively). The numerical heat transfer model integrated with the solar radiation model can be used for evaluating the performance of solar collectors for any location.

Task 2: Development of a test facility and pilot demonstration

The second task targets the development of a test facility and pilot demonstration systems based on parabolic trough and dish technologies. The experimental combined power and cooling setup will be used as a preliminary study of the demonstration system that will be developed.

2.1 Performance analysis of a Rankine-Goswami Combined Cycle

Improving the efficiency of thermodynamic cycles plays a fundamental role for the development of solar power plants. These plants work normally with Rankine cycles which present some disadvantages due to the thermodynamic behavior of steam at low pressures. These disadvantages can be reduced by introducing alternatives such as combined cycles which combine the best features of each cycle. In the present study a combined Rankine-Goswami cycle is proposed and a thermodynamic analysis is conducted. The Goswami cycle, used as a bottoming cycle, uses ammonia-water mixture as the working fluid and produces power and refrigeration while power is the primary goal. Figure 5 shows a schematic of the Rankine-Goswami cycle.

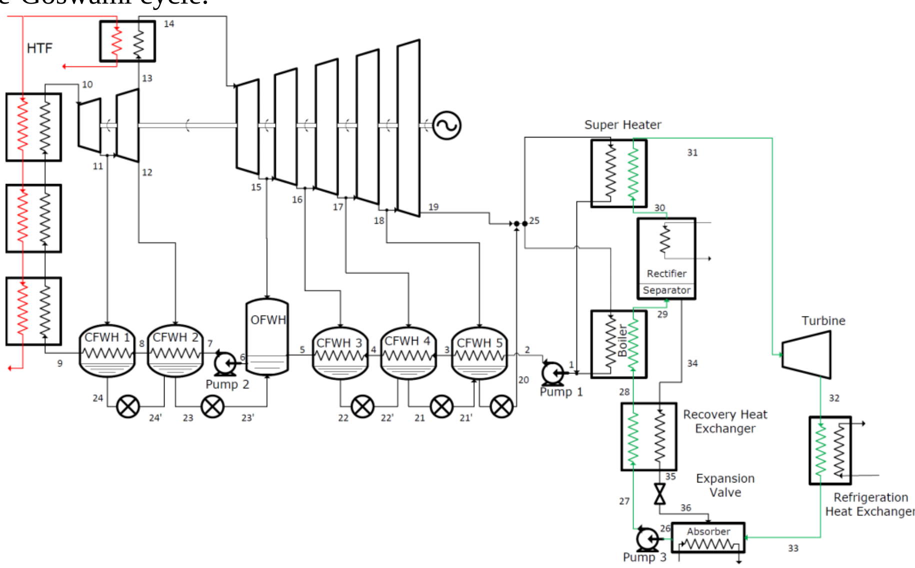

Figure 5

The detailed explanation about the parameters that were used for simulation is given in the paper. Different cases were also considered for parametric studies which are shown below.

Case	Rectifier	Superheater	Controlled Parameter
R	Yes	No	$x_{rectifier} = 0.995$ $T_{superheater} = T_{rectifier}$
R+S	Yes	Yes	$x_{rectifier} = 0.98$ $T_{superheater} = T_{boiler}$
B (Base)	No	No	Saturated vapor condition at the boiler exit

The thermodynamic properties of water and steam were implemented in Python 2.6 by using the international-standard IAPWS-IF97 steam tables. For the Goswami cycle, the properties of ammonia water were obtained from a Gibbs free energy formulation given by Xu and Goswami. In this study the amount of the electric work obtained from the topping cycle was held constant at 50 MWe while for the bottoming cycle the turbine work was considered as an output parameter. Figure 6 shows the effect of the high pressure side on the rectifier temperature and absorber concentration, In this case, the ammonia concentration range was selected such as the absorber was kept at least under atmospheric pressure.

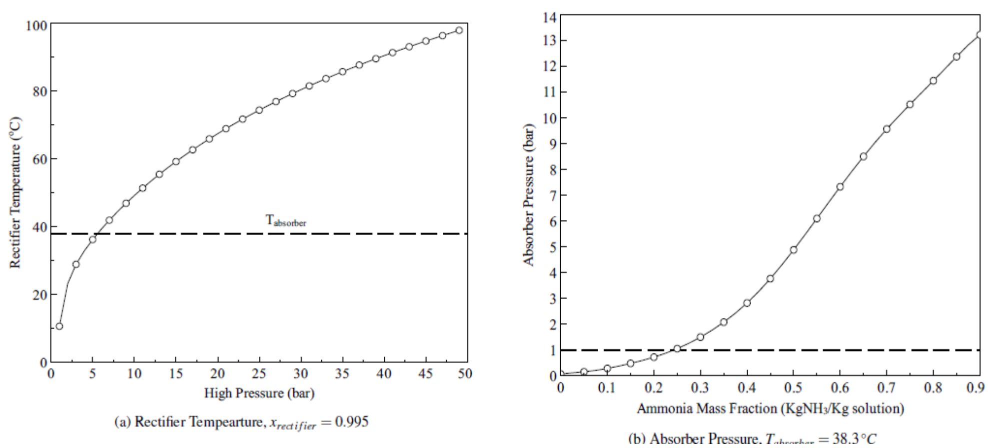

Figure 6

Figure 7 shows the effect of the condenser pressure on the Goswami bottoming cycle exit quality for different cases and ammonia mass fraction. Moreover, Figure 8 shows the effect of the variations of the net -work with the condenser pressure for ammonia mass concentration of 0.3, in all the studied cases.

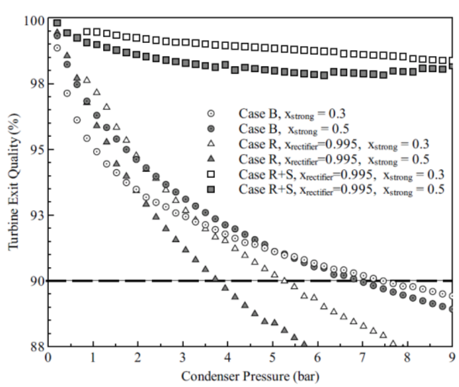

Figure 7

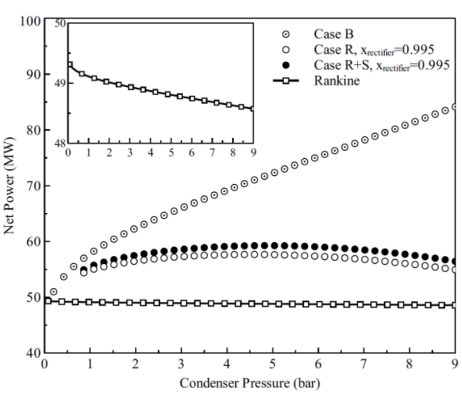

Figure 8

The effect of condenser pressure on the effective First Law efficiency is also illustrated in Figure 9 while the cooling capacity of the Goswami bottoming cycle is presented in Figure 10. The effective exergy efficiency in the cycle as a function of the condenser pressure and ammonia mass fraction is also presented in Fig.11.

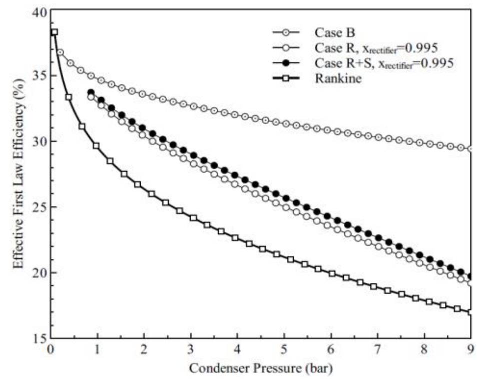

Figure 9

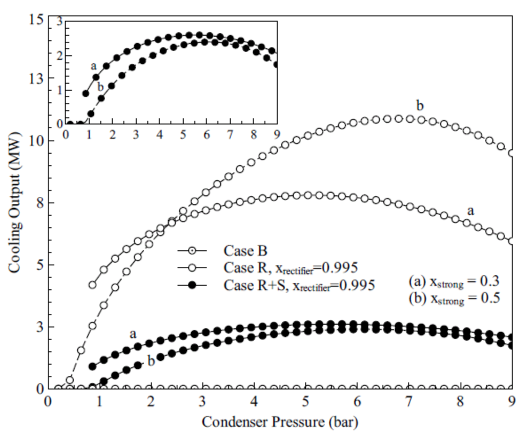

Figure 10

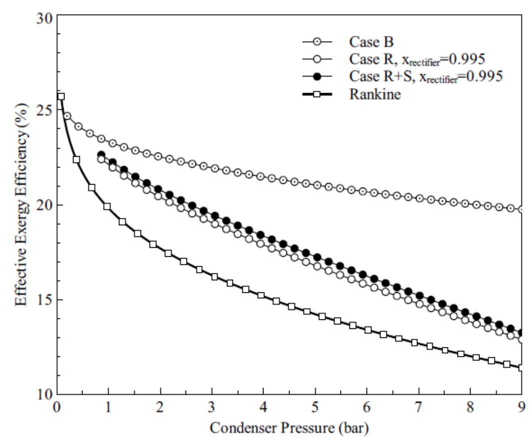

Figure 11

Task 3. Installation and Operation of 50 kW_e Solar Power Plant

Sopogy Inc. Honolulu, Hawaaii is the main contractor for the installation of a 50kW_e Solar Power Plant at USF. Parabolic collectors (Soponova 4.0) were received from Sopogy and were assembled. Power block for generating electricity from GulfCoast Green Energy was also received and installed. Power block is a Green Machine Elite 4000 manufactured by Electratherm. This machine will produce about 50kW_e electricity from the thermal energy collected by the solar field that has 199 Soponova 4.0 parabolic concentrators from Sopogy Inc. Fig. 12 shows a photo of the Electratherm power generator with an air-cooled condenser. Installation of the system is almost complete and commissioning of this system is expected to take place sometime in the first week of Nov. 2013.

Figure 12. Electratherm power generator with air-cooled condenser.

Task 4: Thermal Energy Storage

We are currently working on the development of low cost thermal energy storage (TES) systems for Concentrating Solar Power (CSP). The objective is to research and develop a thermal energy storage system (operating range 300^0C – 450 ^{0}C) based on encapsulated phase change materials (PCMs). The system will be able to meet the utility-scale base-load concentrated solar power plant requirements at much lower system costs compared to the existing TES concepts. This project is developing a TES system concept that will allow for an increase of the capacity factor of the present CSP technologies to 75% or greater and reduce the cost to less than $\$15/kWh_{th}$ as compared to the present cost of about $\$40/kWh_{th}$.

We have successfully prepared capsules of phase change materials that will allow for the volumetric expansion during PCM melting and hence impose less stress on the encapsulating material. We have developed the encapsulation techniques and selected low cost encapsulating materials that will be used to encapsulate the PCM. Currently we are optimizing the process for encapsulating the PCMs for various salts and salt eutectics in the temperature range from 300 to 1000^0C. We are also preparing about 900 capsules for a laboratory test of a PCM based packed bed thermal energy storage system.

Publications

1. Chen, H. and Goswami D.Y. (2008) “The conversion of moderate temperature heat into power and refrigeration,” in the Proceedings of the Annual Meeting of the American Institute of Chemical Engineers, Philadelphia, November.

2. Chen, H. and Goswami D.Y. (2009) “The conversion of moderate temperature heat into power and refrigeration with CO_2 and organic binary working fluid, in the Proceedings of biennial

international student conference of Education without Borders", Dubai, UAE, March-April.

3. Chen, H. and Goswami D.Y. (2010) "Converting Low-Grade heat into Power using a Supercritical Rankine cycle with Zeotropic Mixture Working Fluid," in the Proceedings of ASME 2010 4th International Conference on Energy Sustainability, Phoenix, Arizona May.

4. Chen, H., and Goswami, Y. (2008) "Simulation of a Thermodynamic cycle with Organic Absorbents and Co_2 as Working fluids," in the Proceedings of the ASME 3rd International Conference on Energy Sustainability, Jacksonville, FL, August.

5. Chen, H., Goswami, D. Yogi, Rahman, M.M., and Stefanakos, E.K. (2011) "A supercritical Rankine cycle using zeotropic mixture working fluids for the conversion of low-grade heat into power," *Energy*, vol. 36 (1), pp. 549-555.

6. Chen, H., Goswami, D.Y., and Stefanakos, E.K. (2010) "A Review of Thermodynamic Cycles and Working Fluids for the Conversion of Low-Grade Heat," *Renewable and Sustainable Energy* Reviews, 14 (9), 3059-3067.

7. Chen, H., Goswami, D.Y., Rahman, M.M., and Stefanakos, E.K. (2011) "Energetic and Exergetic analysis of CO_2- and R32-based Transcritical Rankine Cycles for Low-Grade Heat Conversion," *Applied Energy*, 88, pp. 2802-2808.

8. Chen, H., M.M. Rahman, D.Y. Goswami, E.K. Stefanakos (2011) "Optimizing energy conversion using organic Rankine cycles and supercritical Rankine cycles," in the Proceedings of the Proceedings of the ASME ESFuelCell 2011 Conference, Washington, D.C., August.

9. Demikaya, G., Vasquez Padilla, R., and Goswami,D.Y. (2013) "A review of combined power and cooling cycles," *WIRES Energy Environ* 2013. Doi: 10.1002/wene.75

10. Demirkaya, G., Besarati, S., Vasquez Padilla, R., Ramos Archibold, A., Goswami, D.Y., Rahman, M.M., Stefanakos, E.K. (2012) "Multi-objective optimization of a combined power and cooling cycle for low-grade and mid-grade heat sources," *Journal of Energy Resources Technology (ASME)*,134, 032002-1.

11. Demirkaya, G., Besarati, S.M., Vasquez Padilla, R., Ramos, A.A., Rahman, M.M., Goswami, D.Y., and Stefanaksos, E. (2011) "Multi-Objective Optimization of a Combined Power and Cooling Cycle for Low-Grade and Mid-Grade Heat Sources," in the Proceedings of the ASME ESFuelCell 2011 Conference, Washington, D.C., August.

12. Demirkaya, G., Padilla, R.V., Goswami, D.Y., Stefanakos, E., Rahman, M.M. (2011) "Analysis of a combined power and cooling cycle for low-grade heat sources," *International Journal of Energy Research*, 35 (13), pp. 1145-1157.

13. Goswami, D.Y. "Keynote address: Emerging CSP Market in India," SolarPACES conference, Berlin, Germany, September 2009.

14. Li, C., Besarati, S., Goswami, Y., Stefanakos E., and Chen, H. (2012) "Reverse osmosis desalination driven by low temperature supercritical organic rankine cycle," (pre press accepted and available online, October 2012) *Applied Energy*.

15. Li, C., Besarati, S., Goswami, Y., Stefanakos, E., and Chen, H. (2013). "Reverse osmosis desalination driven by low temperature supercritical organic rankine cycle," *Applied Energy,* 102, pp. 1071-1080.

16. Padilla, R. V., Ramos, A.A., Demirkaya, G., Besarati, S., Goswami, D.Y., Rahman, M.M., and Stefanakos, E.K. (2011) "Performance Analysis of a Rankine-Goswami Combined Cycle," Proceedings of the ASME 2011 "ESFuelCell 2011" (5th International Conference on Energy Sustainability and 9th Fuel Cell Science Engineering and Conference), Washington, DC, August.

17. Padilla, R.V., Demirkaya, G., Goswami, D.Y., Stefanakos, E., and Rahman, M.M. (2011) "Heat transfer analysis of parabolic trough solar receiver," *Applied Energy,* Vol. 88 (12), pp. 5097-5110.

18. Padilla, R.V., Demirkaya, G., Goswami, D.Y., Stefanakos, E., and Rahman, M.M. (2010) "Analysis of power and cooling cogeneration using ammonia-water mixture," *Energy,* Vol. 35 (12), pp. 4649-4657.

19. Padilla, R.V., Demirkaya, G., Goswami, Y., ad Stefanakos, E.K. (2010) "Parametric study of a combined power and cooling thermodynamic cycle for low temperature sources," in the Proceedings of the 2010 ASME International Mechanical Engineering Congress and Exposition, 6, pp. 165-174.

20. Vasquez Padilla, R., Demirkaya, G., and Goswami, D.Y. (2009) "Parametric Study of a Combined Power and Cooling Thermodynamic Cycle for Low Temperature Heat Sources," in the Proceedings of the 2009 ASME Internaitonal Mechanical Engineering Congress and Exposition Conferenece (IMEC-E 2009), Lake Buena Vista, FL, November.

21. Vasquez Padilla, R., Ramos Archibold, A., Demirkaya, G., Besarati, S., Goswami D.Y., Rahman, M.M., ad Stefanakos, E.K. (2012) "Performance analysis of a rankine cycle integrated with the Goswami combined power and cooling cycle." *Journal of Energy Resources Technology, 134, 032001-1.*

22. Vidhi, R., Goswami, D.Y., Chen, H., Stefanakos, E., and Kuravi, S. (2011) "Study of supercritical carbon dioxide power cycle for low grade heat conversion," Proceedings of the Supercritical CO_2 Power Cycle Symposium, Denver, Colorado, May.

23. Besarati, S.M., Vasquez Padilla, R., Goswami, D.Y., and Stefanakos, E. (2013) "The potential of harnessing solar radiation in Iran: Generating solar maps and viability study of PV power plants," *Renewable Energy,* 53, pp. 193-199.

University of South Florida

Solar Photovoltaic Manufacturing Facility to Enable a Significant Manufacturing Enterprise within the State and Provide Clean Renewable Energy

(Final Report)

PI: Don L. Morel **Co-PI**: Chris Ferekides, Lee Stefanakos
Students: K. Jayadevan (MS), S. Bendapudi (MS 5/11), R. Anders (PhD), Y. Wang (PhD), Manikandan Sampathkumar (MS)

Description: The primary goal of this project is to enable the establishment and success of local solar photovoltaic manufacturing companies to produce clean energy products for use within the state and beyond and to generate jobs and the skilled workforce needed for them. Thin film technologies have shown record efficiencies of 20%, and present tremendous opportunities for new Florida start-up companies. USF, UCF, and UF are collaborating to develop a pilot line facility for thin film solar technologies, which will serve as a test bed for making ongoing improvements in productivity and performance of solar modules, develop advanced manufacturing protocols, and help train a skilled workforce to ensure the success of new companies.

Budget: $1.6M
Universities: USF, UCF, UF
External Collaborators: Mustang Solar, a Division of Mustang Vacuum Systems

Summary of Final Report

Just before submitting the Fifth Annual Report we were told that our funding had been taken over by DSR and we were not to spend any further on the project which officially ended June 30th of this year. Consequently the Fifth Report constitutes the final Report for the project.

Over the past year progress has continued to be made on the two main task areas of the project, development of the Thin-Film Pilot Line deposition system and development and advancement of laboratory scale processes for CIGS related materials and devices. As a result of the changing landscape related to CIGS manufacture the Pilot Line System was modified to focus on the key elements currently controlling commercialization of the technology. Simulation tools that address cost factors as well as technology were developed and utilized to guide the redirection of the design. It was determined that deposition rates of 20 Å/s and above were needed to hit the targeted cost factors for capital equipment utilization. The design of the deposition machine and the process recipes will allow attainment of these rates.

The key factor for machine and process design on the technology side is the arrival rate and sequence of the CIGS constituents. Simulation tools have been developed and utilized that allow determination and control of these species. The deposition tool set utilizes two pair of metal deposition sources and several Se sources distributed over the deposition zones. The two-dimensional deposition profile of the components are individually simulated and then combined to simulate the overall two-dimensional profile. Imbedded in the simulations is the ability to control the evolution of the metal ratios across the deposition zone. And, simulation of the Se/metal profiles within a targeted range completes the capture of the entire deposition process. The insights provided from these simulations have guided the design of the deposition system. It will be versatile enough to enable access to a large range of deposition space that contains the optimum parameters for performance and cost control. The machine components have been delivered, and it is currently being assembled.

Based upon CIGS laboratory scale experimentation that has been underway two process recipes have been chosen to implement in the Pilot Machine. The initial configuration of the machine will be directed toward determining which of these has the most potential for success. On a longer timeframe we have also been developing CuZnSnSe(CZTS) as a sustainable substitute for CIGS. With increasing production volume the availability of In may drive up its cost. CZTS uses earth abundant materials and has demonstrated efficiency in the 10% range. We have been developing the material, and with new insights gained from use of Raman spectroscopy have made significant progress in improving material quality. Initial results from devices made with the upgraded material are also promising.

Thin Film Pilot Line

As progress is being made in the manufacture of CIGS solar panels new challenges and opportunities are emerging for ongoing growth of the technology. Champion large area module efficiencies of 16% are being reported, and average production efficiencies are catching up. So it is clear that performance parameters for large scale applications can be met. What remains is to demonstrate that costs are competitive and have a pathway to remaining so. The key to cost is throughput and materials utilization. These translate to fast deposition rates and management of In and Ga utilization. From the beginning of our research endeavors at USF we have always pursued deposition technologies that would be able to pass commercialization muster while avoiding those that allowed fast pathways to high efficiency, but had no chance at commercialization. There has been a series of companies that failed by trying to commercialize the easy high efficiency technologies. With this backdrop we have designed our new deposition system to accommodate the commercialization drivers. The system will incorporate tools to evaluate deposition approaches that have not been reported in the literature. Our objective is to demonstrate that one of these surpasses commercialized technologies in performance and cost.

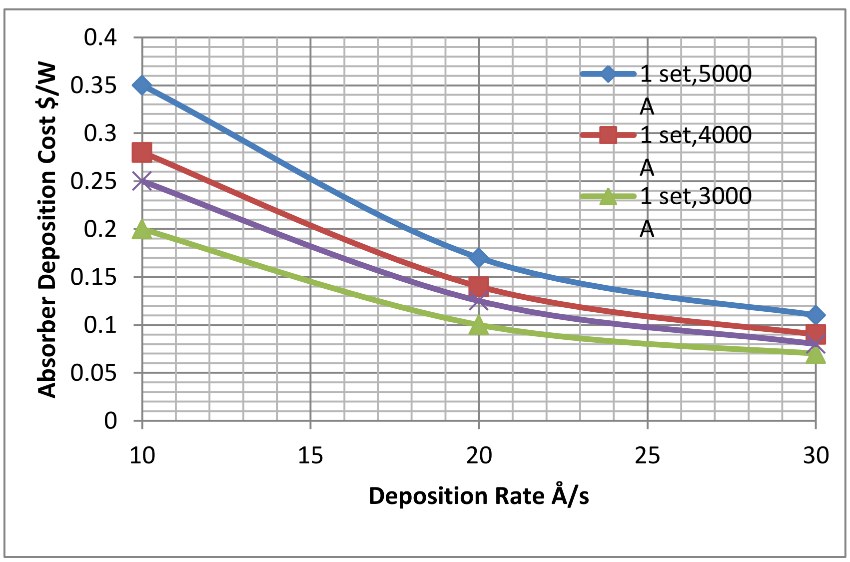

Figure 1. Projected capital equipment cost in $/W for CIGS deposition as a function of deposition rate

Cost Simulation

Throughout the project we have developed and used simulation tools to guide our technology development. Of particular importance to the design of the deposition system is the projected capital cost/Watt for the deposition tool. The drivers for this cost factor are the capital cost of the equipment, the throughput, the efficiency and the yield. There are also variations for series and parallel target configurations that have various cost tradeoffs. An example of results for a few of these configurations is shown in Fig. 1. This component for the cost of a finished module should be about 20%, which for a selling price of \$0.60/W should be around \$0.12/W. As can be seen in the figure, this threshold can be reached for deposition rates of 20 Å/s and higher.

At this point it is necessary to bring another technical factor into the cost discussion. Deposition rates of 20 Å/s can be attained by both sputtering and thermal evaporation of the source materials. While thermal evaporation is the technology that has been used to progress efficiencies to the 20% level, it has not proven to be a successful technique for large area manufacturing. Sputtering is considered the technology of choice for large area manufacture because of its ability to deposit uniformly and reproducibly over large areas. Ideally one would like then to just sputter from a CIGS target or maybe a combination of CuSe, In_2Se_3 and Ga_2Se_2 targets. These approaches have not worked largely because of loss of Se, but even if they did, sputter rates of 20 Å/s and higher are not realistic for "ceramic" targets. Thus sputtering of metals is what must be pursued, and that is what we, and others, are working at. Depositing Cu, In and Ga at these rates is not the problem, it is rather how to selenize the metal layers. This is where innovations are needed to enable the emergence of this technology and what is guiding our efforts and the design of our deposition tool.

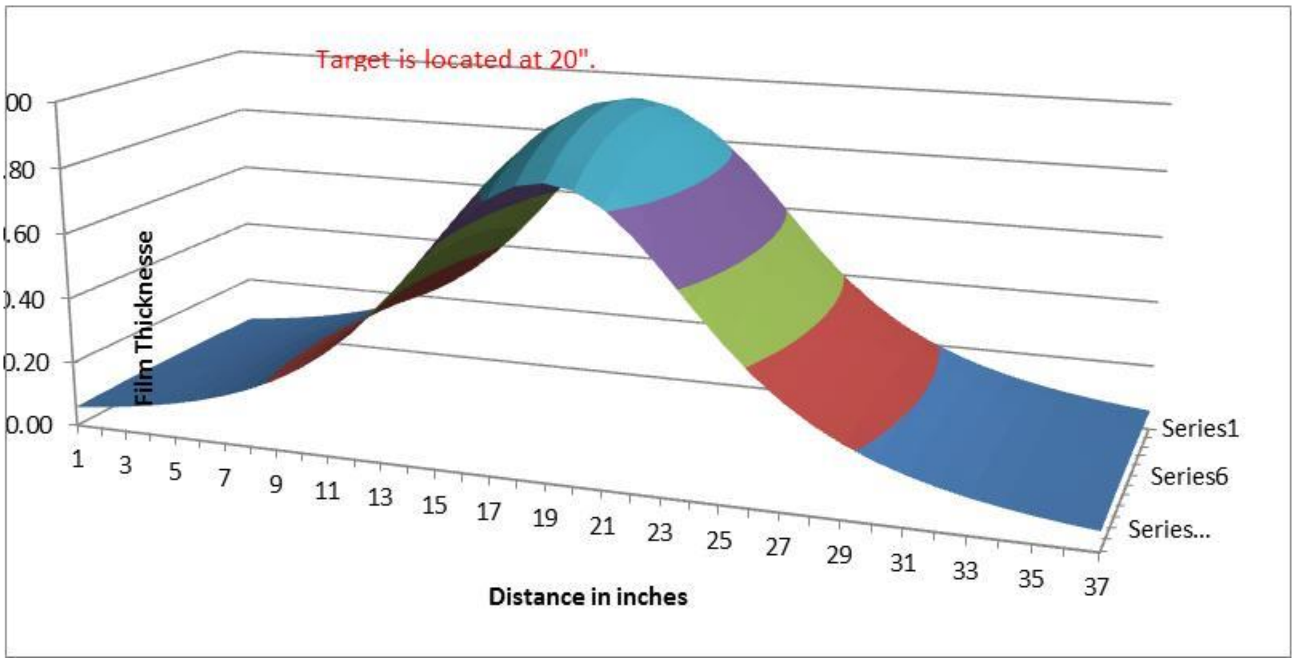

Figure 2. Thickness Profile of a Sputtered Film on the Web.

Deposition Simulation

The process recipes that we will be developing are based upon sputtering of the metal components. We will pursue a couple of different approaches to Se delivery and determine which is most effective. The deposition system will be in a roll-to-roll configuration and will be able to handle "plastic" as well as stainless steel coils. The width of the substrate will be 4". Champion efficiency cells are made in deposition systems on small substrates onto which all four components, Cu, In, Ga and Se are delivered to the substrate simultaneously and carefully controlled. This is not possible in a manufacturing scale system based upon sputtering. In these systems the components are delivered to a moving substrate by multiple sputtering sources. Consequently there are time offsets in the arrival of the constituents.

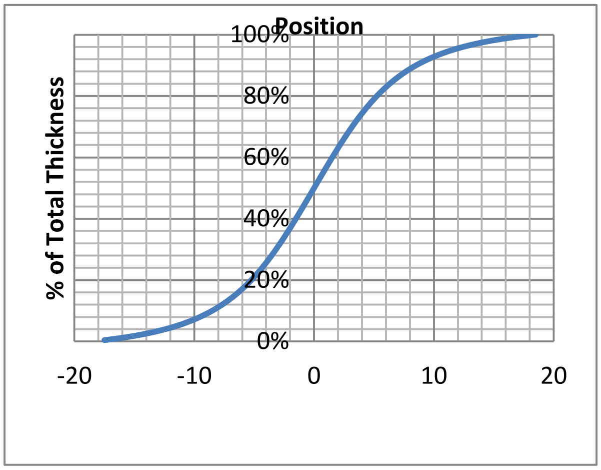

Figure 3. Cumulative thickness as a function of web position.

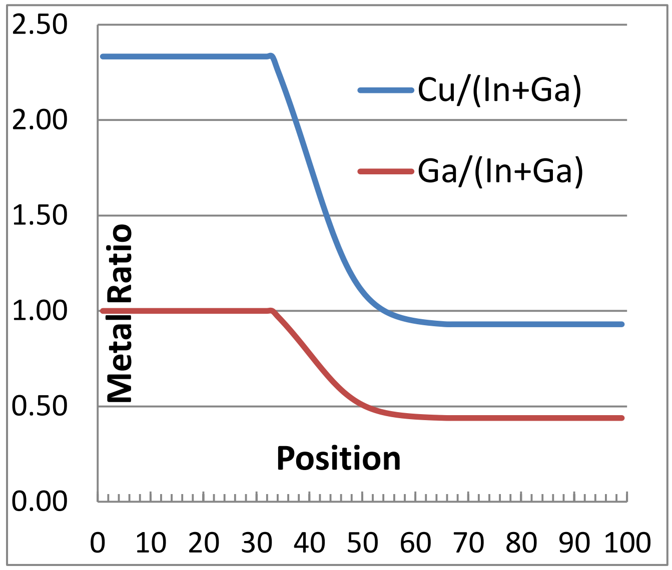

Figure 4. Metal ratio profiles from four sputtering sources.

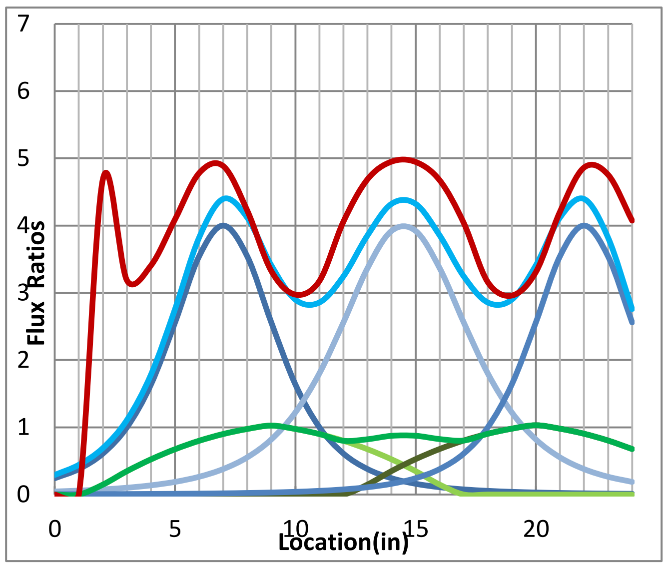

Figure 5. Flux ratios for two sputter sources and Se sources.

Given the complex phase space of CIGS and the potential for formation of unfavorable phases it is important to understand the formation chemistry and to design the deposition tools to be able to access the region of deposition space that produces high quality, single-phase CIGS. Throughout the years we have explored and studied many regions of this phase space and have designed the deposition tool to access regions that we know to be viable. To effectively use this understanding we have developed deposition simulation tools to guide design of the deposition tools. Figure 1 shows the instantaneous thickness profile, or equivalently the flux, of the deposition along the web for a sputter target located at 20". Fig. 3 shows the resulting thickness increase as the web moves over the sputtering source. There is a corresponding profile for a second sputter source adjacent to the first one. It has the same profile, but offset from the first source. Thus the instantaneous composition at any location on the web can be determined. Further, the composition can be changed by adjusting the separation distance between the sources, the sputter gun angle and the deposition rates. Fig. 4 is an example of the emergence of the metal ratio profile as a function of position for four sputtering sources resulting in targeted ratios of 0.9 for Cu/(In + Ga) and 0.4 for Ga/(In + Ga).

In addition to controlling the metal fluxes it is important to attain the proper delivery profile for Se. It is necessary to have an overpressure of Se to achieve full selenization of the films. A simulation result for one of the two pairs of sputter sources used for the Fig. 4 simulation is shown in Fig. 5. The targeted ratio of Se/metal is 3 – 5. The red(top) curve in the figure is this ratio and indicates that the desired range is achieved. The underlying curves are the contributions from the individual sources.

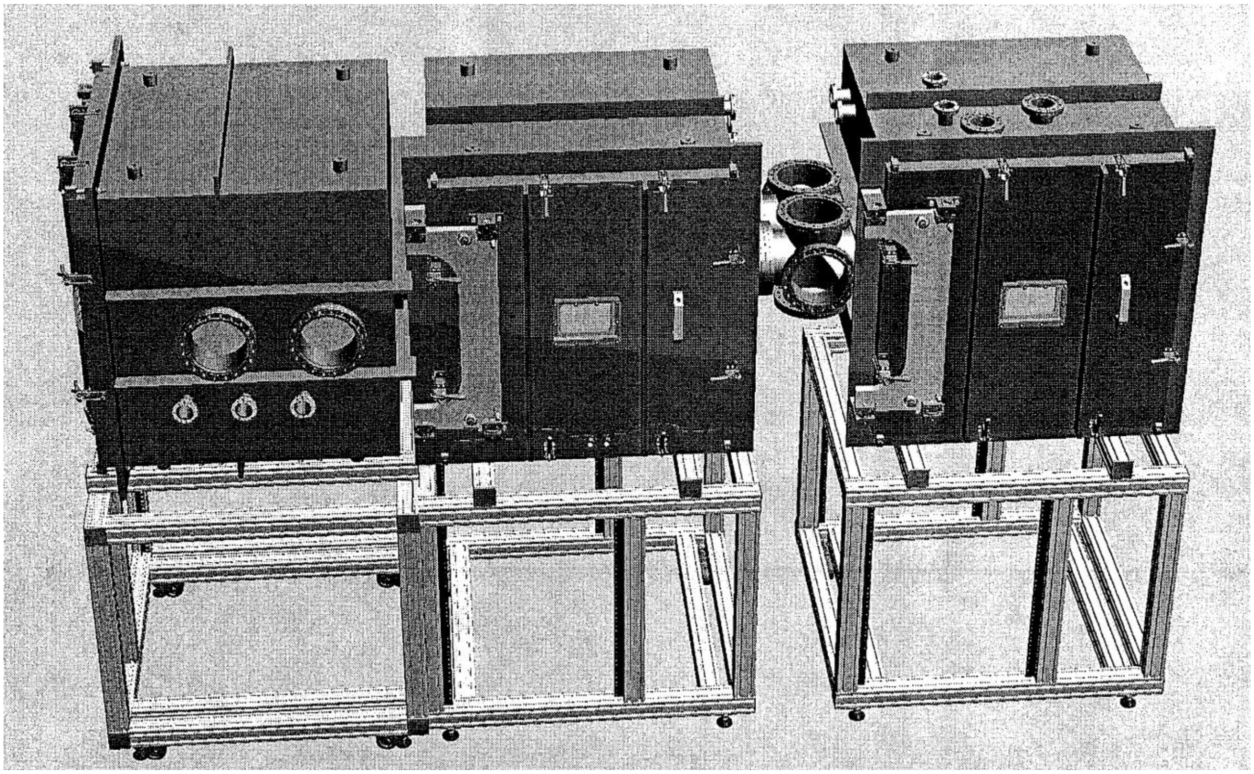

Figure 6. Pilot-Line Deposition system.

The insights gained from the above analysis were used to guide the development of the Pilot-Line deposition system shown above which has a total length of 10 feet. This figure is before all of the operational hardware has been installed. We hope to report next time on installation and operation of the system and initial results.

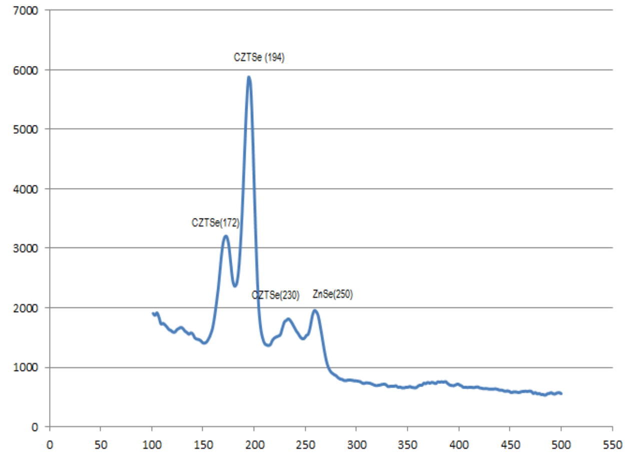

Figure 7. Raman spectrum of CZTS.

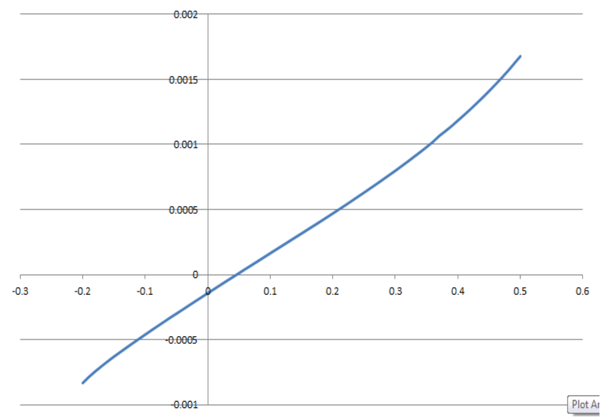

Figure 8. CZTS IV curve.

One of the cost issues for CIGS is Indium. In is currently available and cost-effective, but going forward to large volumes this might not remain true. Consequently we and others have been pursuing alternative CIGS-related compounds. In particular we have focused our efforts on CuZnSnSe. Efficiencies of 5 – 10% have been reported for CZTS made with different techniques. We have chosen a deposition pathway that we believe will meet the requirements for large scale manufacture. Our efforts thus far have concentrated on attaining good materials properties. This material is more complex than CIGS because of the various locations that the metals can take in the lattice. These properties are also difficult to characterize by the usual techniques of XRD because of the similarities of the fingerprints for the relevant phases. We developed an optical technique which we reported previously and which was helpful in identifying the presence of ZnSe[1]. Our attempts at making devices were being thwarted by the formation of ZnSe. Recently we started using Raman spectroscopy to gain further insights to the structural composition of our material. In Fig. 7 we show a Raman spectrum for a sample made at an annealing temperature of 300 °C. The main peak at just under 200 cm^{-1} is that of CZTS with two satellite peaks on either side. The peak at 265 cm^{-1} , although identified to be ZnSe, is more likely CuSe. With additional processing at higher temperatures we find that this peak disappears. It is known that CuSe forms at lower temperatures and then reacts with the other constituents to form CZST. We are using these insights to guide further development of our material and believe that the electronic quality is now significantly better. However, the ultimate proof of material quality is in device performance. We have started making devices with the upgraded materials process and are seeing encouraging results. An IV curve of a device showing PV response is shown in Fig. 8. Once we advance the performance of CZTS at the laboratory level, we can also transfer the process to the Pilot-Line machine for further development.

[1] Y. Wang, S. Bendapudi, C. S. Ferekides and D. L. Morel, "*Optical Determination of Phase Composition and Processing Effects on $Cu_2ZnSnSe_4$ Film Quality and Device Performance*", Proceedings of the 38th IEEE PV Specialist Conference, Austin, June, 2012.

FESC Phase 2 Technology Commercialization Projects

High Efficiency Black Polymer Solar Cells
(Final Report)

PI: Dr. Franky So
External Collaborators: John Reynolds, Georgia Tech
Industry Partner: Sestar Technologies, LLC
Students: Cephas Small and Song Chen

Description: The objective of the proposed project is to synthesize broadly absorbing, black colored (PBLACK) polymers with especially high charge mobilities and to fabricate the highest performance polymer solar cells possible. Specifically, we will synthesize polymers with absorption band ranging from 400 nm to beyond 1 μm with carrier mobilities higher than 10^{-4} cm^2/Vs. Polymer-fullerene (both $PC_{60}BM$ and $PC_{70}BM$ along with more recently developed derivatives) blend morphology will be optimized using different solvent/heat treatments as well as additives to the blends. The final device will be enhanced using anode and cathode interlayers to enhance carrier extraction to the electrodes. With the ability to synthesize broadly absorbing polymers, control the donor-acceptor phase morphology and engineer the device structure, it is expected that the power conversion efficiency of polymer solar cells can reach 10% at the end of the two-year program.

Summary of Progress

Polymer bulk heterojunction solar cells based on low bandgap polymer:fullerene blends are promising for next generation low-cost photovoltaics. While these solution-processed solar cells are compatible with large-scale roll-to-roll processing, active layers used for typical laboratory-scale devices are too thin to ensure high manufacturing yields. Furthermore, due to the limited light absorption and optical interference within the thin active layer, the external quantum efficiencies (EQEs) of bulk heterojunction polymer solar cells are severely limited. In order to produce polymer solar cells with high yields, efficient solar cells with a thick active layer must be demonstrated. In this work, the performance of thick-film solar cells employing the low-bandgap polymer poly(dithienogermole-thienopyrrolodione) (PDTG-TPD) was demonstrated. Power conversion efficiencies over 8.0% were obtained for devices with an active layer thickness of 200 nm, illustrating the potential of this polymer for large-scale manufacturing. Although an average EQE > 65% was obtained for devices with active layer thicknesses > 200 nm, the cell performance could not be maintained due to a reduction in fill factor. The SCL photocurrent regime is reached for device with active layer over 200nm, leading to limited charge collection efficiency in the devices due to space-charge accumulation. The onset of space-charge accumulation also coincides with reductions in FF and hence power conversion efficiency in thick devices. These results indicate that although high efficiencies can be obtained in solar cells with low-bandgap conjugated donor-acceptor polymers, the high density of photogenerated charge carriers could severely limit the performance of solar cells with a thick active layer.

Goals and Objectives

The objective of the proposed project is to synthesize broadly absorbing, black colored (PBLACK) polymers with especially high charge mobilities and to fabricate the highest performance polymer solar cells possible. Specifically, we will synthesize polymers with absorption band ranging from 400 nm to beyond 1 μm with carrier mobilities higher than 10^{-4} cm^2/Vs. Polymer-fullerene (both $PC_{60}BM$ and $PC_{70}BM$ along with more recently developed derivatives) blend morphology will be optimized using different solvent/heat treatments as well as additives to the blends. The final device will be enhanced using anode and cathode interlayers to enhance carrier extraction to the electrodes. With the ability to synthesize broadly absorbing polymers, control the donor-acceptor phase morphology and engineer the device structure, it is expected that the power conversion efficiency of polymer solar cells can reach 10% at the end of the two-year program.

Project Activities, Results and Accomplishments

Extensive efforts have been directed at developing polymer bulk heterojunction (BHJ) solar cells because of their potential for low-cost energy harvesting. The device geometry of typical laboratory-scale polymer solar cells comprises a bottom indium tin oxide (ITO) anode, an anode interfacial layer, a photoactive layer and a low-work-function top metal cathode. Because vacuum deposition of low-work-function metals is required for these top cathode devices, it is not viable to use this device architecture in large-scale roll-to-roll (R2R) processing. To avoid the low-work-function metals used in such devices, we recently report a new method for enhancing charge collection with inverted geometry of polymer BHJ solar cells using a ZnO–poly(vinyl pyrrolidone) (PVP) composite sol–gel film as the ETL, and demonstrate inverted polymer solar cells that operate with laboratory-measured PCEs in excess of 8% and certified efficiencies of 7.4% under AM 1.5G illumination at 100 mW cm^{-2}.

The photo J–V characteristics for inverted PDTG–TPD:$PC_{71}BM$ solar cells were measured under AM 1.5G solar illumination at 100 mW cm^{-2}. The photovoltaic (PV) performance results for the inverted cells with ZnO–PVP nanocomposites are shown in Figure 1. On initial light exposure the inverted solar cells had a low FF of 25.5% and J_{sc} of 10.9 mA cm^{-2}. With continuous illumination, device performance was enhanced significantly over time. After 10 min of light soaking, an enhanced FF of 63.7% and J_{sc} of 12.9 mA cm^{-2} were obtained, resulting in an average PCE of 7.0%. Previously, we reported inverted PDTG–TPD-based polymer solar cells with a FF of 68% using colloidal ZnO nanoparticlesas the ETL. We suspected that by using ZnO-PVP composite as the ETL, the ZnO-PVP surface would be compositionally rich in PVP, creating a contact barrier between the ZnO nanoclusters and $PC_{71}BM$ leading to the lower FF of our present devices.

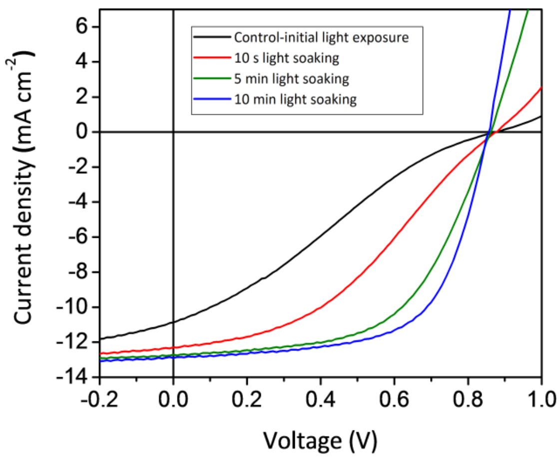

Figure 1. Effect of light soaking on device performance for inverted solar cells with as-prepared ZnO-PVP nanocomposite ETL.

To ensure a good contact between the ZnO nanoclusters and $PC_{71}BM$, we performed UV-ozone treatment on the ZnO–PVP nanocomposite films to remove PVP from the surface. Previous work has shown that UV-ozone treatment can remove PVP on colloidal nanoparticle film surfaces34. The removal of PVP did not alter the size, shape or distribution of the nanoclusters in the films. Based on these findings, we believed that the UV-ozone treatment would improve electronic coupling between the photo-active layer and the ZnO nanoclusters. The photo J–V characteristics for the inverted PDTG–TPD:$PC_{71}BM$ solar cells with UV-ozone treated ZnO–PVP nanocomposites are shown in Fig. 2a. All devices were tested under initial light exposure, and no additional light soaking was applied to the devices. The ZnO–PVP nanocomposite films were UV-ozone treated for 5, 10, 20 and 30 min, leading to significant enhancements in the J_{sc} and FF values for the inverted PDTG–TPD:$PC_{71}BM$ solar cells compared to cells with as-prepared nanocomposite films. Table 1 summarizes the device performance for inverted solar cells with treated ZnO–PVP nanocomposite films. UV-ozone treating the ZnO–PVP nanocomposite films for 10 min led to an optimal device with enhancements in both J_{sc} and FF compared to the light-soaked devices without UV-ozone treatment, and resulting in an average PCE of 8.1%. This average PCE of 8.1+0.4% is based on measurements from 102 fabricated solar cells. Our best
device had a J_{sc} of 14.4 mA cm^{-2}, V_{oc} of 0.86 V, FF of 68.8% and PCE of 8.5%. For devices with ZnO–PVP nanocomposite films that had been UV-ozone treated for less than or more than 10 min, a reduction in FF was observed. For the shorter treatment, we attribute this reduction in FF to incomplete removal of the PVP from the surface of the composite film. For the longer treatment, excess oxygen is present on the ZnO film surface, which reduces the electron extraction efficiency. Based on these findings, we conclude that removal of extra PVP from the ZnO–PVP nanocomposite film surface by UV-ozone treatment greatly enhances the charge collection efficiency of these devices.

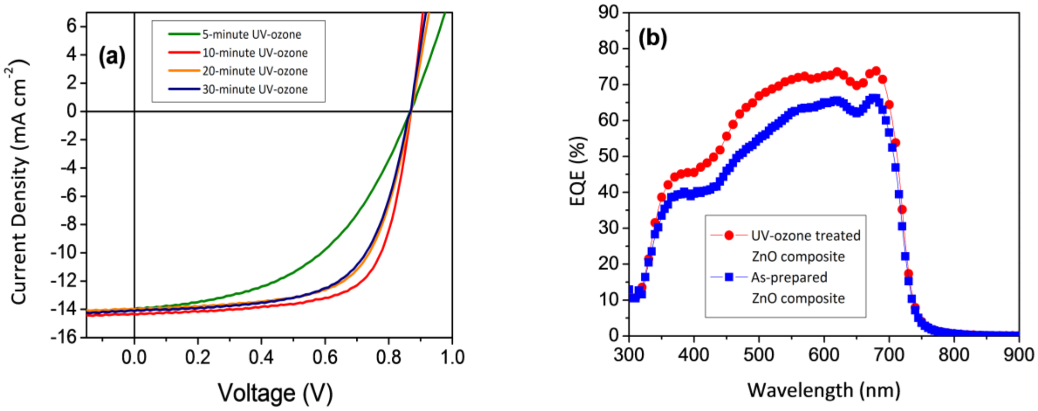

Figure 2. (a) Photo J-V curves of inverted PDTG-TPD:PC71BM solar cells with UV-ozone treated ZnO-PVP nanocomposite films as ETLs for various treatment times (5, 10, 20, 30 min) under initial AM 1.5G solar illumination at 100 mW cm-2. (b) Corresponding EQE for the devices with as-prepared and 10 min UV-ozone treated ZnO-PVP nanocomposite films

.

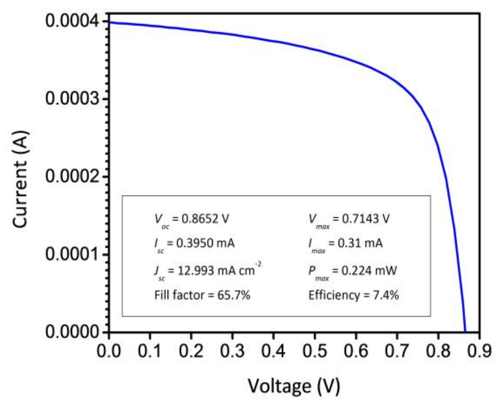

Figure 3. Certified I-V characteristics for an inverted PDTG-TPD:PC71BM solar cell with 10 min UV-ozone treated ZnO-PVP nanocomposite ETL.

To confirm the accuracy of the photo J–V measurements, the external quantum efficiency (EQE) spectra for the solar cells with as-prepared and 10 min UV-ozone treated ZnO–PVP nanocomposite films were measured; these are compared in Fig. 2b. An enhanced efficiency is observed throughout the full spectral range from 350–700 nm for cells with UV-ozone treated ZnO–PVP nanocomposite films when compared to cells without UV-ozone treatment. The maximum EQE for the optimized inverted PDTG–TPD:PC_{71}BM solar cell with UV-ozone treated nanocomposite films was 73.6%. The J_{sc} value was then calculated by integrating the EQE data with the AM 1.5G spectrum. The calculated J_{sc} value of 14.5 mA cm^{-2} is in good agreement with the directly measured J_{sc} value.

Encapsulated devices with UV-ozone treated ZnO–PVP nanocomposite films were then sent to NEWPORT Corporation for certification. The photo J–V characteristics and the corresponding solar cell parameters are shown in Figure 3. A PCE of 7.4+0.2% was certified for the devices. Although this certified efficiency is 9% less than that measured in our laboratory because of a reduction in J_{sc} and FF in the certified device, we attribute the reduction in PCE in the certified cells to degradation because of a non-optimized encapsulation process. The devices were retested in our laboratory after certification and we obtained an efficiency (7.2%) comparable to the certified results.

Based on the demonstration of high efficiency polymer solar cells based on a low bandgap donor-acceptor copolymer with alternating dithienogermole-thienopyrrolodione (DTG-TPD) repeat units last year, we further present high efficiency inverted polymer solar cell with thicker active layers that will potentially facilitate the production yield of roll-to-roll printing process. One key factor for improving the large-scale R2R processing compatibility of polymer solar cells is the active layer thickness required to ensure high manufacturing yields in PV modules. Most high efficiency laboratory-scale devices demonstrated have an active layer with a thickness of about 100 nm which is too thin for R2R processing to ensure a pinhole-free film. Obtaining high efficiency devices with active layers thicker than 200 nm is critical for commercialization. To achieve high efficiency with an active layer thickness larger than 200nm, we fabricated the device containing a bottom transparent oxide electrode, a ZnO-PVP composite layer with UV-ozone treatment, a photo-active layer composed of PDTG-TPD and fullerene, a layer of molybdenum oxide and a top electrode—silver. In addition, the efficiency loss mechanism in the thick devices was studied in depth by the measurement of field dependent external quantum efficiency spectra and photoconductivity analysis. The work is done in collaboration with Dr. John Reynolds at Georgia Institute of Technology.

Figure 4 shows the photocurrent density–voltage ($J-V$) characteristics and the corresponding external quantum efficiency (EQE) spectra for inverted PDTG-TPD:$PC_{71}BM$ solar cells with 105 nm, 204 nm, and 258 nm-thick active layers. Figure 4 a shows that the short-circuit current density (Jsc) increases with increasing active layer thickness due to enhanced light absorption, with the highest Jsc of 16.1 mA cm^{-2} obtained for the device with an active layer thickness of 258 nm. The integrated current density from the EQE spectra, shown in Figure 4 b, is consistent with the measured Jsc with 5% deviation. The difference in the EQE spectra is due to optical interference effects between the incident light and light reflected from the Ag back electrode. For devices with thickness $L \geq 200$ nm, the interference effects no longer affect the photocurrent density of the device and the active layer absorbs most of the incident light below 700 nm, resulting in EQEs above 70% from 400 nm to 700 nm.

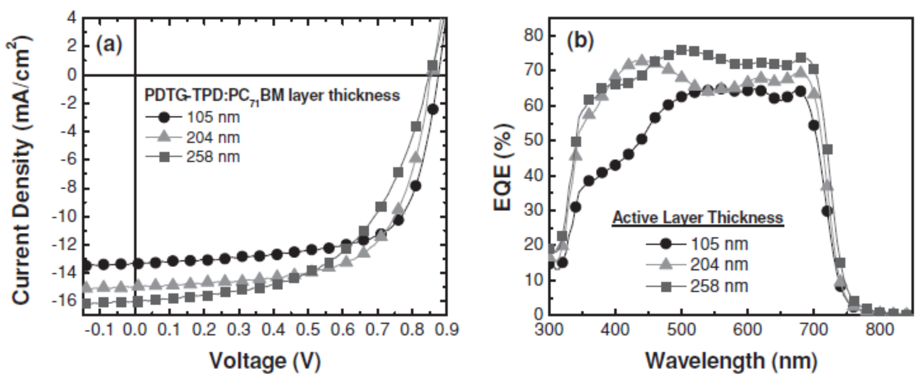

Figure 4 (a) Current density versus voltage characteristics for PDTG-TPD:PC 71 BM solar cells with 105 nm, 204 nm, and 258 nm-thick active layer. (b) Corresponding external quantum efficiency (EQE) spectra for the devices.

Table 1 summarizes the average solar cell parameters for the PDTG-TPD:PC_{71}BM devices with an active layer thickness varying from 90 nm to 409 nm. The reduction in FF observed for PDTG-TPD solar cells with increasing active layer thickness is the major factor limiting the device performance. A power conversion efficiency (PCE) of 7.9% is obtained for the device with a 105 nm thick active layer, which is consistent with our previous report. The efficiency remains constant for devices with $L \leq 204$ nm, with an average PCE of 8.2% being obtained for devices with an active layer thickness of 204 nm. Above 200 nm, the FF reduction becomes significant, dropping from 69% in 105 nm film to 42% in 409 nm film.

Table 1 Averaged solar cell performance for PDTG-TPD:PC 71 BM devices with various active layer thickness under initial AM 1.5G solar illumination.

Active Layer Thickness	J_{sc} (mA cm^{-2})	J_{sc} (EQE) (mA cm^{-2})	V_{oc} (V)	FF (%)	PCE (%)
90 nm	12.5 +/−0.1	12.3	0.88	68.5 +/−0.1	7.5 +/−0.1
105 nm	13.3 +/−0.2	13.0	0.87	68.7 +/−0.3	7.9 +/−0.1
153 nm	13.5 +/−0.4	13.5	0.86	68.1 +/− 0.3	8.0 +/−0.2
204 nm	14.9 +/−0.3	14.7	0.86	64.5 +/−0.7	8.2 +/−0.2
258 nm	16.1 +/−0.2	16.0	0.85	54.1 +/−0.9	7.4 +/−0.1
409 nm	15.2 +/−0.1	14.9	0.82	41.6 +/−0.9	5.2 +/−0.1

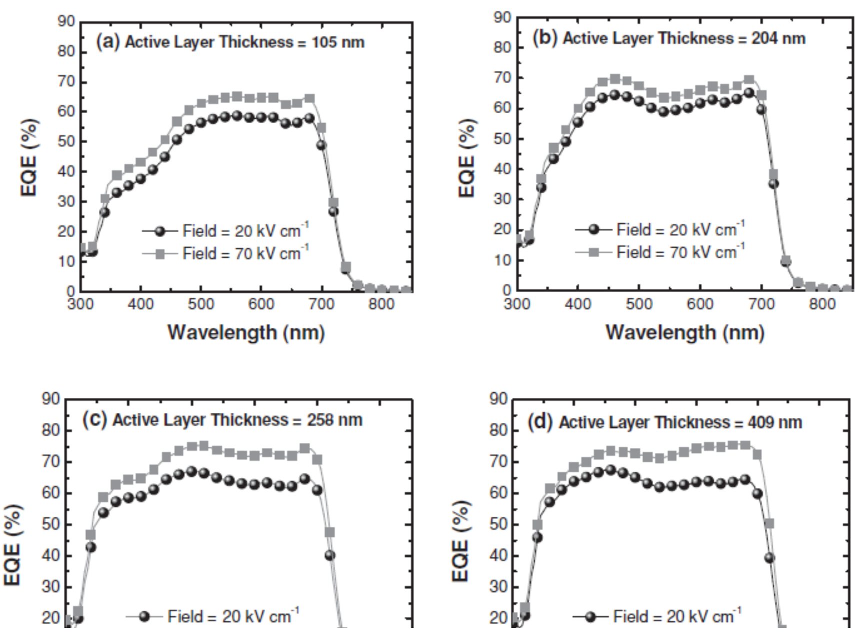

Figure 5 Field-dependent EQE spectra for PDTG-TPD:PC 71 BM solar cells with (a) 105 nm, (b) 204 nm, (c) 258 nm and (d) 409 nm-thick active layer. The EQE spectra were measured at internal electric fi eld values of 20 kV cm− 1 and 70 kV cm− 1.

To determine the root cause for the reduction in FF observed in thick-film PDTG-TPD:PC_{71}BM solar cells, the EQE spectra for the thin-film and thick-film devices were measured under different values of internal electric field. **Figure 5** shows the field-dependent EQE spectra for devices with 105 nm, 204 nm, 258 nm, and 409 nm-thick active layers, respectively. By measuring the EQE as a function of internal electric field (E), approximated as $E = (Voc-V)/L$, the effect of series resistance can be eliminated. For the device with an active layer thickness ≤ 204 nm, increasing the applied fi eld from 20 kV cm^{-1} to 70 kV cm^{-1} leads to a uniform enhancement in EQE across the entire spectral range. The increased applied field enhances the extraction of photogenerated charges equally across the EQE spectrum. Interestingly, for devices with $L > 204$ nm, a stronger field dependent enhancement in EQE is observed in the spectral range from 500 to 750 nm when the applied field is increased from 20 kV cm^{-1} to 70 kV cm^{-1}. This wavelength range corresponds to the absorption spectrum for a pristine PDTG-TPD film. For devices with a thick active layer, the build-up of charges in PDTG-TPD:PC_{71}BM will hinder charge collection and contribute to the FF reduction in thick solar cells.

To study the role space-charge accumulation plays in PDTGTPD: PC_{71}BM solar cells with a thick active layer, we employed the SCL photocurrent model to confirm that the electrostatic space-charge limit was reached in our thick devices. We compared the results for PDTG-TPD:PC_{71}BM solar cells with similar devices based on P3HT:PC_{61}BM, since P3HT solar cells provide a model system for studying space-charge effects. The effective photocurrent J_{ph}, normalized to the saturation photocurrent $J_{sat} = qG_{max}L$, was plotted on a double logarithmic scale against the effective voltage across the device, given by $V_{eff} = V_0 – V$. Here, V_0 is defined as the voltage where J_{ph} = 0 and is slightly larger than *V*oc. This "corrected" photocurrent analysis is a widely used tool for analyzing recombination loss processes in organic solar cells. **Figure 6a** shows the results for the PDTG-TPD:PC_{71}BM solar cells with 105 nm, 258 nm and 409 nm-thick active layer. For the device with a 105 nm thick active layer, two different voltage regimes can be observed. For V_{eff} < 0.30 V, J_{ph} steadily increases with voltage due to the competition between diffusion and drift for photo-generated carrier transport at low field. For V_{eff} > 0.30 V, the photocurrent saturates with increasing voltage. In this saturation regime, the internal field is strong enough to efficiently extract photogenerated carriers and the high field is responsible for the dissociation of *e-h* pairs. The voltage corresponding to the short circuit condition falls within the saturation regime, indicating that the high J_{sc} and FF obtained for this device is due to efficient charge collection by the internal electric field. For the device with a 105 nm active layer, space charge effects were not observed based on the data shown in Figure 6a. As the active layer thickness for PDTG-TPD cells increased above 200 nm, a square-root effective voltage dependence on J_{ph} is observed. This $J_{ph} \propto V^{1/2}$ corresponds to the onset of space-charge limited photocurrent in thick PDTG-TPD cells assuming a $J_{ph} \propto G$¾ dependence is also observed. The solid lines in Figure 6a correspond to $J_{ph} \propto V^{1/2}$. For the 409 nm-thick device, the $J_{ph} \propto V$ ½ regime extends to the short circuit condition, which correlates well with the reduction in *J*sc and FF observed in this device. These results are in contrast with those found in **Figure 6b** for P3HT:PC_{61}BM.

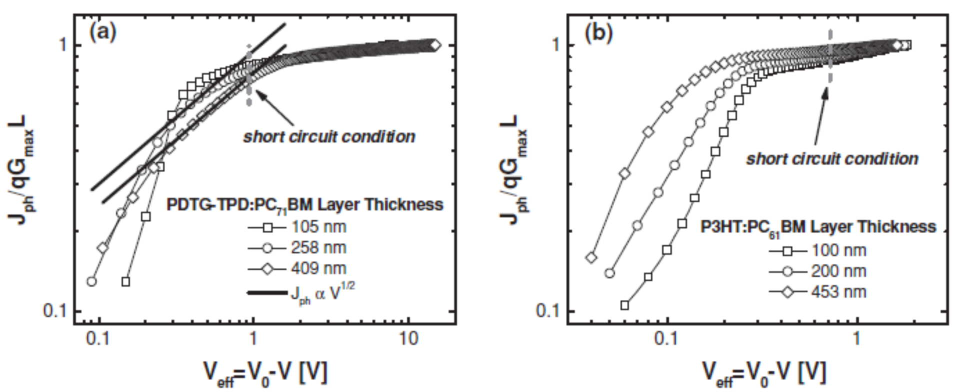

Figure 6 Effective photocurrent density (J ph) normalized by J sat = qG max L as a function of effective voltage (V_{eff}) under 100 mW cm^{-2} illumination for (a) PDTG-TPD:PC_{71}BM cells with 105 nm, 258 nm, and 409 nm-thick active layer, and (b) P3HT:PC 61 BM cells with 100 nm, 200 nm, and 453 nm-thick active layer. Dashed lines highlight the value of V_{eff} corresponding the short-circuit condition ($V_{eff} = V_0$). The solid lines correspond to $J_{ph} \propto V^{1/2}$ fits of the photocurrent in the SCL regime for PDTG-TPD solar cells.

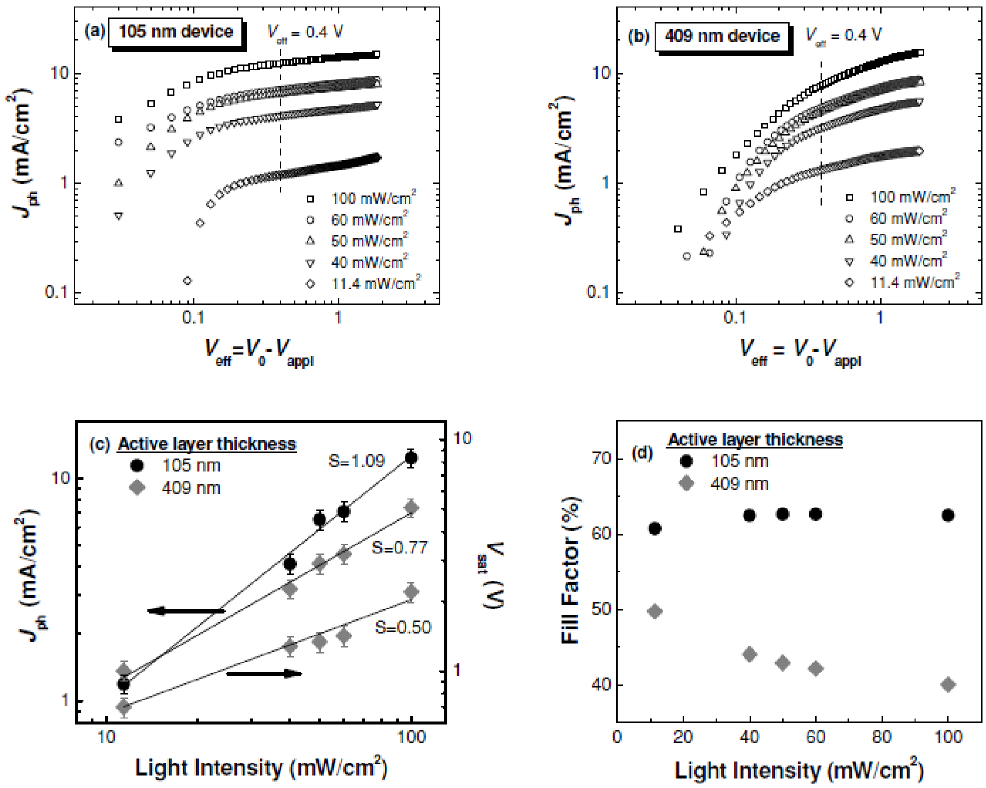

Figure 7 Light Intensity Dependent Study For Pdtg-Tpd:PC71BM Solar Cells with Thin and Thick Active Layer. Jph − Veff Curves for the (a) 105 nm-thick and (b) 409 nm-thick devices under various light intensities (from 11.4 to 100 mW cm− 2). (c) Effective photocurrent density (J ph), saturation voltage (Vsat), and (d) fill factor as a function of incident light intensity for the same devices. The Jph − P0 curves were measured at Veff = 0.4 V.

The dependence of J_{ph} and FF on incident light intensity (P_0) was plotted for the 105 nm and 409 nm-thick PDTG-TPD:PC$_{71}$BM solar cells (see **Figure 7**). Neutral density filters were used to control the incident light intensity, which was varied from 11.4 to 100 mW cm^{-2}. The $J_{ph} - P_0$ data for the thin and thick PDTG-TPD:PC$_{71}$BM devices, shown in Figure 7c, was extracted from the $J_{ph} - V_{eff}$ curves shown in Figures 7a and b. For the solar cell with a 105 nm-thick active layer, J_{ph} showed a linear dependence on light intensity with the slope of the linear fit tothe data equal to 1.09. In contrast, a slope of 0.77 is observed for the 409 nm-thick PDTG-TPD solar cell. The ~ 3/4 power dependence of J ph on the incident light intensity confirms the occurrence of SCL photocurrent in PDTG-TPD:PC$_{71}$BM solar cells at low bias. The dependence of the saturation voltage (V_{sat}) on incident light intensity provides further evidence, in which a slope of 0.50 is extracted from the $V_{sat} - P_0$ data. To form a more clear physical picture, the light-intensity dependence of the FF was also analyzed and plotted in Figure 7d. The FF remained relatively constant with incident light intensity for the 105 nm-thick solar cell, which is expected since the device is not space-charge limited at P_0 = 100 mW cm $^{-2}$ and the thickness is sufficiently thin to ensure efficient charge extraction. For the 409 nm-thick PDTG-TPD solar cell, a 24% enhancement in FF was observed as the incident light intensity was decreased from 100 mW cm^{-2} to 11.4 mW cm^{-2}. By lowering P_0 and, consequently, reducing the generation rate of charge carriers in the thick PDTG-TPD:PC 71 BM active layer, space-charge buildup was reduced. As a result, enhanced charge carrier collection and FF was observed in the solar cell. Despite this enhancement, the FF of the 409 nm-thick device at low light intensity does not reach the value obtained in the 105 nm device. This result indicates that the reduced photocurrent observed for thick-film devices could not be completely recovered despite lowering the incident light intensity. There is still some degree of limited charge collection occurring in thick-film PDTG-TPD:PC$_{71}$BM solar cells.

To conclude, the loss mechanism in thick-film PDTGTPD:$PC_{71}BM$ solar cells have been investigated. For polymer solar cells with an active layer thickness up to 200 nm, efficiencies in excess of 8.0% were obtained for devices under AM 1.5G illumination at 100 mW cm^{-2} . For L > 200 nm, the SCL photocurrent regime is reached, leading to limited charge collection efficiency in the devices due to space-charge accumulation. The onset of space-charge accumulation also coincides with reductions in FF and hence power conversion efficiency in thick devices. These results indicate that although high efficiencies can be obtained in solar cells with low-bandgap conjugated donor-acceptor polymers, the high density of photogenerated charge carriers could severely limit the performance of solar cells with a thick active layer.

Concluding Remarks

Polymer bulk heterojunction solar cells based on low bandgap polymer:fullerene blends are promising for next generation low-cost photovoltaics. While these solution-processed solar cells are compatible with large-scale roll-to-roll processing, active layers used for typical laboratory-scale devices are too thin to ensure high manufacturing yields. Furthermore, due to the limited light absorption and optical interference within the thin active layer, the external quantum efficiencies (EQEs) of bulk heterojunction polymer solar cells are severely limited. We demonstrated high performance polymer solar cells with high yields, efficient solar cells with broadly absorbing polymers. The next step is to extend the absorption wavelength to the NIR region to increase the light harvesting efficiency.

Publications

1. T.-H. Lai, S.-W. Tsang, J. Manders, S. Chen and F. So “Properties of interlayers for organic Photovoltaics, invited review paper, Materials Today (2013)
2. R. Casalini, S.W. Tsang, J.J. Deninger, F. A. Arroyave, J.R. Reynolds and F. So, “Investigation of the Role of the Acceptor Molecule in Bulk Heterojunction PV Cells using Impedance Spectroscopy”, J. Phys. Chem. C, (2013) dx.doi.org/10.1021/jp401435s
3. M. Hartel, S. Chen, B. Swerdlow, HY Hsu, J. Manders, K. Schanze, F. So, “Defect-induced loss mechanisms in polymer-inorganic planar heterojunction solar cells”, ACS Appl. Mater. Interfaces, (2013)
4. Cephas E. Small, Sai-Wing Tsang, Song Chen, Chad M. Amb, Jegadesan Subbiah, John R. Reynolds, Franky So, “Loss Mechanism in Thick-Film Organic Photovoltaic Cell with Low Bandgap Polymer”, Advanced Energy Materials, DOI: 10.1002/aenm.201201114(2013)
5. S.W. Tsang, S. Chen and F. So, “Energy Alignment and Sub-bandgap charge generation in polymer:fullerene bulk heterojunction solar cells”, accepted for publication, Adv. Mater. adma.201204495. (2013)
6. J. Manders, S. Chen, S.W. Tsang, C. Amb, J.R. Reynolds and F. So, "Solution-Processed Nickel Oxide Hole Transport Layers in High Efficiency Polymer Photovoltaic Cells", Adv. Funct. Mater. 2012, 10.1002/adfm.201202269 (2013)
7. K. Chan, S.W. Tsang, H.K.H. Lee, F. So and S.K. So, “Admittance spectroscopy study of charge transporting properties of semiconducting polymers and their blends”, J. Polymer Science: Polymer Physics (2013)
8. Kenneth R. Graham, Romain Stalder, Patrick Wieruszewski, Michael Hartel, Jianguo Mei, Franky So, John R. Reynolds, “Improved Performance of Molecular Bulk-Heterojunction Photovoltaic

Cells through Predictable Selection of Solvent Additives", Advanced Functional Materials, Volume 22, Pages 4801-4813, November 2012.

9. Song Chen, Cephas E. Small, Chad M. Amb, Jegadesan Subbiah, Tzung-han Lai, Sai-Wing Tsang, Jesse M. Manders, John R. Reynolds, Franky So, "Inverted Polymer Solar Cells with Reduced Interface Recombination", Advanced Energy Materials, DOI: 10.1002/aenm.201200184, Volume 2, Page 1333-1337, November 2012.

10. C.E. Small, S.W. Tsang, J. Kido, S.K. So, F. So, "Origin of Enhanced Hole Injection in Inverted Organic Devices with Electron Accepting Interlayer", Advanced Functional Materials, DOI: 10.1002/adfm.201200185, Volume 22, Pages 3261-3266, August 2012.

11. S. Chen, J. Manders, S.W. Tsang, J.R. Reynolds, F. So, "Metal-oxides for organic photovoltaics", Invited Review, Journal of Materials Chemistry, Volume 22, Pages 24202-24212, August 2012.

12. C. Xiang, W.H. Koo, S. Chen, X. Liu, X. Kong, Y. Wang, F. So, "Solution processed multilayer cadmium-free blue/violet emitting quantum dot light emitting diodes", Applied Physics Letters, Volume 101, July 2012.

13. Pierre Beaujuge, Hoi Nok Tsao, Michael Ryan Hansen, Chad Amb, Chad Risko, Jegadesan Subbiah, Kkaushik Choudhury, Alexy Mavrinskiy, Wojciech Pisula, Jean-Luc Bredas, Franky So, Klauss Mullen, John Reynolds, "Synthetic Principles Directing Charge Transport in Low Band-Gap Dithienosilole-Benzothiadiazole Copolymers", Journal of the American Chemical Society, Volume 134, Pages 8944-8957, May 2012.

14. K. K. H. Chan, S. W. Tsang, H. K. H. Lee, F. So, S. K. So, "Charge injection and transport studies of poly(2,7-carbazole) copolymer PCDTBT and their relationship to solar cell performance", Organic Electronics, Volume 13, Pages 850-855, May 2012.

15. S. Chen, S.W. Tsang, C.E. Small, J.R. Reynolds, F. So, "Inverted polymer solar cells", Invited Paper, Breakthroughs in Photonics, IEEE Photonics Journal, Volume 4, Pages 625-628, April 2012.

16. C. M. Amb, M.R. Craig, U. Koldemir, J. Subbiah, K. Roy Choudhury, S.A. Gevorgyan, M. Jorgensen, F.C. Krebs, F. So, J. R. Reynolds, "Aesthetically Pleasing Conjugated Polymer: Fullerene Blends for Green Solar Cells Via Roll-To-Roll Processing", Applied Material Interfaces, Volume 4, Pages 1847-1853, March 2012.

Florida Advanced Technological Education Center (FLATE)

Education - Technician Based Workforce
(Progress Report)

PI: Marilyn Barger

Description: FLATE (Florida Advanced Technological Education Center) will partner with FESC to develop statewide curriculum frameworks for technical A.S./A.A.S. degree programs supporting existing and new energy business sectors. FLATE will develop and have processed through the FLDOE the industry-validated student competencies of the frameworks. FLATE will also develop new courses required for each new program of study. Additionally FLATE will help state and community colleges implement the new frameworks in their institutions. To support the new curriculum, FLATE will work closely with the FESC Public Outreach and Industry Partnership programs to provide professional development opportunities for teachers and faculty to upgrade and update their knowledge base.

Budget: $300,000.
Universities: FLATE/Hillsborough Community College

FLATE External Collaborators: Brevard Community College; Tallahassee Community College; Daytona State College; Central Florida Community College; Polk State College; Florida State College at Jacksonville; Valencia Community College; Palm Beach State College; School District Hillsborough County; Florida Department of Education – Division of Adult and Career Education; West Side Technical School; USF College of Engineering; Madison Area Technical College ATE project for Alternative Energy certifications; Milwaukee Area Technical College Energy Conservation and Advanced Manufacturing Center (ECAM); Florida Energy Workforce Consortium (FEWC); TECO; Progress Energy; ISTEC (Ibero Science and Technology Education Consortium), Usurbil GLBHI (Spain); TKNIKA - Innovation Institute for Vocational Training (Spain); Center for Energy workforce Consortium (CEWD); UF Industrial Assessment Center; CREATE NSF Center for Alternative Energy; EST2 NSF ATE Grant project; DOE's Office of Energy Efficiency & Renewable Energy; Gulf Coast State College; Palm Beach State College; University of South Florida's College of Engineering; University of Miami; University of Alabama; Rutgers University; Energy Reduction Solution, SMC Corporation of America, Energy Conservation Group; Florida Solar Energy Consortium; Tampa Bay Regional Business Plan Energy Efficiency and Conservation Sub-Committee.

Progress Summary
Since October 1, 2012 FLATE has achieved several milestones. Together with the National Science Foundation-funded Energy Systems Technology Technicians (EST²) project team, FLATE has developed a new Industrial Energy Efficiency (IEET) specialization for the Engineering Technology (ET) Degree and associated College Credit Certificate, in addition to the existing Alternative Energy Specialization. The IEET program framework has been approved by the FL Department of Education and colleges will be able to implement it in the 2014-2015 academic year.

FLATE coordinated a second highly successful **energy workshop** (the last one was held in September 2011 in Gainesville), for high school and college educators, as well as industry partners, hosted by the Florida Solar Energy Center (FSEC) in Cocoa, FL on January 25, 2013. Forty attendees attended a wide variety of presentations, went on a tour of the amazing FSEC facilities and participated in a Professional Development activity focused on solar energy applications.

FLATE's **Third Annual Summer Energy Camp** was a huge success with the highest attendance ever and feedback from both teachers and students overwhelmingly positive! Thirty 7th and 8th grade students were treated to four days of exciting, hands-on activities centered on capturing and keeping their interest in STEM (Science, Technology, Engineering and Math) subjects – specifically renewable energy.

Finally, FLATE regularly updates / presents information about energy curriculum and training issues at the statewide Florida Engineering Technology Forum that meets twice per year at various colleges across the state. Many of these schools are looking to add "energy" curriculum and/or programs and are requesting guidance on what industry is asking for across the state and what and how other colleges are implementing credit programs. The goal of these activities is to keep colleges working together and sharing curriculum rather than develop independent programs not properly aligned to statewide frameworks. The ET Forum most recently met October 4 - 5 in Tampa at Hillsborough Community College.

Florida Advanced Technological Education Center (FLATE), Dr. Marilyn Barger

The development of the process for the Florida State College System to respond to FESC's long term strategy to bring energy related technologies out of the Florida University System is well underway. FLATE has the college contacts and process in place to respond to any FESC and/or regional economic development authority request to provide assistance to a designated State College. These requests can be focused on the technician workforce development need as identified or triggered by industrial partners, FESC university partners or from expanding energy- related companies' operations in the State.

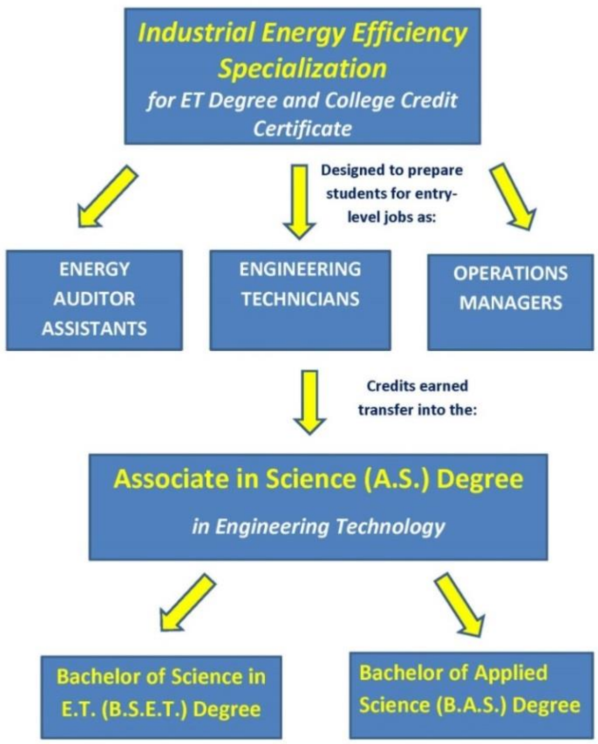

Since October 1, 2012 FLATE has achieved several milestones. Together with the National Science Foundation-funded Energy Systems Technology Technicians (EST²) project team, FLATE has developed a new Industrial Energy Efficiency specialization for the Engineering Technology (ET) Degree and associated College Credit Certificate, in addition to the existing Alternative Energy Specialization. Experts from industry, government and academia have been involved in this collaborative effort and instrumental in ensuring that the new specialization is directly aligned with current industry needs. It will help students prepare to become a **SEP-Superior Energy Performance Certified Systems Practitioners** and **CEM Certified Energy Managers**. In addition, the program will train workers who will assist a company in achieving the ISO 50001 standards related to energy management, as well as ISO 14001:2004 to assure a company's stakeholders that measures are being taken to improve their environmental impact. Credits earned in this certificate will transfer into the Associate in Science (A.S.) degree in Engineering Technology.

FLATE and FESC coordinated an Advisory Working Group Meeting in Orlando (DACUM), FL on February 28, to develop a curriculum plan for the Industrial Energy Efficiency Technician (IEET) Specialization. Sixteen members from academia and industry worked on the following focus statement for the workshop, “An industrial energy efficiency technician implements energy efficiency strategies in industrial processes and systems in order to improve an organization's bottom line and reduce environmental impacts." The meeting summary was circulated to the atteendees and others who were not able to be there for final input. The finalized document established the courses that would be developed for the A.S. specialization tract in Engineering Technology and the related College Credit Certificate. The 7 new courses will have to be submitted to the state Common Course Numbering System office to be given a state number before they are available for colleges to adopt.As a result of the meeting, a comprehensive list of IEET Resources was compiled and classes were identified as well as their associated learning outcomes.

All courses are 3 credit hours

- Fundamentals of Industrial Energy Efficiency
- Industrial Systems
- Energy Benchmarking and Performance Analysis
- Energy Efficiency Instrumentation and Measurement
- Industrial Energy Analytics and Troubleshooting
- Industrial Controls and System Integration
- Industrial Energy Efficiency Capstone

The course creation validated the IEET program framework content that was submitted to the FL Department of Education for approval this year, and colleges will be able to implement it in the 2014-2015 academic year. Curriculum content modules are currently being developed to support the newly defined courses (from the DACUM) – available in Dec 2013.

Engineering Technology Energy-Related Programs as of January 2013

COLLEGE CREDIT CERTIFICATES	COLLEGES OFFERING
Alternative Energy Systems Specialist (CCC) **Career Cluster:** Manufacturing **CIP #:** 0615000003 **Program Length:** 18 (Primary) or 15 (Secondary)Credits	Brevard Community College, Tallahassee Community College, State College of Florida, Gulf Coast State College
Industrial Energy Efficiency Specialist (CCC) **Career Cluster:** Manufacturing **CIP #:** 061500000x **Program Length:** 21 (Primary) or 24 (Secondary)Credits	Florida State College at Jacksonville (2013)
A.S. DEGREE SPECIALIZATIONS (60 credit hours)	**COLLEGE OFFERING**
A.S. Eng Tech Alternative Energy Technology	Brevard Community College, State College of Florida, and Gulf Coast State College
A.S. Eng Tech Industrial Energy Efficiency	Florida State College at Jacksonville (2013)

Frameworks are posted on the FLDOE website:
http://www.fldoe.org/workforce/dwdframe/mfg_cluster_frame12.asp

FLATE and FESC coordinated a second highly successful **energy workshop** (the last one was held in September 2011 in Gainesville), for high school and college educators, as well as industry partners, hosted by the Florida Solar Energy Center (FSEC) in Cocoa, FL on January 25, 2013. Forty attendees attended a wide variety of presentations, went on a tour of the amazing FSEC facilities and participated in a Professional Development activity focused on solar energy applications. Feedback received was overwhelmingly positive.

FLATE's **Third Annual Summer Energy Camp** was a huge success with the highest attendance ever and feedback from both teachers and students overwhelmingly positive! Thirty 7th and 8th grade students from Beth Shields and Pierce Middle Schools were treated to four days of exciting, hands-on activities centered on capturing and keeping their interest in STEM (Science, Technology, Engineering and Math) subjects – specifically renewable energy. By participating in the camp, students also learned about the many diverse and exciting careers available in the field of clean energy. Camp participants were all part of Hillsborough County School District's AVID (Advancement Via Individual Determination) Excel Program, consisting of first generation college-bound, English language learners.

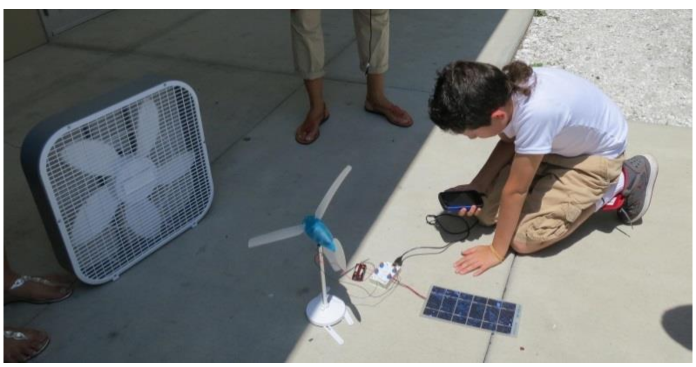

On the final day of camp, students raced hydrogen-fueled cars and were given a fabulous "Green" tour of Hillsborough Community College's SouthShore campus which is LEED (Leadership in Energy and Environmental Design) silver-certified by the USGBC (U.S. Green Building Council), and boasts an earth-friendly, energy-conscious functionality incorporating a number of sustainable features. These include solar panels, a rainwater recycling process, maximum use of natural light and a raised-floor HVAC system that provides greater efficiencies for cooling. Students' feedback from the final camp survey illustrated strongly how much they learned about energy while at the same time having fun. Student comments included, "*"The experiments we did were a magnificent experience for an 8th grader," "We got to be creative and at the same time learn something," "The thing I like about energy is we do these awesome projects of energy"*. One hundred percent of the students said that they learned new things about energy and 95% stated that they felt the camp would help them making future career choices with over half saying that they would consider a career in clean energy.

Finally, FLATE regularly updates / presents information about energy curriculum and training issues at the statewide Florida Engineering Technology Forum that meets twice per year at various colleges across the state. Many of these schools are looking to add "energy" curriculum and/or programs and are requesting guidance on what industry is asking for across the state and what and how other colleges are implementing credit programs. The goal of these activities is to keep colleges working together and sharing curriculum rather than develop independent programs not properly aligned to statewide frameworks. The ET Forum most recently met October 4 - 5 in Tampa at Hillsborough Community College.

Activities for the 2012-2013 year are listed below.

- Presented at the Florida Association of Science Teachers Conference in October, 2012 with Mark Dick (Tallahassee Community College), "Energy Camps that are Energizing", highlighting the Teacher Energy Workshops and Energy Summer Camps for students offered over the summer by all EST 2 partners.
- Attended the Florida Energy Workforce Consortium Meeting in November 2012 and March 2013.
- Presented "Industrial Energy Efficiency Competencies for Associate Degree Programs", at the Interstate Renewable Energy Council (IREC) Clean Energy Workshop in Albany, NY, November, 2012.
- Attended the Manufacturers Association of Florida Summit in December 2012 and surveyed 40 manufacturers about the need for energy efficiency trained technicians. The overwhelming majority of manufacturing members who completed the survey strongly supported the new IEET CCC since manufacturers need solutions to their high cost associated with energy consumption. A focus group meeting was held in Orlando, in February 2013 with industry, university faculty, tech center faculty and state college personnel/faculty. The focus group meeting was a scaled down, Designing a Curriculum (DACUM) that produced potential courses and course content for the proposed IEET program. The course creation validated the IEET program framework content that was submitted to the FL Department of Education for approval this year, and colleges will be able to implement it in the 2014-2015 academic year. Curriculum content modules are currently being developed to support the newly defined courses (from the DACUM) – available in Dec 2013
- Coordinated a second Community College Energy workshop for 40 attendees at the Florida Solar Energy Center (FSEC) in Cocoa, January 25, 2013.
- Was instrumental in the selection of Hillsborough Community College as a winner of the (Sustainability Education and Economic Development) Green Genome Award which recognizes exemplary community colleges nationwide that have taken a strategic leadership role in sustainability and green economic and workforce development.
- Attended and was part of an Energy Efficiency and Conservation Panel at 2013 Beyond Sustainability 37th Annual Conference at Hillsborough Community College, Plant Ybor City in February.
- Participated in, "An Energy Literate Citizenry from K-to-Gray: A Webcast on the Department of Energy's Energy Literacy Initiative", in March.
- FLATE hosted the Engineering Technology (ET) Forum in St. Petersburg in April, and in Tampa in October. (Energy Efficiency Specialization was presented).

- A third summer energy program for under-represented middle school students, was held July 8-11 at HCC's SouthShore Campus in Ruskin, FL in conjunction with the EST2 grant partners (BCC, TCC and FSCJ). We had the best attendance to date and teachers have requested that we add a high school camp next year.

Funds leveraged/new partnerships created: FLATE has leveraged its NSF and FESC resources to help Brevard Community College to apply for and be awarded a very competitive NSF grant, $ 500,000, implement two energy related specialization within the A.S. Engineering Technology Degree. In addition, FLATE was able to secure a $ 100,000 award from NSF to develop a faculty/student interchange that will allow Florida to benefit from the well advanced energy related technology educations practices at technology colleges in Spain.

FLATE External Collaborators: Brevard Community College; Tallahassee Community College; Daytona State College; Central Florida Community College; Polk State College; Florida State College at Jacksonville; Valencia Community College; Palm Beach State College; School District Hillsborough County; Florida Department of Education – Division of Adult and Career Education; West Side Technical School; USF College of Engineering; Madison Area Technical College ATE project for Alternative Energy certifications; Milwaukee Area Technical College Energy Conservation and Advanced Manufacturing Center (ECAM); Florida Energy Workforce Consortium (FEWC); TECO; Progress Energy; ISTEC (Ibero Science and Technology Education Consortium), Usurbil GLBHI (Spain); TKNIKA - Innovation Institute for Vocational Training (Spain); Center for Energy workforce Consortium (CEWD); UF Industrial Assessment Center; CREATE NSF Center for Alternative Energy; EST2 NSF ATE Grant project; DOE's Office of Energy Efficiency & Renewable Energy; Gulf Coast State College; Palm Beach State College; University of South Florida's College of Engineering; University of Miami; University of Alabama; Rutgers University; Energy Reduction Solution, SMC Corporation of America, Energy Conservation Group; Florida Solar Energy Consortium; Tampa Bay Regional Business Plan Energy Efficiency and Conservation Sub-Committee.